UNIVERSITY OF CALIFORNIA,
IRVINE

Disaggregate Control of Vehicles Using In-Vehicle Advisories and Peer-to-Peer Negotiations

DISSERTATION

submitted in partial satisfaction of the requirements
for the degree of

DOCTOR OF PHILOSOPHY

in Civil Engineering

by

Riju Lavanya

Dissertation Committee:
Professor R. Jayakrishnan, Chair
Professor Amelia Regan
Professor WenLong Jin

2021

Table of Contents

List of Figures

Page

List of Tables

Page

Acknowledgements

I would like to express my deepest appreciation to my advisor and dissertation committee chair, Dr. R. Jayakrishnan, who has accompanied me on this intellectual journey from the very beginning. His passion for scientific inquiry and his willingness to be skeptical about so-called settled questions with pat answers continue to amaze me. His joyful approach to teaching is something I aspire to emulate. He placed his unwavering faith in me, even during times when I gave him no ostensible reason to do so. Without his persistent help in all dimensions of my life, this work would not have been possible.

I would like to thank my committee members, Professor Amelia Regan and Professor Wenlong Jin, for their intellectual and moral support, constant encouragement, and timely feedback. I am grateful to all professors in ITS for the rigorous training I received as a graduate student. In particular, I would like to thank Professor Michael McNally for all the stimulating conversations about topics far and wide. My deepest gratitude to Professor Stephen Ritchie for going out of his way to ensure students in ITS have stability in their lives so they can focus on their research without distractions.

I would like to acknowledge the generous fellowship support I have received from PSR-UTC. Many thanks to the administrative support staff at ITS and CEE who work tirelessly behind the scenes to make sure our lives run smoothly. I have had responses from April Heath to my inquiries that have been faster than some automatic out-of-office email replies.

I want to express my gratitude to some of my colleagues in ITS. In am in debt to Dr. Daisik Nam, who has immensely enriched my intellectual and spiritual life. Many thanks to Bumsub Park and

Lu Xu for their radiant positivity. I wouldn't have been able to finish my journey without the constant support from Navjyoth Sarma and Koti Reddy Allu. I am honored and blessed to call them my friends. I am grateful to Koti for his contributions to my chapter on future research and I look forward to a long-lasting professional relationship with him.

To all my friends, thank you for the much-needed reminder that there are more important things than a PhD dissertation. To Xavier Atero, Ronne Toledo, Amit Kanvinde, Marc Carreras, and Joel Benito, thank you for helping me survive the most stressful periods of my life. In 2019, I experienced the most devastating loss in my life. By virtue of pure happenstance I met a group of people volunteering with the Bernie Sanders campaign who inadvertently rescued me from my intellectual and emotional stasis. That experience helped me find meaning in the middle of apparent senselessness. Many thanks to Ashley Call, Stuart Hiller, Carly Jugler, and Barret Lybbert for their friendship, wit, and capacity to love.

Most of all, I'd like to thank my parents, Umesh Sharma and Vinod Sharma, for the best gift any parent can give to their child: the feeling that the world loves and accepts them unconditionally.

Curriculum Vitae

Education

Spring 2012 – present	Doctor of Philosophy in Civil and Environmental Engineering – Transportation Engineering, University of California, Irvine, CA 92697. Advisor – Professor R. Jayakrishnan
Fall 1999 – Winter 2002	Master of Science in Civil and Environmental Engineering – Transportation Engineering, University of California, Irvine, CA 92697
July 1995 – April 1999	Bachelor of Technology in Civil Engineering, Indian Institute of Technology (IIT Bombay), Bombay, India.

Honors and Awards

Spring 2006	Stradling Yocca Carlson & Rauth Business Plan Competition. Main open competition finalist. Awarded a "wild card" to the Tech Coast Angels Seed Financing Invitational.
Spring 2004	Excellence in Teaching Award, awarded by the Division of Undergraduate Education, UCI.
Spring 2003	Best teaching assistant in the School of Engineering, awarded by the Division of Undergraduate Education, UCI.
2003-2004	University of California Transportation Center Grant

Research Experience

2012 – present	**Lane-based exit control of traffic vehicles**. Development and simulation of traffic mitigation strategies, relying on lane-based instead of link-based traffic information.
2016 – present	**Estimating local traffic density by probe vehicles.** Development and simulation of a suite of algorithms to estimate local density by using sensor-equipped vehicles.
2017 – present	**Addressing Degradation of High-Occupancy Vehicle Lanes in California**. Explore best practices to address HOV lane degradation to strengthen the incentives these lanes provide for carpooling, transit, and ZEV purchase.

2004 - 2008	**Kinetic Theory of Traffic Flow for Networkwide Freeway Traffic Control"** - Conducted extensive theoretical modeling as well computational simulation to evaluate and develop a framework for individual level speed control.
2003 - 2005	Distributed Simulation in Paramics - Assisted in developing a test platform for distributed large-scale simulation. Development of the methodology on distributing the simulation, along with algorithmic details for different types of distribution schemes. Funded by CALTRANS.
2001- 2003	**High Coverage Demand-Responsive Transit: "A new design concept and simulation-evaluation of operational schemes for future technological deployment".** Development of routing algorithms for point-to-point shortest path problems. Simulation of the proposed system using PARAMICS. Funded by PATH.
2001	**Dynamic Traffic Assignment Prototype Evaluation and Field Test** (Development of TrEPS: Phase 1.5B Technical Assistance) - Generated real-time freeway and arterial surveillance data. Funded by FHWA and ORNL.
1999 – 2000	**A Microscopic Simulation Approach to the Evaluation of Transportation Improvement Projects** – Evaluated benefits of freeway improvement projects proposed by CALTRANS. Funded by California Advanced Transportation Management Systems (ATMS) Testbed Research Facility.

Publications/Presentations:

Nam, D., Lavanya, R., Jayakrishnan, R., Yang, I., Jeon, W.H. (2020). A Deep Learning Approach for Estimating Traffic Density Using Data Obtained from Connected and Autonomous Probes. *Sensors*, Vol 20, No. 17, pp. 4824.

Nam, D., Lavanya, R., Yang, I., Jayakrishnan, R. (2018). A Long Short-Term Memory Neural Network Approach for Traffic Density Estimation with Sensor-equipped Probe Vehicles. Proc. International Symposia of Transport Simulation (ISTS) and the International Workshop on Traffic Data Collection and its Standardisation (IWTDCS).

Nam, D., Lavanya, R., Yang, I., Jeon, W.H., Jayakrishnan, R. (2017). Traffic Density Estimation Method from Radar Sensor-equipped Probe Vehicles. Proc. ITS World Congress. 2017 Montreal.

Riju Lavanya, R. Jayakrishnan, “Dynamics of Speed Distributions from Microscopic Simulators In Comparison to Kinetic Theory of Traffic Flow,” (2005) Paper 05-2739, Proc. Transportation Research Board 2005 Annual Meeting, Washington D.C

Yue Zhang, MingJie Lai, Raymond Klefstad, Riju Lavanya, R. Jayakrishnan (2005), “A Distributed, Scalable, and Synchronized Framework for Large-Scale Microscopic Traffic Simulation,” Proc. The 8th International IEEE Conference on Intelligent Transportation Systems (ITSC), September 13-16, 2005, in Vienna, Austria

R. Jayakrishnan, Cristián E. Cortés, Riju Lavanya and Laia Pagès (2003). “Simulation of Urban Transportation Networks with Multiple Vehicle Classes and Services: Classifications, Functional Requirements and General-Purpose Modeling Schemes”. Paper presented at the 82nd Annual Transportation Research Board Meeting, January 11-16, 2003, Washington D.C.

R. Jayakrishnan, Cristián E. Cortés, Riju Lavanya and Laia Pagès (2003). “High-Coverage Point to Point Transit Systems: A New Design Concept and Simulation Evaluation of Operational Schemes. Paper presented at the Pan-American Conference and Workshop on the Interface between Automobile Traffic Networks under Dynamic Traffic Assignment and Bus Rapid Transit Systems", funded by the National Science Foundation, and the Puerto Rico Highway and Transportation Authority.

Cristián E. Cortés, Riju Lavanya, Jun-Seok Oh, and R. Jayakrishnan (2002) "A General-Purpose Methodology for Link Travel Time Estimation Using Multiple Point Detection of Traffic" Paper presented at the 81st Annual Transportation Research Board Meeting, January 13-17, 2002, Washington D.C. and accepted for publication in Transportation Research Record: Journal of the Transportation Research Board

Abstract

Disaggregate Control of Vehicles Using In-Vehicle Advisories and Peer-to-Peer Negotiations

By

Riju Lavanya

Doctor of Philosophy in Civil Engineering

University of California, Irvine, 2021

Professor R. Jayakrishnan, Chair

Traffic advisories to travelers are based upon traffic state information at the link level. This is due to existing infrastructure which sometimes can only provide link-level information. However, the primary justification for providing link-level data is the reluctance of Traffic Management Agencies to consider more detailed traffic state data for operational and safety reasons. However, with the advances in automotive technology, sensing equipment, and the Internet of Things (IoT), we can do better. Research shows that faster and more accurate travel paths can be obtained by using lane data rather than link data. Our contention is that for vehicles to be able to change lanes to improve their travel times, operationally, they would need to enter into Peer-to-Peer negotiations with surrounding vehicles, where they can trade their position in time and space in accordance to their own perceptions of their values of time and satisfaction and possibly in exchange for monetary benefits. Our work is an exploration of this idea.

We begin with a simple in-vehicle advisory control policy, partially inspired by the Kinetic theory of traffic. We then move towards an individual-level Peer-to-Peer negotiated lane change framework by first investigating its efficacy by means of microsimulation studies. We then

propose an agent-based optimization framework for this system, which minimizes both travel time and the ”envy” induced among drivers when they are assigned paths that are inferior to their peers. Numerical results from running our optimization on an illustrative network show that the proposed model converges to both envy-free and system optimum traffic states, even at a net zero budget, meaning this system can be used by transportation agencies without exacting tolls or giving subsidies.

Our proposed framework of routing vehicles on a lane to lane basis can only be realized in the field if the mediating agency (TMC, or a mobility service) has accurate information about traffic conditions. We propose multiple algorithms, including a LSTM (Long Short Term Memory) neural network architecture-based framework to estimate traffic states solely using information collected from sensor-equipped probe vehicles, without the need for any other data such as those obtained from traditional embedded loop detectors.

Chapter 1. Introduction

Government investment in infrastructure is a crucial indictaor of the health of a nation's economy and the well being of its people. Failure to invest in infrastructure gives rise to inequalities and inequities in both economic and social dimensions. In the US, the neoliberal movement of the last few decades has exacerbated the withdrawal of the government from what used to be its essential functions. Figure 1.1 depicts just one of many examples of this trend. These developments in the political economy of infrastructure have serious implications for transportation agencies, who will need to be more efficient with existing infrastructure and lower future budgets.

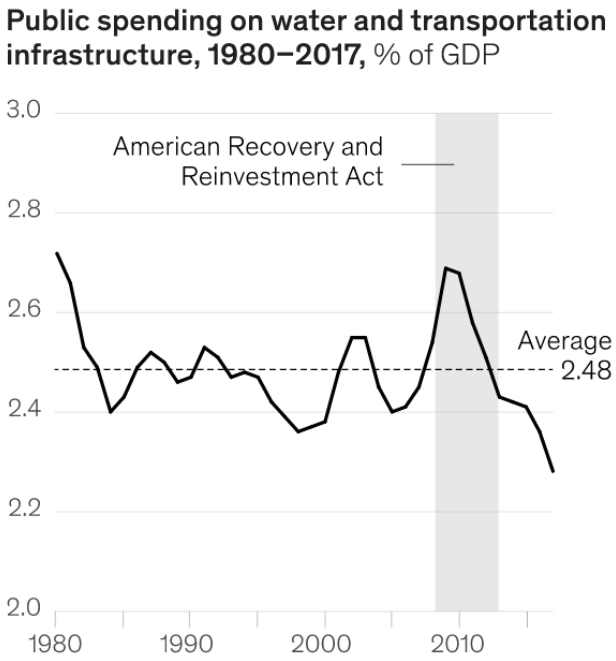

Figure 1.1 Public spending on infrastructure (Source: 2017 Report Card, ASCE)

At a basic level, it also spells the death of the idea that agencies can build their way out of congestion. The appetite for investing in massive capital projects, such as new highways, is low.

The very places where urban congestion is at its worst are also the places where land values are the highest, making it prohibitively expensive to purchase land for constructing additional highway capacity.

Therefore, it is crucial to make efficient utilization of the existing transportation capacity. Advancements in computing, sensor, wireless, and autonomous vehicle technologies over the last decade can be leveraged to develop smart mobility systems that can relieve traffic congestion by making more efficient use of the existing road capacity. One of the consequences of these technological advances has been the gradual shift of modern traffic control approaches from centralized/aggregate to decentralized/disaggregate control. Centralized control applications have a single system controller that computes the inputs and control actions. Even if a centralized system contains subsystems, in the end it is the system controller that determines the control actions of its subsystems. Centralized systems suffer from the usual problems of scalability and robustness, especially as the system becomes large. On the other hand, decentralized and distributed control systems have their control actions distributed over various independent or quasi-independent subsystems that use local measurements as their inputs. The control of Connected and Autonomous Vehicles (CAVs) falls under the broad umbrella of distributed control, and is widely expected to yield dividends in the future in terms of efficient use of highway capacity.

1.1 Motivation

There is a significant body of literature on the control of CAVs to improve system performance. We present a review of the control methodologies in later chapters, but we note here that the basic goal of these frameworks is systemic benefits. These are good for society in the long run (speed

harmonization, lower emissions, etc.) but individual users are not able to directly perceive benefits specific to them, making it near impossible to achieve compliance. In other words, even if a driver knows that slowing down their car by a few miles per hour could result in a traffic condition that would be ultimately beneficial for all, they may still not want to slow down because they prioritize their individual short-term incentives. This also means that most CAV control frameworks are more appropriate for companies that own large fleets of vehicles that they can have absolute control over. Indeed, one of the most promising avenues for CAVs to be fully functional in the real world is in the field of freight and logistics.

Furthermore, these frameworks do not lend themselves naturally to MaaS (Mobility as a Service) platforms where individual characteristics like Value of Time can be leveraged to provide real time path choices, based on tailor-made incentives. Therefore, there exists an opportunity for mobility services to leverage information about user heterogeneity and traffic conditions at the most granular level.

It is evident that not all lanes in traffic move at the same speed. Drivers often change lanes when they perceive that their current lane is slower than their adjacent lane, to avoid incidents and road hazards, or to get to their destination faster. The California Department of Transportation (Caltrans) operates a web-based software tool called PeMS (Performance Measurement System) for collecting and analyzing various traffic data from detectors installed on highways throughout California. For some freeway facilities in California, PeMS provides traffic data at the lane level. (Miller 2008) analyzed PeMS data to show that faster and more accurate travel paths can be obtained by using lane data rather than link data. They also show that if vehicles can be routed by to make optimal lane changes, travel time savings as high as 33% can be achieved.

Consider a two-lane freeway stretch, shown in Figure 1.2, composed of several segments, and a vehicle traveling from ingress I to egress E. A possible "lane-path" for the vehicle could be *2r-3r-4r-5l-6r* (where *l* denotes the left lane and *r* denotes the right lane).

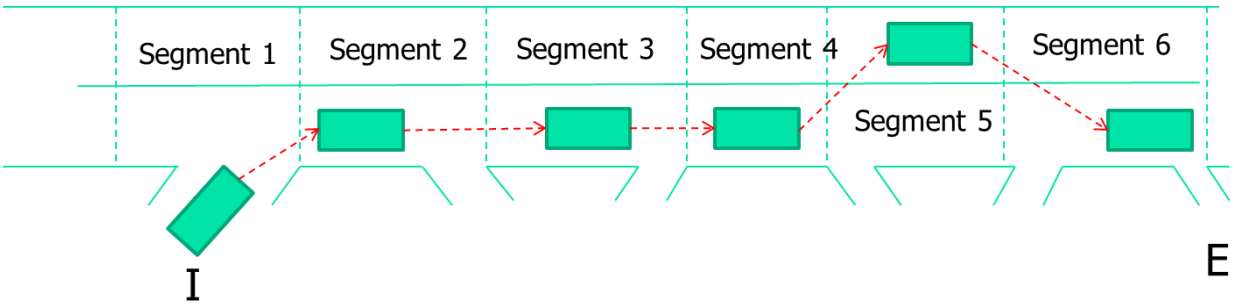

Figure 1.2 A possible lane-path on a freeway stretch between I and E

We can also envision an alternative lane-path, *2r-3l-4r-5l-6r* as shown in Figure 1.3.

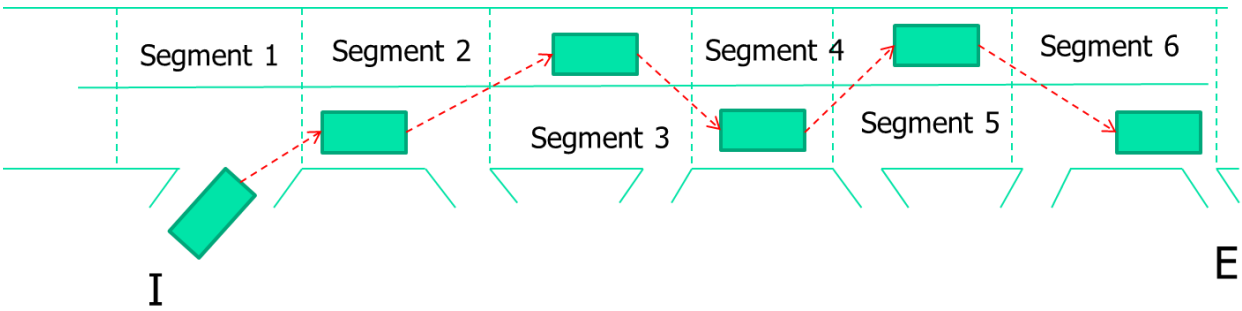

Figure 1.3 Alternative lane-path between I and E

Of course, in real traffic, it is not always possible for vehicles to make optimal lane changes throughout the course of their travel, but the kernel of the idea remains. What if vehicles could be routed at the lane level? What would such a system look like?

1.2 Revisiting First-In First-Out (FIFO) Assumptions

Our contention is that for vehicles to be able to change lanes to improve their travel times, operationally, they would need to enter into negotiations with surrounding vehicles. This prompts us to reconsider the very idea of the traditional First-Come First Served (FCFS) nature of transportation supply (Lloret-Batlle and Jayakrishnan, 2016; Lloret Batlle, 2017).

Conventional transportation paradigms only consider the built physical infrastructure as part of the transportation supply. However, even a vehicle traveling on a road segment has something to offer: its position in the time-space region it currently occupies. A classic example of this idea in practice is of a vehicle traveling slower than the average traffic speed delaying all vehicles behind it. A less obvious, but equally interesting example is of a vehicle traveling comfortably at average traffic speed "delaying" another vehicle behind it simply because the vehicle behind wishes to travel faster. This may be due to several reasons: the vehicle behind it might have an emergency, or its driver might have a higher value of time and values travel delays more than the driver in front. If we consider the different Values of Time (VOTs) of the vehicle drivers, clearly the overall system would improve if the two vehicles could switch their positions. The vehicle with the higher VOT now experiences less time delay and the vehicle with a lower VOT experiences more time delay (but valued at a lower rate). This also implies that the vehicle agreeing to sacrifice their position in time and space and accepting higher delays would need to be compensated in some manner.

Complex negotiations between human drivers have not been possible in the past due to safety reasons but advances in automotive, sensor, and wireless communication technologies give us an opportunity to revisit this fundamental assumption. In this environment, such ad hoc collaborative negotiations are possible and may even become necessary, for example, in disaster routing

scenarios. The focus of our research is to establish a framework under which vehicles can collaboratively perform lane-changing maneuvers and "trade" their supply (position in a queue) to others in exchange for payments, all in the service of certain system goals of society, network operating agencies, and other stakeholders.

1.3 Need for Independent Sources of Traffic Data

The American Society of Civil Engineers, in their annual report card for the country's infrastructure, state that as much as 43% of the country's roads are in poor or mediocre condition. Ths represents a challenge to traffic management agencies who primarily rely upon detectors embedded in roads to obtain traffic data that is used to control traffic. Furthermore, it raises questions regarding the accuracy of the data obtained from traditional detectors. More accurate density estimation technologies are needed to effectively utilize data from alternate sources of traffic data, which do not depend on expensive and invasive infrastructure such as loop detectors. Sensor equipped probe vehicles that estimate traffic density are expected to play an important role in improving the accuracy of road congestion mitigation techniques. A significant contribution of this dissertation is the development of sensor-based traffic state estimation methodologies that can act in concert with our proposed real-time lane negotiation framework to route vehicles more efficiently.

1.4 Dissertation Outline

The dissertation is organized as follows:

Chapter 2 provides our first attempt at moving towards a more disaggregate control approach by means of speed advisories to separate classes of vehicles, categorized by their speed. This approach

was inspired by Kinetic theory of traffic, a statistical traffic flow model. We present a study that validates the parameters of this model using microsimulation, and propose a basic variable speed limit control method.

Chapter 3 contains a review of existing CAV control methodologies, including cooperative driving and lane change control methods. We present a simulation framework in which we study the effects of our proposed lane change negotiations on traffic on network performance.

Motivated by the results obtained in chapter 3, we provide an optimization framework for these lane change negotiations using a dynamic traffic assignment model in chapter 4. We describe the network transformation in a prescribed lane change environment and discuss the optimization results, both in terms of traffic and in terms of social incentives to users who yield their way for higher VOT vehicles.

We present a traffic-estimation framework in Chapter 5 that would enable the deployment of our prescribed lane negotiations in the field. We present a deep-learning technique used to estimate traffic conditions using data obtained from sensors embedded in proble vehicles.

Finally, chapter 6 provides a summary of the conclusions and directions for future research.

Chapter 2. Dynamics of Speed Distributions from Microscopic Simulators

This chapter provides a preliminary approach to traffic control using speed advisories that are disaggregated by classes of vehicles, instead of the traditional speed advisories which provide the same information to all vehicles. We provide a discussion of the kinetic theory of traffic, evaluate its suitability in a microsimulation context, and describe a simple open-loop speed control study. This represents our first attempt at speed control, before we proceed to agent based simulation approaches that are described in the subsequent chapters.

Ever since (Prigogine and Herman, 1971) outlined a Boltzmann-like statistical approach to traffic flow there has been sustained interest in the scientific community for developing new and improved kinetic theory models. Most, if not all, gas kinetic models cannot be described purely as microscopic, mesoscopic, or macroscopic in nature. These models, in their essence, attempt to describe the change in speed distributions of vehicles in traffic with respect to time and space.

Information about speed distributions can be used by the traffic management agency for, say, formulating a traffic control policy. But before that happens, it would first be necessary to observe how vehicles are distributed in different speed classes, and to understand how these distributions change spatially and dynamically. Very few studies have been performed that have attempted to evaluate or calibrate these models. This is perhaps due to the requirements of the huge data set needed for such a study. One would require data on individual vehicle speeds at different traffic densities, levels of congestion, road geometry, and at various places on the network. This is prohibitively expensive, and perhaps virtually impossible. In addition, the theoretical models have

generally been developed for idealized traffic, and the applicability of kinetic theory models to complex traffic scenarios such as under different control strategies such as speed control, lane usage control, etc, as well as under realistic geometric situations and traffic vehicle mixes are all open topics. It is clear that validating kinetic theory models or their future extensions with real world data under more complex traffic scenarios is probably not a viable idea. In this chapter, we make an initial attempt at examining whether detailed simulation data could be used for such purposes.

Due to the developments in computing technology it is now possible to simulate large networks using microsimulation. Their detail-oriented design makes it easier to evaluate different traffic scenarios and add multiple modeling contexts. It is also possible to obtain traffic information from individual vehicles throughout the course of the simulation. Most microsimulation models have been validated and calibrated for different network contexts, and although such calibration studies are limited in scope, deviations from ground truth traffic data have been found to be acceptable, within limits. The kinetic theory characteristics of traffic simulated by the commonly used microsimulators have rarely been examined in the past. In this chapter, we report the initial results from such a study. The intent is to make an initial attempt at assessing whether microsimulators are useful at all in reverse-validation of kinetic theory models and premises under realistic traffic scenarios. For reasons outlined above microscopic simulation is chosen to be the tool for performing this study.

We use microscopic simulation with different commercial software to determine speed distributions along a simple stretch of a multi-lane freeway stretch and make an exploratory comparison with the results obtained from kinetic theory. The premise behind the study is that

microsimulators need to first pass the test in replicating at least some of the traffic behaviors predicted by basic kinetic theory under simple scenarios, before we can even consider the case of using them to model the speed distribution characteristics under complex scenarios in the future.

2.1 Background

After the seminal work by Prigogine and Herman, a number of researchers have improved upon the basic kinetic theory model. Notable among those are (Paveri-Fontana, 1975) who postulated a desired speed distribution that is not constant. (Nelson, 1995) introduced the concept of a mechanical model to describe car following behavior and a correlation model to describe the follower-leader pairwise distribution. In recent years there has been renewed interest in kinetic theory of traffic, particularly in the scientific community. (Hoogendoorn and Bovy, 1998) developed multi-class gas-kinetic models by introducing the concept of "Multiclass Phase-Space-Density." (Helbing, 1996) developed a gas-kinetic model similar to (Hoogendoorn and Bovy, 1998), but with additional terms such as a velocity diffusion term, a lane-changing term, and multiple entry and exits. (Treiber et al., 1999) derive a gas-kinetic model based on an underlying microscopic traffic model and include a discussion on its calibration.

A limited number of studies have been performed to analyze the speed distributions observed in traffic. (Edie et al., 1980) use observational data from the New Jersey Turnpike to study speed distributions. For different values of traffic densities, they calibrate a parameter β, which is a combination of passing probability P and relaxation time constant T found in the basic kinetic theory equations. They also estimate τ, the relaxation time, found to lie between 7 and 20

seconds. (Gafarian et al., 1971) performed an experimental validation of the Prigogine-Herman model using the Bureau of Public Roads data. They concluded that their results did not agree with the basic kinetic theory equations.

Any speed distribution could be divided into histograms to see how many vehicles lie in a particular speed interval. This leads to a discussion of (Prigogine and Herman, 1971) model of traffic flow that is similar to the kinetic theory of gases and develops relationships for the time evolution of the speed distribution $f(x, v, t)$ for density *k(t)*. The model is composed of three separate processes: relaxation, interaction and the adjustment process. The change in the speed distribution is described as:

$$\left(\frac{\partial f}{\partial t}\right) = \left(\frac{\partial f}{\partial t}\right)_{relaxation} + \left(\frac{\partial f}{\partial t}\right)_{interaction} + \left(\frac{\partial f}{\partial t}\right)_{adjustment} \tag{2.1}$$

$$= \frac{-(f - f_0)}{T} + \quad (1 - P)k(\overline{v} - v)f \quad + \quad \lambda(1 - P)k[\delta(v - \overline{v}) - f]$$

where

$f(x, v, t)$: number of vehicles per unit length of the highway at *(x,t)* in the speed range *(v, v + dv)*

f_0 : desired speed distribution,

$\overline{v}$: mean speed, variable function of time and space

k : density, variable function of time and space

(1 – P) : probability that a potential interaction between a fast moving car and a slow moving car occurs, resulting in the fast car having to adopt the speed of the slow car.

λ : a constant parameter for the adjustment term,

$\delta()$: Dirac-delta function

Relaxation term: If the speed distribution changes it has a tendency to "relax" to a "desired" speed distribution. The relaxation term captures this effect. By looking at the nature of this function we can see that an exponential relaxation rate over time is assumed. Figure 1 illustrates how traffic at time *t* is trying to eventually relax to a certain desired speed distribution.

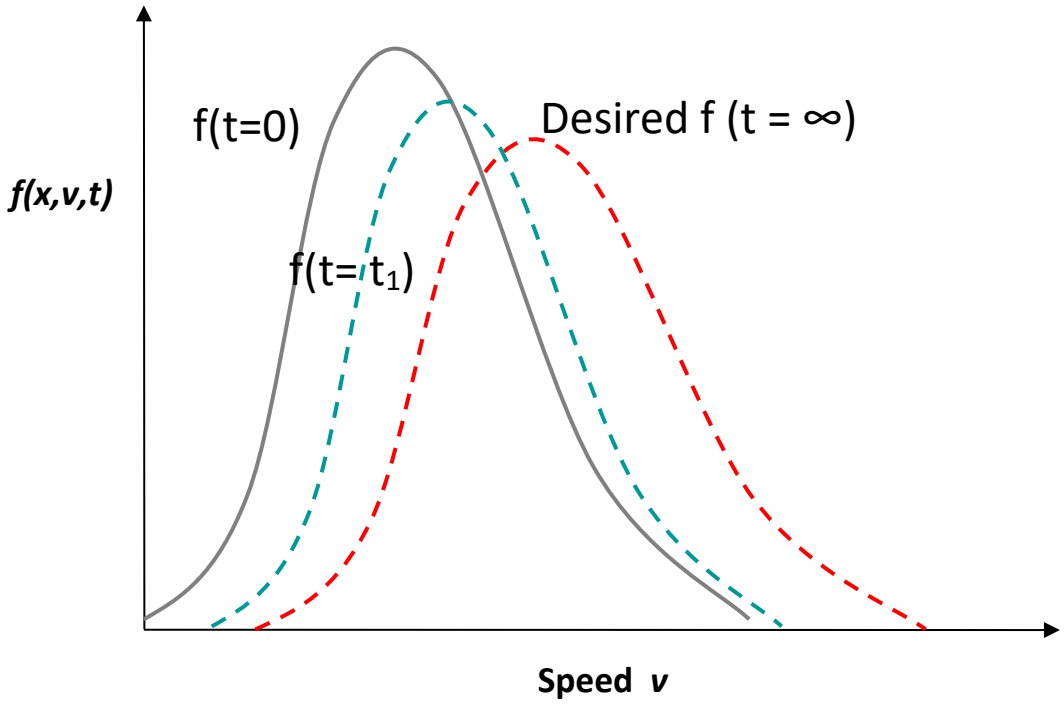

Figure 2.1 Time dynamics of speed distributions under relaxation

Interaction term: This represents the number of vehicles affected by a given car traveling at a particular speed and location in a small time interval. This effect is two-fold; i.e. it represents the interaction of vehicles that are slowed down because of a speed v_0 and the interaction of the vehicles traveling at lower speed that cause the vehicles traveling at v_0 to slow down. The combined effect is described by the second term of equation 1.

Adjustment term: This term was added later to account for the collective local effect where traffic tends to adjust the speeds to the local average speed. This term attempts to capture the platooning behavior due to local speed conditions.

Some of the parameters in the above expression have not been adequately defined. This is one of the reasons why very few studies have been undertaken to validate the above model with any data; real or simulated. For the same reason, those studies have treated the change in the speed distribution as a whole, without isolating the individual components involved. We will focus upon a preliminary investigation of only the first term, i.e. relaxation term in the above expression.

2.2 Inherent Stochasticity in Kinetic Theory Characteristics

Any microscopic simulation study needs to use multiple simulations due to the stochasticity of the results. This is even more important in the current study where we look at the stochasticity of an extremely specific aspect of the simulation, the dynamics of the speed distributions over small time periods (say tens of seconds) over small stretches of highways (say 0.1 miles). Thus, there is a natural reason for performing a large number of simulation runs. Note that speed distributions are the cornerstone of the kinetic theory model. The very word "distributions" implies stochasticity and the speed distribution function is nothing but the *expected* number of vehicles in a certain speed range at any given point in time and space. When the study is based on the vehicle speeds over small stretches over small time periods, as required here, the stochasticity in the simulation results is much more than when we look at aggregated simulation results such as section densities or average flows.

We consider it important to stress this topic in this section, as there is hardly much existing literature that specifically points to the need for large data sets (from the real world or from simulation) to properly make conclusions on distribution dynamics as presumed in kinetic theory. The discussion here is intended both to show the results of the study as well as to bring out the fact that simulations need to be replicated a large number of times and that any real-world data would also correspondingly have to be large to see any identifiable distribution dynamics over short time periods.

For the above reason it is clear that the study needs to sample the data from a large number of simulations, each with the same set of initial conditions but with different seed value for the random number generators in the simulation model, fixed at the beginning of each simulation. Multiple simulations would effectively bring out the stochasticity in traffic evolution and would give more robust values for the traffic properties of interest (speed distribution dynamics, in this case). The number of simulations has to be calculated based upon the variance of the traffic counts in each time step, and the desired value of tolerance and confidence interval.

We used a simple freeway section to simulate different scenarios to obtain f and f_0 distributions at different times and for different locations. The study site for the analysis is a stretch of Interstate freeway 405, Irvine, California. Figure 2.2 shows the stretch of freeway. The freeway section is northbound direction from Jeffrey to Culver. The simulation was based on traffic input volumes matching the measurements from actual freeway detectors using the capabilities in the ATMIS Research Testbed at University of California, Irvine.

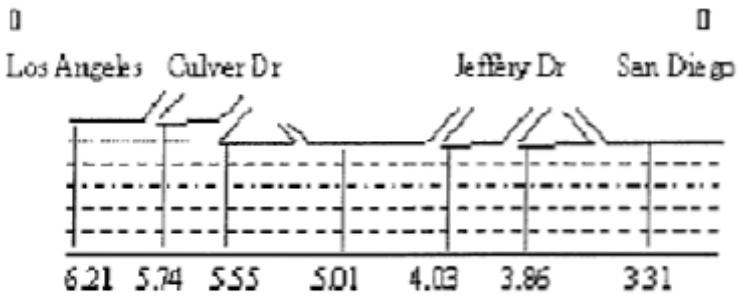

Figure 2.2 Section of the 405-freeway used for simulation

For each specific location and for various time instants, the number of vehicles in each speed class was counted. This poses a practical problem. Since the kinetic model involves a derivative with respect to time, we cannot evaluate the speed distributions with time instants spaced far apart. For instance, calculating the changed in the speed distribution every 5 minutes would destroy the continuity of f, and also ignore any temporal variations that occur during the interval. On the other hand, choosing a small time interval would mean that, for a particular instant, very few - or in some cases even zero - vehicles are captured in each speed class. The speed distribution, in that case, would be unfit for any analysis. These are two conflicting objectives. To solve this apparent conflict, we used a large number of simulation runs with very small time intervals of gathering data. This ensures both continuity and reasonable number of vehicles in each speed class.

Based upon a specified level of tolerance and the calculated standard deviation of vehicle counts in different categories, the sample size, i.e. the number of simulations required, was calculated. The number of simulations required for different values of the time-aggregation interval for two different microscopic simulators used for this study (the next section discusses these models) range from around 30 when the aggregation interval is 60 seconds to around 1000 when the aggregation interval reduces to 1 second. This is intuitive because, as the aggregation time interval decreases, the number of "captured" vehicles that are present in each category also decreases. This makes the

data fluctuate a lot, thus, necessitating a large number of simulations to "smooth" out the data. Both PARAMICS and AIMSUN give, roughly the same numbers.

2.3 Using Different Simulation Software

The initial intuition in a study like this would be to consider developing a simple microscopic simulator using a car-following model and a lane changing model. While this would be a "cleaner" and simpler way to study the speed distribution dynamics, it would defeat the purpose behind this study, in that validating kinetic theory with a simple microscopic model is not the intent. The objective is to examine whether a comprehensive microscopic simulator would yield behavior as predicted by kinetic theory (though such prediction is possible only for simpler scenarios), so that we could make some conclusions on whether data can be developed to validate extensions of kinetic theory for complex and detailed traffic scenarios using such comprehensive models which include several additional microscopic behaviors such as lane choice, route choice, multiple vehicle classes, etc. For this reason, it was considered more appropriate to select two widely used microscopic simulators – PARAMICS (Cameron and Duncan, 1996) and AIMSUN (Barceló et al., 1999). The two models also have somewhat different microscopic models in them, along with differences in other details such as the simulation time step length. A brief description of these models is presented below.

PARAMICS: This software package was developed at the Edinburgh Parallel Computing Center at the University of Edinburgh in Scotland, is a suite of software tools for microscopic traffic simulation of congested traffic networks. Individual vehicles are modeled in detail for the duration

of their entire trip, providing dynamic information about traffic, transit time, and congestion. The PARAMICS model has been validated for a number of data sets in the UK as well as US.

The car-following model in PARAMICS is derived from the psycho-physical car-following model by (Fritszhe, 1994), and incorporates a number of behavioral assumptions, among those are that speed differences between vehicles are not easily perceptible by drivers unless they are more than a certain threshold. In addition the model also specifies other thresholds that belong to the following driver's phase-space. The model itself does not have an easy closed form to reproduce here, however the main variables involved are:

- AD, the desired separation between the leading and following car.
- AR, the "risky" distance, at which the drivers decelerate to avoid collisions.
- AS, the "safe" distance at which the following car still accelerates.
- AB, the braking distance needed to avoid any potential collisions.

The psycho-physical car-following model in PARAMICS, which is similar to what is used in other commercial microsimulators as well, may be contrasted with a "more traditional" model, as used in the AIMSUN model described next.

AIMSUN2: This package is part of GETRAM (Generic Environment for Traffic Analysis and Modeling), which is a simulation environment comprising a traffic network graphic editor (TEDI), a microscopic traffic simulator (AIMSUN2), a network data base, a module for storing results, and an Application Programming Interface (API) to aid with interfacing the simulator to any user-specified application (for example, a emission model or a vehicle routing routine).

AIMSUN2 was used in a pilot study of traffic management schemes on an environmental cell for the city of Dublin. Measured flows and speeds were used as calibration variables. The Center for Transportation Studies of the University of Minnesota used AIMSUN2 in a simulation study of the I-494 freeway in Minneapolis where AIMSUN2 was calibrated and validated against the flow and speed values provided by freeway detectors.

The car-following model in AIMSUN is based on the well-known (Gipps, 1981) microsimulation model. The main behavioral assumption in this model is that the vehicle chooses its speed such that it can come to a complete stop safely, if the vehicle ahead of it suddenly stops. Mathematically, the model can be described by the following equation.

$$v_n(t+T) = v_n(t) + 2.5a_nT(1 - v_n(t)/V_n)(0.025 + v_n(t)/V_n)^{1/2} \quad (2)$$

Where:

a_n is the maximum desired acceleration of vehicle *n*

V_n is the desired speed of vehicle *n*

$v_n(t)$ is the speed of vehicle *n* at time *t*

T is the value of reaction time for all vehicles

The two simulation models were determined to be adequate for an initial comparison of how the individual vehicle behavior from two essentially different microscopic models (the psycho-physical model in PARAMICS and the Gipps model in AIMSUN) yield collective speed distribution dynamics as in the kinetic theory. We leave out a discussion of the lane-changing

dynamics, as both models use somewhat ad hoc models for lane-changing for which the current state-of-art is limited, as far as theoretical soundness is concerned. In any case, it is also deemed that the relaxation behavior that we focus on is much less affected by the lane-changing dynamics than the interaction behavior in Kinetic theory, which is left for a more involved subsequent study.

Both AIMSUN and PARAMICS have ways to model their underlying speed distributions. For instance, in PARAMICS, the vehicles travel at speeds that are consistent with their level of aggression, which is set to be normally distributed across the driving population. This is a realistic assumption, and we expect such models of speed distribution to be present in one form or the other, in most microsimulators. These underlying speed distributions may be thought of as "desired" speed distributions since this is how the vehicles travel in free-flow conditions. It is evident that the exact nature of relaxation and the final "relaxed" distribution will depend on the assumed "desired" distribution embedded in the simulator, but how fast this relaxation is achieved may be more dependent on the car-following model parameters that govern these simulations. For the purposes of our study we used the default speed distributions in both PARAMICS and AIMSUN.

The simulation set up for this experiment was similar to that described in the earlier section. Speed distributions were obtained every 5 seconds. This was also the length of the "time-window" used to collect probe data from the simulation. The probe data set corresponds to the vehicles that are tagged when they cross certain predefined points on the network. Since, for the purposes of this study we are only interested in exploring the relaxation in further detail, we chose the level of the demand to be very low – in effect, increasing the headway at the beginning section, and removing most "interactions" from the process. Thus, any change in the speed distribution may be reasonably attributed to the relaxation term in the kinetic equation. Also, in order to further see the effect of

relaxation we introduce a lower speed limit on a particular link for a certain time. After that time the speed limit is relaxed and the vehicles accelerate, presumably towards their desired speed distributions.

The time period of the simulation was 80 minutes. The first set of simulation runs was to obtain reasonable estimates for desired speed distribution, and thus the demand level was chosen to be low and the corresponding headway was set at a high value. In the second set of simulations, to observe a "relaxation" effect, the speed limit of a link was set at 35 mph for the first 20 minutes of the simulation. After the twenty minutes, this speed limit was relaxed and the vehicles were free to travel at their desired speeds. With respect to data, our main interest was the few time steps after relaxing the speed limit at that location. The values of $f\text{-}f_0$ and rate of change of f were computed for that particular time interval. Assuming the relaxation law postulated by Prigogine and Herman, a linear regression was then performed, with the dependent variables being discrete values of $\Delta f/\Delta t$ and the independent variables being the discrete values for $(f\text{-}f_0)$.

The estimated time constant, which can be thought of as the time taken by $1/e^{th}$ of the vehicles to achieve their desired speed distribution when passing probability is 0.5, is shown in the following table. These values are in agreement with the estimated time constant values obtained by (Edie et al., 1980).

Table 1 Estimated value of Time Constant for different speed classes

	Relaxation time constant (seconds)

Speed Class	PARAMICS	AIMSUN
50-55 mph	12.21	14.33
55-60 mph	22.07	19.20
60-65 mph	28.87	30.53

The following figures illustrate the variation of the distribution functions for different speed classes, during the few time steps right after the speed limit of 35mph was removed.

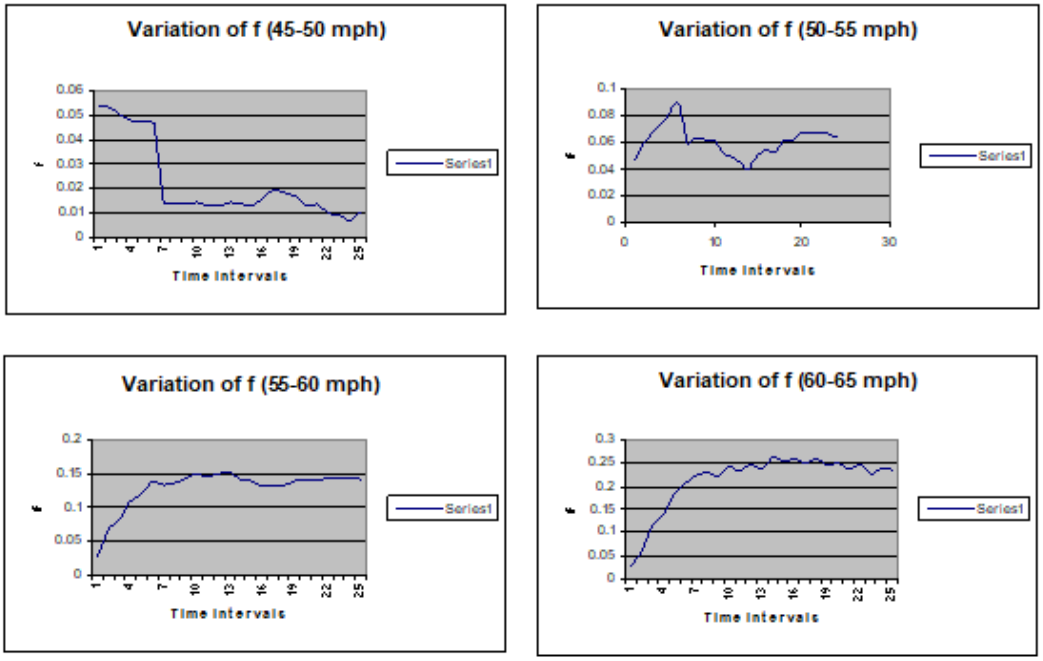

Figure 2.3 Variation of speed distributions after speed relaxation (PARAMICS)

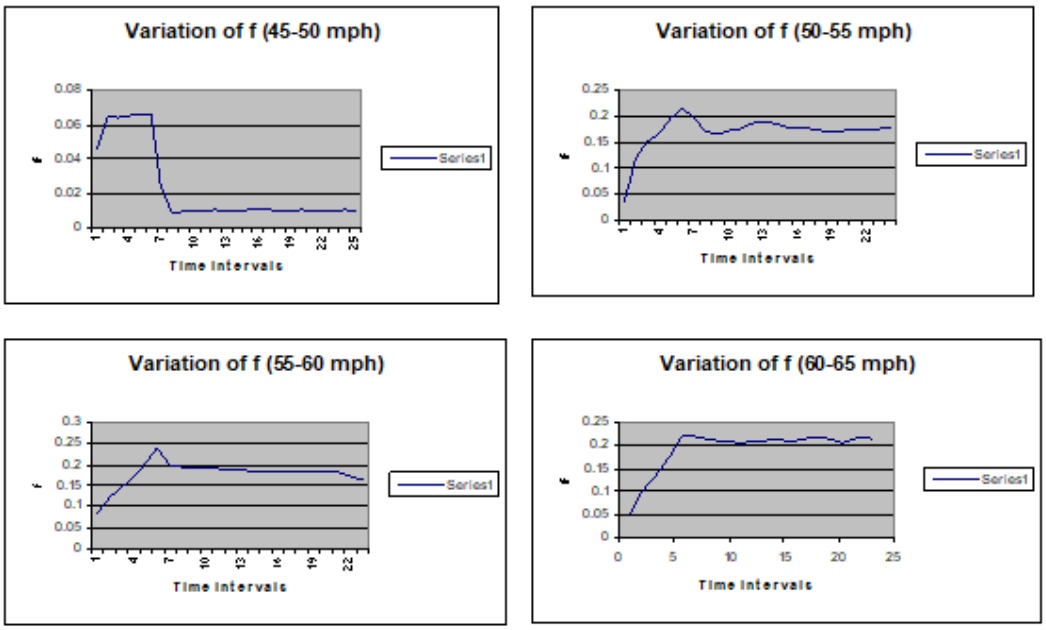

Figure 2.4 Variation of speed distributions after speed limit relaxation (AIMSUN)

As can be seen from the figures above, both simulation models perform similarly, and, except for the 50-55mph case in PARAMICS, all distributions do seem to relax to a near-constant value. However, it is interesting to see that even after a great number of simulations there is still an oscillatory behavior, even though its amplitude is small. To our knowledge, such behavior is not predicted by existing kinetic theory models and perhaps may point to certain additional aspects that still need to be included in kinetic theory models. We also see that this oscillatory behavior appears significant even after aggregation is performed to smooth the data. In fact, this oscillatory behavior is pronounced when the aggregation interval is reduced to one second, even when the number of simulations exceeds 1000. Note that the speed distributions still relax quickly in each case. The oscillations could be due to "overreaction" and "underreaction" by vehicles in each speed class. For instance, a vehicle traveling in the 40-45 mph speed range, desiring to travel in

the 45-50 mph range, may jump into a higher speed class before relaxing towards its desired speed range.

The interaction term was estimated using the same simulation setup as earlier, except that the traffic condition was chosen to be free flow conditions, without any incidents. This ensures that the effect from relaxation term in the equation is minimized, and any speed distribution change would be coming from the interaction term. Simulation runs were performed for different densities. The following figures show the estimated passing probabilities for different density values.

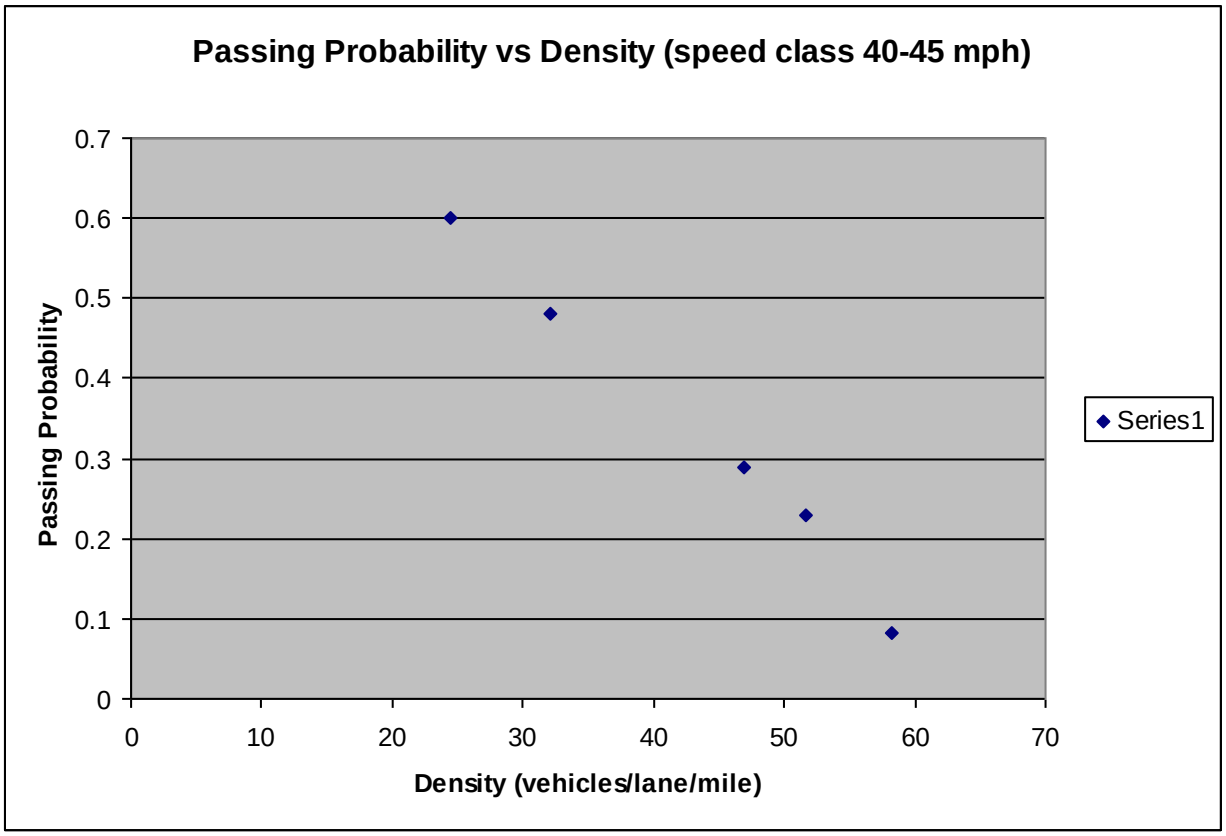

Figure 2.5 Passing probabilities vs density (speed class 40-45 mph)

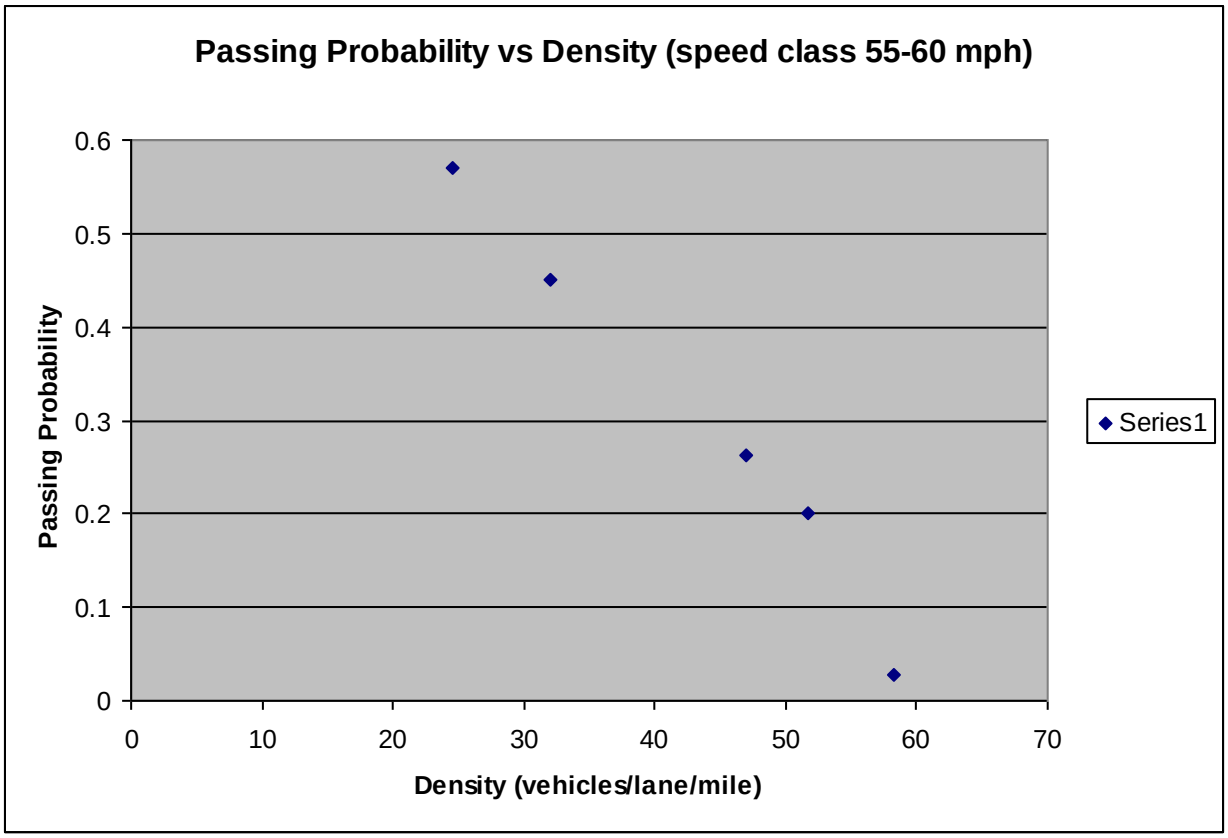

Figure 2.6 Passing probabilities vs density (speed class 55-60 mph)

That both the models showed this characteristic shows the promise of this approach of studying kinetic theory behavior of traffic. It is possible that there is a "collective" over-reaction and associated oscillation that happens in traffic during the relaxation behavior, especially at higher speed ranges in the distribution, which is something not addressed in current literature. One could postulate that vehicles speed up and raise the distribution value at higher speeds, and then reduces their speed. Due to the speed limits, the speed up happens only to a few speed ranges, whereas the speed reduction happens to many other speed ranges, thus the oscillations not being seen clearly at the lower speed ranges. Clearly, much further examination is needed to identify the reasons

behind it or to develop extended kinetic models that show such behavior. It is fair to say that the clear conclusion is the need to start identifying such details that get muddled under stochasticity in traffic. This would require conducting studies with large numbers of replications– which would be impossible in the real world but quite practical in simulations.

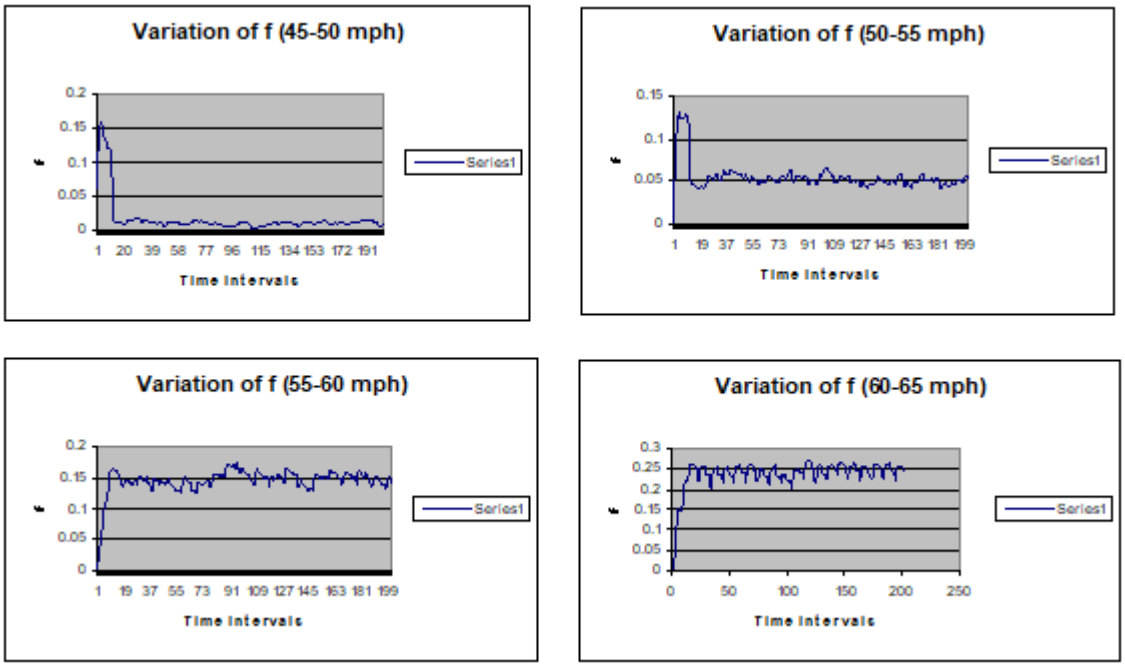

Figure 2.7 Variation of speed distributions (1000 simulations, 1 second aggregation interval)

2.4 A Simple Variable Speed Control

Based upon the idea of an ideal speed distribution as postulated by kinetic theory models and the propensity to relax to that distribution, we devise a simple speed advisory, graphically depicted in the following figure. In effect, we replace the ideal speed distribution with our own desired speed

distribution. In practice, this desired speed distribution can be calculated by the traffic controller using historical data, or postulated to serve certain objectives (traffic calming, for instance).

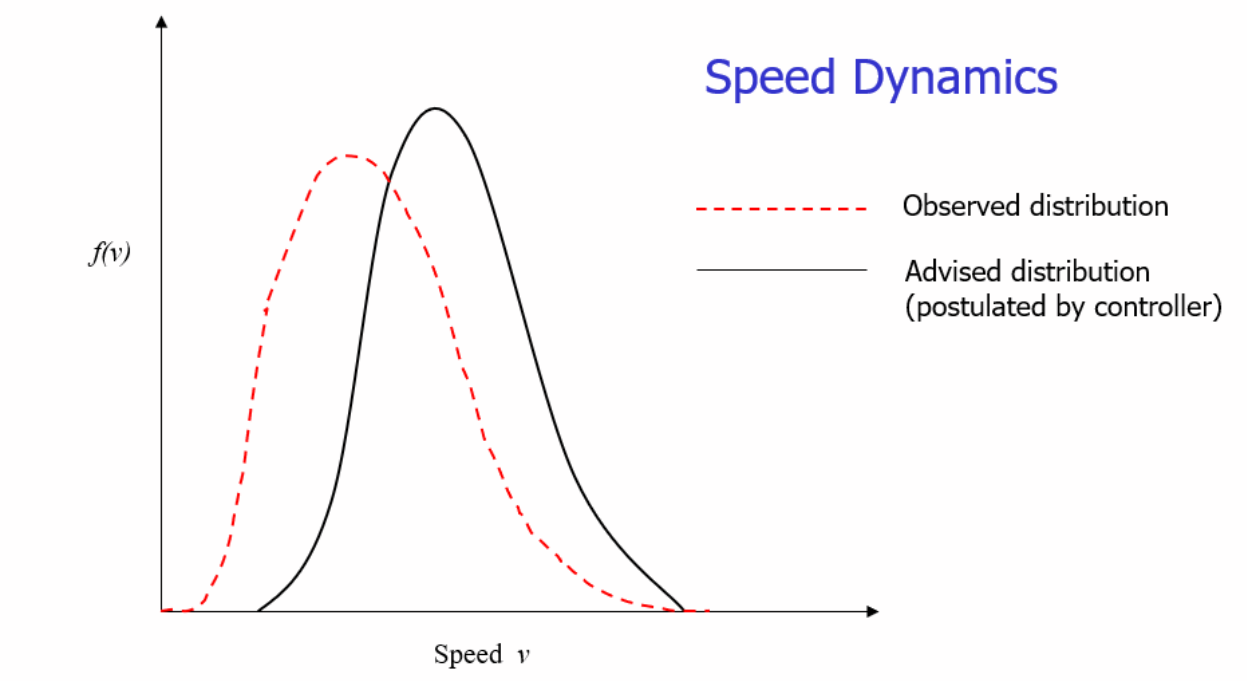

Figure 2.8 Observed distribution vs Advised speed distribution

The speed advisory mechanism is as follows.

1. Postulate a desired speed distribution (candidates can be uniform or triangular distributions)

2. Each vehicle in a speed class is shown the same information (which is the target speed for that class obtained from the desired speed distribution)

3. Vehicles in a speed class change to the advised speed class with a compliance rate *c*

The simulation setup for this experiment in PARAMICS was as described in previous sections and the same road stretch was used as before. The total travel time and throughput was calculated for each simulation run, with varying levels of compliance. Results show an improvement over the base case for both travel time and throughput. At a compliance rate of 25%, a modest travel time improvement of approximately 2% and a throughput improvement of 3.8% were observed, with the values increasing with more compliance.

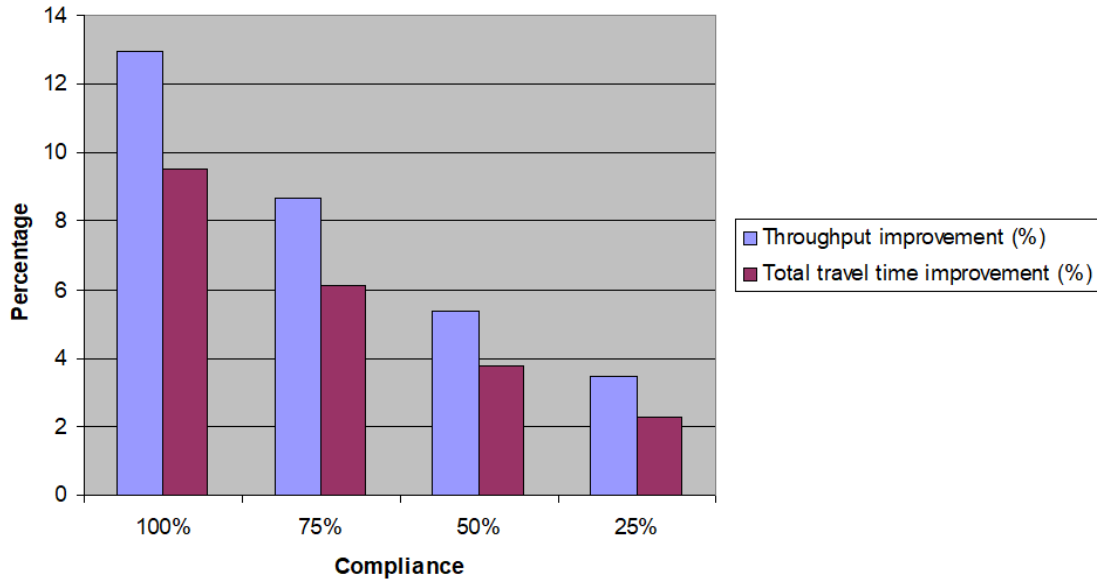

Figure 2.9 Network Performance Results

2.5 Conclusions

The understanding of speed distributions in traffic would be useful for traffic management agencies in formulating control policies to reduce congestion. This would require development of more complex extensions of the kinetic theory models to handle the details of real networks and

realistic traffic. Developing extensions of kinetic theory and perhaps even traffic control and management policies based on kinetic theory models is a possibility for the future. In the absence of real-world data to examine stochastic speed distribution dynamics, microscopic simulation is an attractive option if the results show behavior not counter to what the theory predicts. This is a preliminary study that uses different microsimulation models to investigate speed distributions in traffic, and their variation with respect to time Since it is not possible to obtain meaningful instantaneous point data (large enough so that density and flow can be considered continuous functions, but small enough so that they do not lose their temporal nature) on vehicle speeds in real life, microsimulation seems to be the only tool to analyze these models.

Some comparisons are made with the results obtained from the kinetic theory of traffic proposed by Prigogine and Herman. Due to lack of suitable data and benchmark results it is difficult to observe all the components of the kinetic theory model; however, the easiest terms to observe are the relaxation term and the interaction term.

Encouraged by the results showing a degree of compatibility of simulation software with kinetic theory models, we devised a simple speed advisory given to vehicles in various speed classes and were able to observe modest improvements in the values of total travel time and throughput. The next chapter introduces the idea of agent-based simulation models and an envy-based paradigm used to compare vehicle routes.

Chapter 3. Modern Approaches of Vehicle Control

3.1 Introduction

In the previous chapter we analyzed the possibility of controlling traffic by relaying information to classes of vehicles through in-vehicle advisories, which marked a departure from the traditional CMS-based control that provided the same information to every vehicle on the road. Inherent, still, is a basic assumption that traffic advisories to travelers are based upon traffic state information at the link level. This is due to existing infrastructure which sometimes can only provide link-level information. However, the primary justification for providing link-level data is the reluctance of Traffic Management Agencies (TMCs) to consider more detailed traffic state data for (understandably) operational and safety reasons. However, with the advances in automotive technology, sensing equipment, and the Internet of Things (IoT), we can do better. Due to advancements in computing technology, wireless communications, and modern automative technology, there has been an explosion in research efforts devoted to Connected and automated vehicles (CAVs). Although the idea of automated highway systems goes back to the California PATH (Partners for Advanced Transit and Highways) program in the late 1980s, it is only now that autonomous vehicle control methodologies can be reasonably expected to be implemented in the real world. CAVs have the potential to improve traffic safety, reduce fuel consumption and emissions, increase throughput, reduce headways, and relieve traffic congestion.

In this chapter, we present a literature review of the various forms of control methodologies in a CAV context, propose our methodology based on peer-to-peer negotations, and present a proof of concept of our method by means of a simulation study.

3.2 Control of Connected and Autonomous vehicles: Literature Review

Real-time control of CAVs can be broadly divided into the following categories:

3.2.1 Powertrain control

This refers to the control of power demand for vehicle motion. This includes the control of vehicle components such as the internal combustion engine, transmission, gears, brakes, and so on. The purpose of such control varies from energy consumption, powertrain efficiency, emisssions, and driving cost. These problems are almost invariably formulated as dynamic programming and optimal control problems with the Model Predictive Control (MPC) approach being a popular solution methodology (Ngo et al., 2012; Saerens et al., 2010).

3.2.2 Motion control

This is a broad class of control algorithms used to make sure that the vehicle's logitudinal and lateral motion adheres to a reference trajectory or speed. Predictive cruise control (Asadi and Vahidi, 2011), where a vehicle tracks a known velocity which can be either static (road signs) or dynamic (real time information obtained from the cloud). Adaptive Cruise Control (ACC) detects any vehicle in the vicinity and adjusts the vehicle's speed in order to avoid collisions (Xiao and Gao, 2010). Cooperative Adaptive Cruise Control (CACC) is an extension of ACC in the presence of Vehicle-to-Vehicle (V2V) communications. We will discuss these methodologies in more detail in section 3.3.

3.2.3 Motion Planning

Motion or trajetory planning refers to the process of generating a reference trajectory for a CAV vehicle in time and space. In other words, this process involves decision-making on part of the vehicle, equipped with information about its environment, i.e., surrounding vehicles and road geometry. These behavioral decisions are made at a higher level (whether to make a lane change, for instance) and then numerically translated into a trajectory. These problems are formulated as optimization problems, and being PSPACE-hard are known to be computationally expensive in terms of storage (Paden et al., 2016). General research in this area has been motivated by solving computationally tractable versions of these problems, which can be solved by techniques such as graph search methods (Lima et al., 2018), incremental search methods (Plessen et al., 2018), and variational methods (Gerdts et al., 2009).

3.2.4 Remote Planning and Routing

This refers to the broad umbrella of techniques used for long-term computations of trajectories that involve historical traffic data and are intended to improve expected trip performance. Notable among these techniques are eco-driving planning, and battery charge planning for plug-in hybrid vehicles, that can be enhanced substantially if accurate trip forecasts are available. Dynamic programming (Wang et al., 2014) and mixed-integer non-linear programming formulations (Pourazarm et al., 2015) have been used to study this problem with promising results.

3.2.5 Multi-vehicle trajectory planning

Multi-vehicle coordination and planning has been the subject of research in many fields, including robotics, aerial vehicles, and marine vehicles. We will restrict our discussion specifically to autonomous road vehicles coordinating with each other on highways and intersections. The goals of these frameworks can be varied: speed harmonization, minimizing travel time, maximixing throughput, reducing fuel consumption and emissions. Further still, approaches differ, depending on whether vehicles are allowed to change lanes or not. Highway platoon formation has shown promising results in the case of freight network fleets, where a central authority has complete information about the origins, destinations, and time constraints, which can be used to form platoons (Liang et al., 2015). Note that the successful deployment of these platoons depends heavily on their driving environment, i.e., the degree of their interaction with regular traffic.

3.3 Cooperative Lane Change Control Applications

In the CAV context, lane change algorithims have primarily focused on freeway ramps, which are often significant factors contributing to traffic congestion. (Choudhury et al., 2009, 2006) proposed a merging model with cooperation from target lane drivers, considering variables such as merge urgency, driver characteristics, and traffic conditions. (Park and Smith, 2012) developed a connected vehicle application to advise drivers to make early lane changes and create more space in the ramp merging locations. Park et al. (2014) implemented a lane change merging algorithm on the VISSIM simulation platform and reported an increase in speeds and VMT on a real-world I-66 road network. (Nilsson et al., 2017) tested a lane change algorithm in a field experiment, and reported smoother vehicle trajectories.

Recent work from (Roncoli et al., 2017, 2016, 2015) involves a multi-lane macroscopic flow model for freeways in order to formulate an integrated optimal control problem for traffic in the presence of connected and autonomous vehicles. To make the problem tractable for large networks, they formulate a Quadtratic Program, which has a convex quadratic cost function and linear constraints. (Zhang and Ioannou, 2017) developed a combined model for variable speed limits and lane changes, and reported improved travel times. (Y Ali et al., 2019; Yasir Ali et al., 2019) studied the impact of forced lane changes on traffic safety and develop a game-theoretic lane change model for connected vehicles. (Khattak et al., 2020) proposed an CAV application based on lane control and platooning in the presence of incidents, with lane changes occurring between mainline freeway lanes. They reported more efficient merging as a result, leading to increased vehicle throughputs and lesser volatility in vehicle accelerations and decelerations. (Ntousakis et al., 2016) proposed decentralized algorithms for automated merging control in which every vehicle uses information about surrounding vehicles in its ”cooperation area” to determine the optimal sequence of vehicles to merge onto the mainline freeway from a ramp.

3.4 Peer-to-Peer Negotiations: An Illustrative Example and Simulation Study

Consider a two-lane ring network with a flow-density relationship as shown in the following figure. Traffic states A and B both have the same flow, but with density values of 120veh/mile and 15 veh/mile respectively. The number of vehicles in the system are also different in the two traffic states: 1920 vehicles in state A versus just 240 in state B. In its simplest form, the challenge for a traffic management agency is to move traffic from congested state A to a free-flow condition in state B.

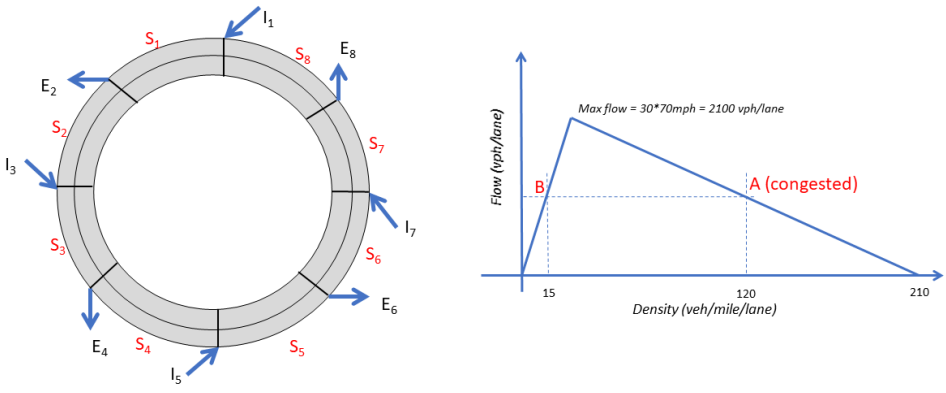

Figure 3.1 Ring Network with Multiple Entries and Exits

One way to accomplish this task could be to achieve high exit flows on the right lanes, the mechanics of which are, of course, non-trivial. Assuming the 4 exit lanes to maintain a certain density of 30 veh/mile and a maximum clearing exit flow of 2100 veh/hour, it is possible to obtain better freeway performance if vehicles can somehow negotiate with other surrounding vehicles to exit more smoothly and quickly. In the past, such schemes would have been truly unthinkable since due to limitations of wireless communication capabilities consumption of transportation supply has traditionally been thought of as First-Come-First-Served (FCFS) in nature.

In the following section, we present a brief description of the simulation software used for the study, followed by a description of a simple peer-to-peer lane change negotiation on a freeways ring network.

3.5 Simulation Framework

Through agent-based simulations, relatively complex global phenomena can be expressed as a sum of small, localized interactions among the agents in the system. The main entities in the traffic network are road segments, vehicles, traffic signals etc., which can be modeled as agents. These agents have the ability to perceive the changes in their environment. Based upon this perception, an agent can modify its behavior to achieve a certain goal. For instance, a vehicle on the road can sense its neighboring vehicles and can change its speed or acceleration, which is analogous to "behavior". Thus, this car-agent behaves as a real-life driver who wants to reach their destination while attaining certain goals. An example of one such goal might be to reach the destination in the shortest time possible without violating any speed limits. We study a system in which there are certain vehicles in the network with a higher value of time than others, who can perceive vehicles around them, and negotiate a lane change to move towards the rightmost lane in order to reach their destination faster. In other words, some vehicles need to slow down to create enough space for higher VOT vehicles to exit the network faster. The trading aspect of this negotation is discussed in the following chapter. Here, we simply model this behavior and study its affect on the overall traffic conditions. In other words, no monetary exchange is assumed in the negotiations modeled in this chapter

PARAMICS is a suite of microscopic simulation tools used to model the movement and behavior of individual vehicles on urban and highway road networks. It offers very detailed modeling for many components of the traffic system. In addition to its default capabilities (Chu et. al. 2003). PARAMICS provides users with an API (Application Programming Interface) through which

users can customize and extend many features of the underlying simulation model without having to access the underlying proprietary code. The following figure depicts the overall, comprehensive framework of PARAMICS, which is used throughout the course of the dissertation.

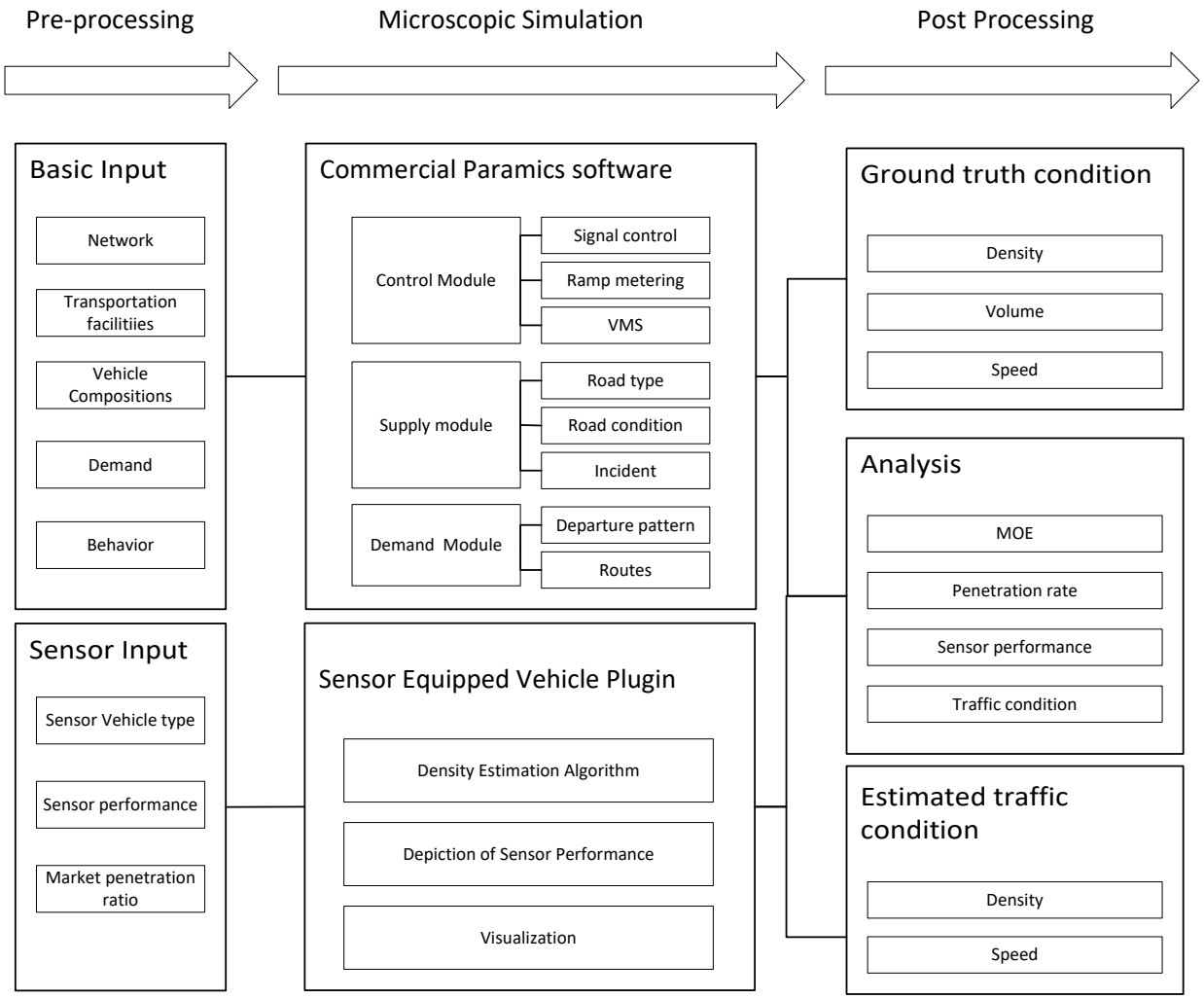

Figure 3.2 Framework of the capability-enhanced PARAMICS simulation

The analysis procedure consists of three steps: pre-processing, simulation, and post-processing. During pre-processing, we define a network, demand, control strategies, and sensor configurations. With these inputs, we run the simulation for a specified period. With the help of PARAMICS API modules, data with outside programs or applications and PARAMICS output data can be communicated back and forth and exchanged. Thus, it is possible to collect information on real-time traffic conditions. Additionally, PARAMICS tracks all vehicles locations at all times and these collected trajectories are used as the ground truth real-time traffic data. In addition to the basic PARAMICS functionalities, we developed customized modules by creating APIs for evaluating the performance of various algorithms. Visual Studio 2012 C++ was used to create the DLLs that interact with PARAMICS. Furthermore, we used the Python programming language to manage the overall testing procedure which includes automated input changes, batch running, and production of reports for statistical comparisons.

3.6 Test Network

For the purposes of testing our negotiation framework, we created a simple network shown in Figure 3.3, comprising a freeway ring with two lanes, several miles in length, containing two origin zones and two destination zones. The network has been created with symmetry in mind, both in terms of network geometry and travel demands. Symmetry in the network and the tempral uniformity of demand pattern provide us with a controlled context with good stability in the traffic dynamics. Zones 1 and 3 are origin zones, and zones 2 and 4 are designated to be destination zones. For each originating vehicle, there are two destinations: one which is closer to it, and another one downstream. This configuration ensures that representatitve vehicle dynamics can be captured in

terms of interactions with vehicles on the mainline lanes as well as vehicles entering or exiting through ramps.

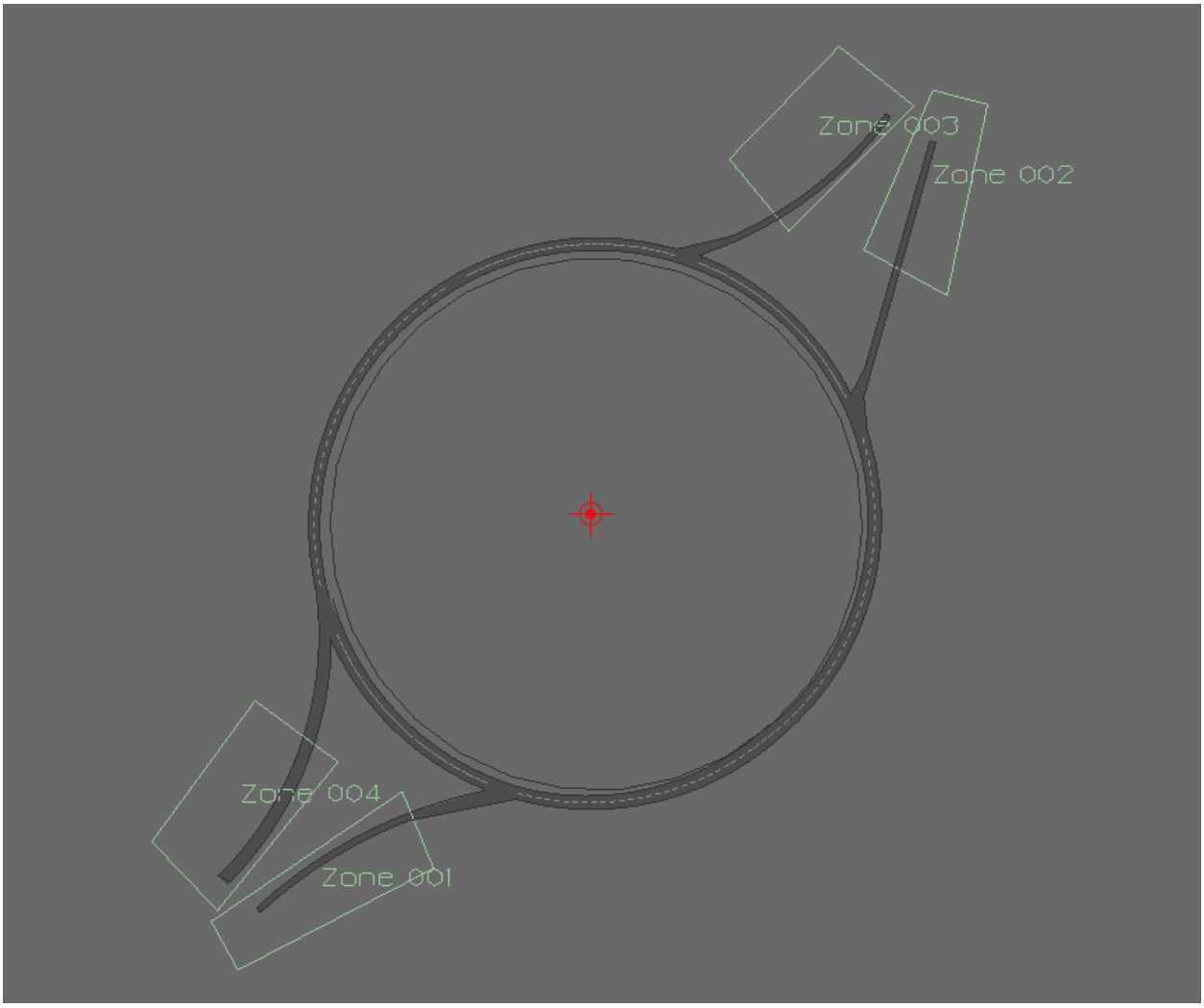

Figure 3.3 Freeway ring network

As mentioned earlier, higher VOT vehicles originating from zones 1 and 3 perceive vehicles in the target lane (in this case the right-most lane to make a quicker exit), through V2V communications modeled through our developed API. These communications are visually depicted in figure 3.4,

where we can see a high VOT vehicle, depicted in blue, interacting with its two immediate vehicles, shown in white, in the target lane. For the purpose of simplicity, we make the assumption that all lower VOT vehicles are open to negotiations. We also stipulate that at any particular instant, a lower VOT vehicle negotiates with only one higher VOT vehicle, i.e., the first high VOT vehicle it negotiates with. Even though we can model multiple negotiations per vehicle on the traffic level in PARAMICS, we preserve this assumption in order to be consistent with our optimization and pricing methodology in the next chapter.

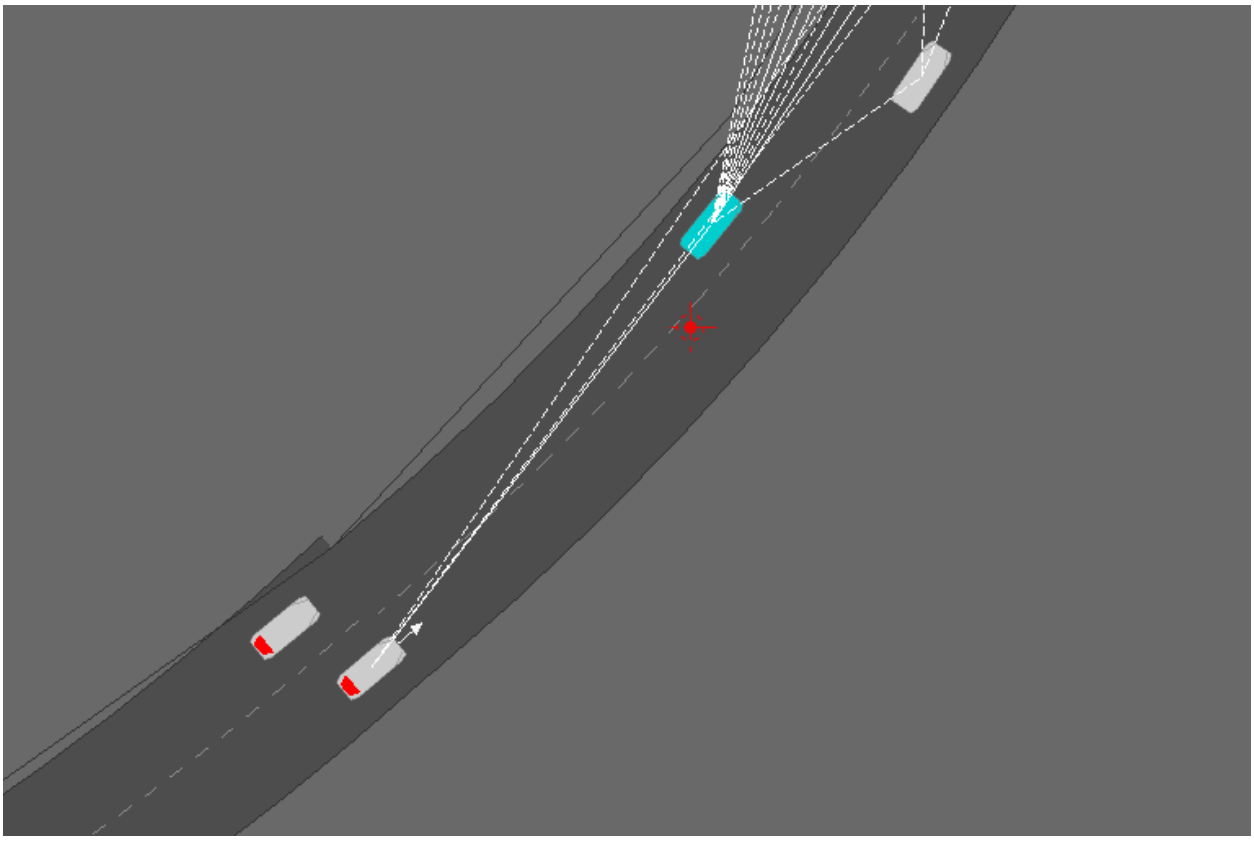

Figure 3.4 Peer-to-Peer communications between vehicles in PARAMICS

The time period of simulation was set to be 1 hour. PARAMICS allows the user to set a demand profile, where they can specify the proportion of vehicles being released every demand period, chosen here to be 12 time periods, each of them 5 minutes in duration. The vehicles are uniformly distributed throughout the simulation period.

We studied the effect of lane-change negotiations on traffic conditions, based upon the proportion of vehicles engaged in these negotiations, and the level of congestion in the network. The output data collected by our API consist of vehicle trajectories, travel times, and headway spacings between vehicles.

3.7 Results

Figure 3.5 shows the improvements in system travel time when the percentage of high VOT vehicles do active lane changes in negotiations with low VOT vehicles. At low market penetration, the travel time savings are statistically insignificant. This is because even if a small number of vehicles improve their travel time, it is still not large enough to make a difference in the overall system travel time. As the market penetration grows, the system travel time goes down, because faster moving high VOT vehicles are able to exit the network quickly, thus lowering overall density on the network. However, as the proportion of vehicles who make lane changes grows even further, overall system travel time also increases. This can be explained by the fact that for every high VOT vehicle making a lane change, there exists a corresponding low VOT vehicle who needs to slow down for this negotiation to succeed. Therefore, too many lane change negotiations will tend to slow down the network.

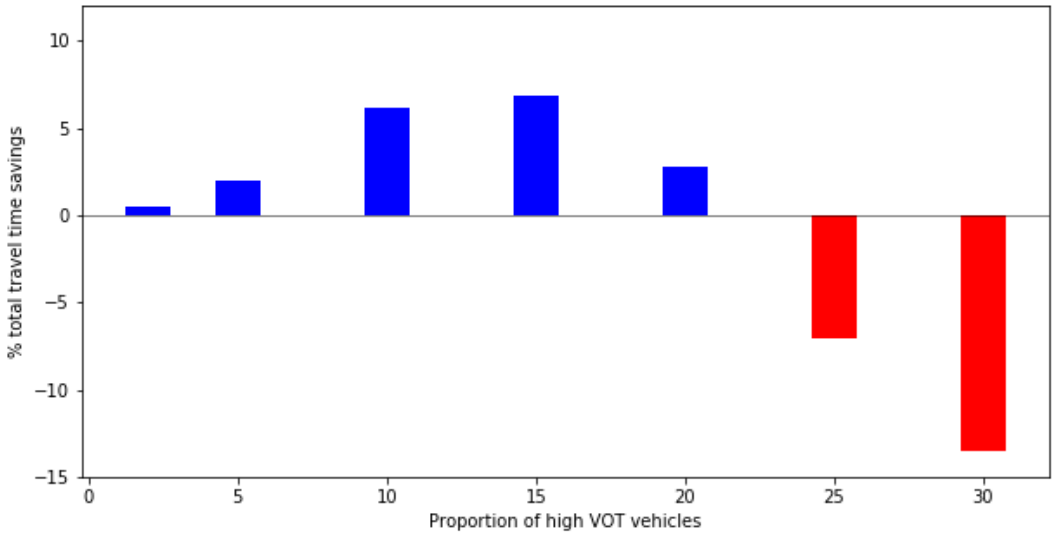

Figure 3.5 Travel time savings with respect to proportion of negotiating vehicles

Figure 3.6 shows the trends of travel time savings for different proportions of lane change negotations when the network OD demand is varied. A larger demand implies a higher level of congestion. These results are intuitive. When the level of congestion in the network is so high that the network traffic density approaches jam density, any lane changes only worsen overall traffic. However, at moderate levels of traffic demand, we observe a modest improvement in travel times at lower market penetrations of high VOT vehicles.

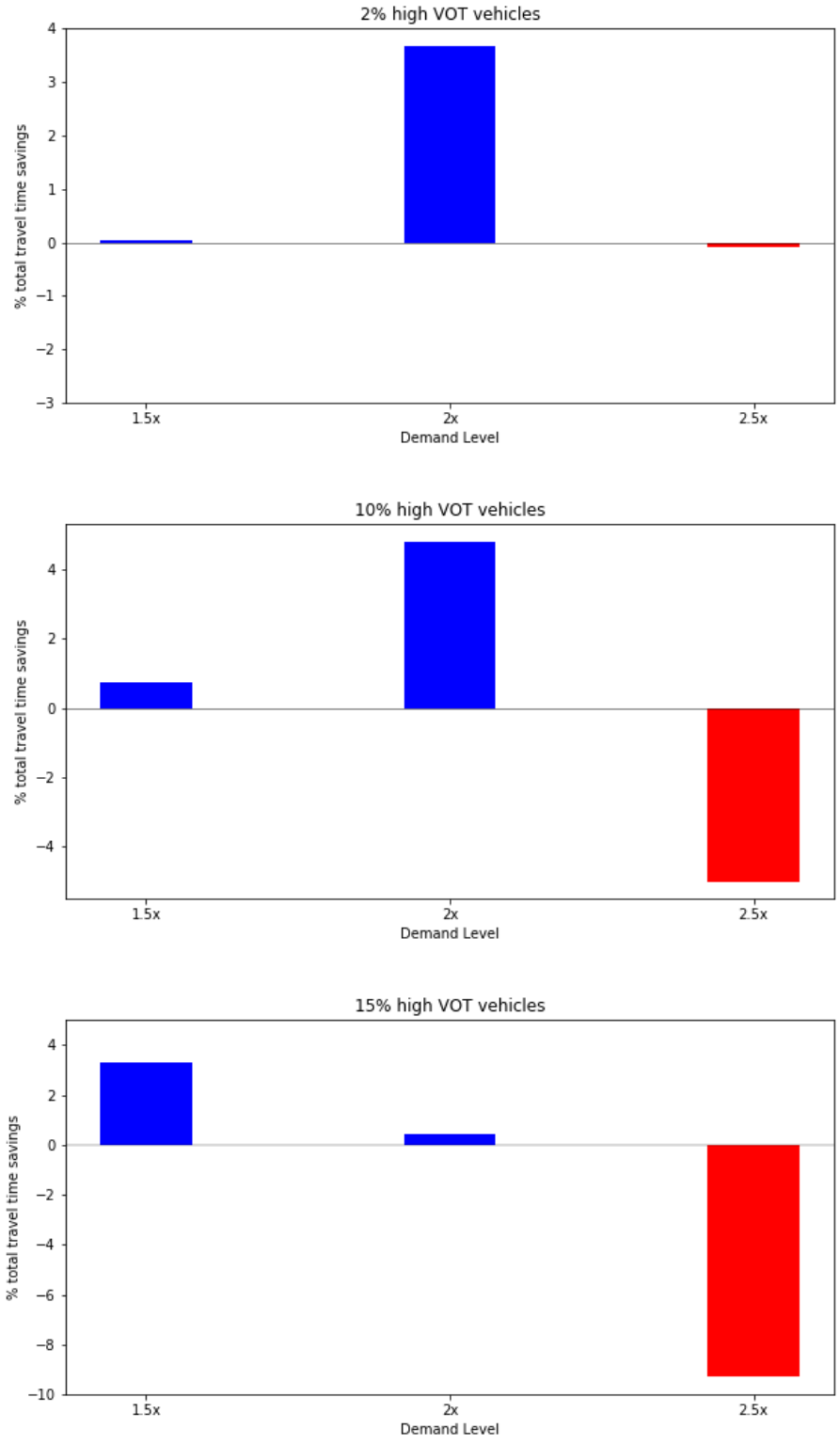

Figure 3.6 Travel time savings with respect to demand

We note that the results shown above are for steady traffic states. Ongoing and future work involves the study of traffic dynamics resulting from lane changes occuring during transient traffic conditions such as incidents or temporary demand increases. Furthermore, the lane changing rules described here have provided us with basic intuition about the effect of lane changes on system travel time, but it remains to be seen if more complex lane changing heuristics validate these results.

Chapter 4. Optimization Framework for Lane-Based Peer-to-Peer Control

Previously, we described lane-to-lane negotiations between vehicles on a network, and used microsimulation to evaluate the traffic performance in such scenarios. In this chapter, we present an optimization framework for this system. We begin with a discussion of agent based models in traffic assignment. We present a brief overview of traditional pricing schemes used to achieve System Optimum traffic conditions and their limitations. This is followed by a description of ”envy” as a metric for agent-level comparisons. Finally, we present a static and a dynamic formulation of our optimization framework, followed by a solution algorithm and numerical results.

Traditional transportation models have been aggregate in nature, with the assumption of homogeneity among users. The reason for this is historic: at the time when transportation planning and assignment were first devised, lack of computational resources necessitated the simplification of traveler behavior. These models are still used for long-term planning studies, or in large scale or regional contexts, where the information about aggregate traffic flows is ususally enough for decision makers. However, they are not appropriate for modeling congestion in real-time traffic networks, where OD the demand varies with time. Agent-based models can capture the complex interactions between individual agents (drivers, network entities, public agencies, etc.), in part due to the innovations in computing technology and the amount of user data available to be analyzed.

4.1 Desirable Traffic Conditions

Wardrop's first principle is a behavioral principle that states that drivers on a transportation network travel in such a way that the travel times on all used routes are equal. This is also known as the User Equilibrium (UE) condition, with the assumption that travelers are selfish individuals who are only concerned with minimizing their own travel time. Even though all travelers experience the same travel time, this condition is not desirable from a system perspective because the overall travel time in the system is not minimized. The total system travel time is minimized under a System Optimal (SO) condition, which can either be achieved when all vehicles travel in cooperation with each other to achieve systemic goals (highly improbable), or under some form of intervention from the Traffic Management Agency.

Note that the SO condition, even if socially desirable, results in routes that have different travel times. This means that some drivers are inadvertently or even deliberately guided by the TMC to experience longer travel times than others, which immediately raises questions about equity and fairness (Roughgarden, 2002).

4.2 Existing Pricing Schemes

There exists a large body of literature on pricing schemes that alleviate unfairness under SO conditions. The most traditional pricing scheme is from road pricing theory that calls for implementing congestion tolling on certain routes at certain times of day, based upon the marginal

travel costs (Beckmann et al., 1956; Burris, 2003; Dial, 1999; Liu and McDonald, 1998; Small, 1992).

However, the success of congestion tolling in the US is, at best, mixed (Zhou et al., 2009). Drivers tend to resent tolling since they expect public roads paid for by their taxes to be free to travel, making tolls politically infeasible (Ben-elia and Ettema, 2009; Nie, 2012; Yang and Wang, 2011; Yang and Zhang, 2003). Furthermore, construction of toll facilities is an investment-heavy endeavor, involving the purchase of right-of-way at precisely the areas in which land in the most expensive (congested urban areas). In today's uncertain political climate, with government spending on infrastructure dwindling, infrastructure-based solutions are not ideal.

The shortcomings of tolling have motivated researchers to propose alternatives. A tradeable credit scheme by (Yang and Wang, 2011) proposes a credit to drivers who are willing to drive on longer routes. Participants can also trade those credits in an open market. (Nie, 2012) proposes a scheme where the government can act as a mediator in the market. (He et al., 2013) extend previous research efforts to create a system in which individual drivers and transportation companies can participate. The author assumes a mixed equilibrium in which that individual drivers act in accordance with Wardrop's first principle, but the transportation companies cooperate to minimize total costs. (Nie, 2015; Nie and Yin, 2013) apply a tradable mobility credit scheme to the departure time selection. A common critique of these schemes is that the credits might not be affordable for some drivers.

(Van Den Bosch et al., 2011) propose a social navigation scheme under the assumption that some drivers are inherently altruistic and do not need incentives to modify their traveled routes. (Pan et al., 2012) use what they term as "Entropy Balanced k shortest paths" to balance traffic. This

concept was used by (Liu et al., 2015) to develop a navigation system where potential traffic routes are displayed to drivers who can choose their desired route based upon metrics such as popularity and estimated travel time.

Recognizing the need to provide real incentives to travelers, (Chiu, 2014) proposes "Metropia," a mobile phone app that suggests various departure time windows to drivers. The algorithm then uses the time window information and the user's historical preferences to generate a set of marginal cost paths. Longer paths come with more incentives, which, in turn, influences travel behavior of drivers.

4.3 Envy as a Metric for Peer-to-Peer System Design

As discussed earlier, optimizing the transportation system to have minimum travel time entails some level of "unfairness" in that some users are forced by the system to travel on less desirable routes. So, system efficiency and social equity are, by definition, in conflict with each other. This implies that any trading mechanism designed by the system operator would necessitate the balancing of these two objectives. This brings us to a discussion of "Envy," a well-known concept in the field of economics, originally formulated to allocate resources fairly to agents. The cake cutting problem (Brams and Taylor, 1996) is a classic example. Note that the term envy is not used as a synonym of "jealousy." It is simply a measure of the desirability of a particular option in contrast with the current option for a given user. A system is said to be "Envy-Free" if each agent in the system is satisfied with their allocation and the overall utility function of the users is maximized at the current level of pricing (Hartline and Yan, 2011). This means that no user has a desire to change their assigned option.

Lloret-Batlle and Jayakrishnan, (2016) and Nam & Jayakrishnan (2018) introduce the envy-based framework in the transportation domain. The following are the brief characteristics of agents in a transportation system operating under such a framework:

1. An agent has their own individual travel preferences, i.e., they can have preferences different from other agents.

2. The distribution of how agents value their travel option (e.g., their value of time) is known to the system manager.

3. Agents can compare their travel options with other agents who have the same origin and destination.

4. Agents feel envy when their valuation of their own travel option is less than that of their valuation of other agents' travel options. This means that an agent only needs to have information about the route allocation of their peers, but not how their peers value those routes. In other words, an agent *i* trading with an agent *j* does not have information about *j*'s socioeconomic characteristics (which would influence *j*'s valuation), so they cannot exploit *j*.

Note that our framework is an agent-based model, which can incorporate heterogeneity among users. Transportation assignment models, even when describing multiclass drivers or commodities, treat members of the same class homogenously. This approach may be suitable for higher level transportation planning for large areas but is not amenable for microscopic frameworks such as peer-to-peer trading where each driver/agent is allowed to enter into a

negotiation with surrounding agents. Agent based models are also flexible in that the definitions and scope of the agents can be easily expanded to accommodate emerging mobility systems, new-age travel forecasting models, and more resilient control models. In our study, we restrict the definition of agents to be just the drivers and the system operator but in the context of Smart Cities and Autonomous Vehicle (AV), we can also have various elements of city infrastructure (freeway beacons, sensors, intersections on arterial roads, etc.) as active agents interacting with one other.

4.4 Notations and Definitions

Based upon our previous discussion, we redefine the current link-based envy framework in Nam and Jayakrishnan (2018) to incorporate lanes into our formulation.

Each driver in the network is an agent *i*, traveling from their origin *r* to destination *s*, using path *k*. We define a path binary $f_{i,k}^{rs}$ for each individual agent that indicates if *i* uses path *k* to go from origin *r* to destination *s*. Instead of link flow, we define lane flow $x_{\mathrm{m}a}$which is associated with a binary variable $\delta_{i,ma,k}^{rs}$ that indicates if agent *i* uses the *m*th lane of link *a* for path *k* between *r* and *s*. Agent *i* has a valuation function (V_i) to compare their travel options to others. This valuation functon can be based upon many factors, but for simplicity, we assume it is obtained from θ_i, the travel time for *i*. The envy felt by agent i towards j is depicted by the term e_{ij}. Table 2 shows the a summary of notations used in this chapter.

Table 2 Notations and Definitions

i	agent $i \in$ I
r, s	origin $r \in R$ and destination $s \in R$
k	a path k in a path set of an origin and destination pair
a	a link $a \in A$
m	lane m $\in M_a$
θ_i	value of time of an agent i
p_i	price for an agent i
e_{ij}	envy of an agent i towards agent j
V_{ij}	valuation function for an agent i agent j's trip
$\delta_{i,\mathrm{m},a,k}^{rs}$	route-lane binary (if lane m is used for link a on route k of r, s, i, then 1, otherwise 0)
$f_{i,k}^{rs}$	path k binary of an agent i of an OD pair r, s (1 if route k is used by i, then 1, 0 otherwise)
x_{ma}	traffic flow of lane m on link a
t_{ma}	travel time of lane m on link a (convex and non-decreasing function of lane flow x_{ma}, $t_a = t_{ma}(\mathrm{x}_{ma})$

4.5 Envy Model Formulation

We introduce a multiobjective optimization function for the static version of the problem as follows:

$$\text{Min: } \alpha \sum_{m\in M_a} \sum_{a\in A} \mathrm{x}_{ma} t_{ma}\,(\mathrm{x}_{ma}) + \beta \sum_{i\in I} \max_{i\neq j}\{e_{ij}\} + \gamma \sum_{i\in I} \mathrm{e}_{\mathrm{is}} \qquad (4.1)$$

Subject to:

$$\sum_{k\in K} -t_a \delta_{i,a,m,k}^{rs} \theta_i + e_{ij} \;\geq\; \sum_{k\prime\in K} -t_a \delta_{j,a,m,k\prime}^{rs} \theta_i \qquad \forall\, i,\ \mathrm{j} \in I,\ \mathrm{i} \neq j \qquad (4.1a)$$

$$x_{ma} \;=\; \sum_{rs} \sum_i \sum_k f_{i,k}^{rs} \delta_{\mathrm{i,ma},k}^{rs} \qquad \forall\ \mathrm{rs, i}\ \in I, k\ \in K^{rs} \qquad (4.1b)$$

$$\mathrm{q}^{rs} = \sum_k f_{i,k}^{rs} \qquad \forall\ k\ \in K^{rs} \qquad (4.1c)$$

$$f_{i,k}^{rs} \geq 0 \qquad \forall\ i\ , j\ , k \qquad (4.1d)$$

$$0 \leq e_{ij} \leq e_{max} \qquad \forall\ i\ ,\ j\ ,\ i \neq\ j \qquad (4.1e)$$

The objective function is composed of three terms. The first term, weighted by the paramater α, is the efficiency term that is the sum of travel times of all vehicles in the system. The second term is a proxy for equity, which we define as the sum of the maximum envy values of each agent *i* with the rest of the agents. Finally, the third term represents the envy value that an agent feels towards the absolute shortest path for their origin and destination.

Equation (4.1a) is a comparison of envy between agent *i* and agent *j*. The term e_{is} is the envy felt by agent *i* towards the shortest path. Note that the valuation function *V* described earlier is set to be θ_i. The maximum allowable envy felt by any agent is set by the operator to be e_{max}. By varying the values of the weighting factors α, β, and γ, and by constraining the values of e_{ij} in this general

formulation, we can implement desirable pricing schemes and arrive at well-known traffic assignment solutions.

4.6 Dynamic Optimization Framework for Envy Minimization

The formulation of the dynamic version of the previous optimization problem is as follows.

$$\min Z = \alpha \sum_{t\in T}\sum_{a\in A} x_{a,t}t_{a,t}\left(x_{a,t}\right) + \beta \sum_{i\in I} \max_{i\neq j}\{e_{ij}\} \quad (4\text{-}1a)$$

Subject to:

$$q_\tau^{rs} = \sum_{i\in I}\sum_{k\in K_\tau^{rs}} h_{i,\tau}^{rsk} \qquad \forall\, r,s \in R, \tau \in T^D \quad (4\text{-}1b)$$

$$h_{i,\tau}^{rsk} = \begin{cases} 1 & if\ path\ k\ is\ used \\ 0 & otherwise \end{cases} \qquad \forall\, i,\tau \quad (4\text{-}1c)$$

$$\sum_i h_{i,\tau}^{rsk} = 1 \qquad \forall\, i,k \quad (4\text{-}1d)$$

$$x_{ta} = \sum_{i\ \in I}\sum_{r,s,k,\tau} h_\tau^{rsk}\delta_{it\tau a}^{rsk} \qquad \forall\, r,s \in R, i\ \in I, k \in K^{rs} \quad (4\text{-}1e)$$

$$\delta_{it\tau a}^{rsk} = \Psi\left[h_{i,\tau}^{rsk},\ \forall i,r,s,k,\tau\right] \qquad \forall\, r,s,q\ \in q^{rs}, k\ \in K_\tau^{rs}, a \in A \quad (4\text{-}1f)$$

$$\sum_{r,s,k,\tau} -t_a\delta_{it\tau a}^{rsk}\theta_i + e_{ij} - p_{i\tau}^{rs} \geq \sum_{r,s,k',\tau} -t_a\delta_{jt\tau a}^{rsk'}\theta_i - p_{j\tau}^{rs} \qquad \forall\, i,j \in I,\ i \neq j \quad (4\text{-}1g)$$

$$0 \leq e_{ij} \leq e_{max} \qquad \forall\, i,\ j,\ i \neq\ j \quad (4\text{-}1h)$$

$$\sum_{i\in I} p_i^{rs\tau} = B^{rs\tau} \qquad \forall\, r,s,\tau \quad (4\text{-}1i)$$

The objective function is composed of two parts: the first captures system efficiency, which is the total travel time in the system, and the second represents the level of equity in the system by summing the envy across all users, for all time steps.

4.7 Solution Algorithm for the Dynamic System Optimization Framework

We present a solution algorithm for the formulation proposed above, by combining a Dynamic Traffic Assignment model to compute optimal time-dependent OD flows, and use those results as input to a linear programming agent-based model to make the system envy-free. The output of this two-step solution approach is a set of optimal benefits or prices allocated to users with inferior paths. We implement a simulation-based DTA model, as described in Yang, Jayakrishnan (2011) and Nam (2019). Figure 4.1shows the overall bi-level optimization solution framework. The Step

1 in the solution framework is the Dynamic System Optimal assignment step, based upon the well-known gradient project method proposed by Jayakrishnan et el., (1994).

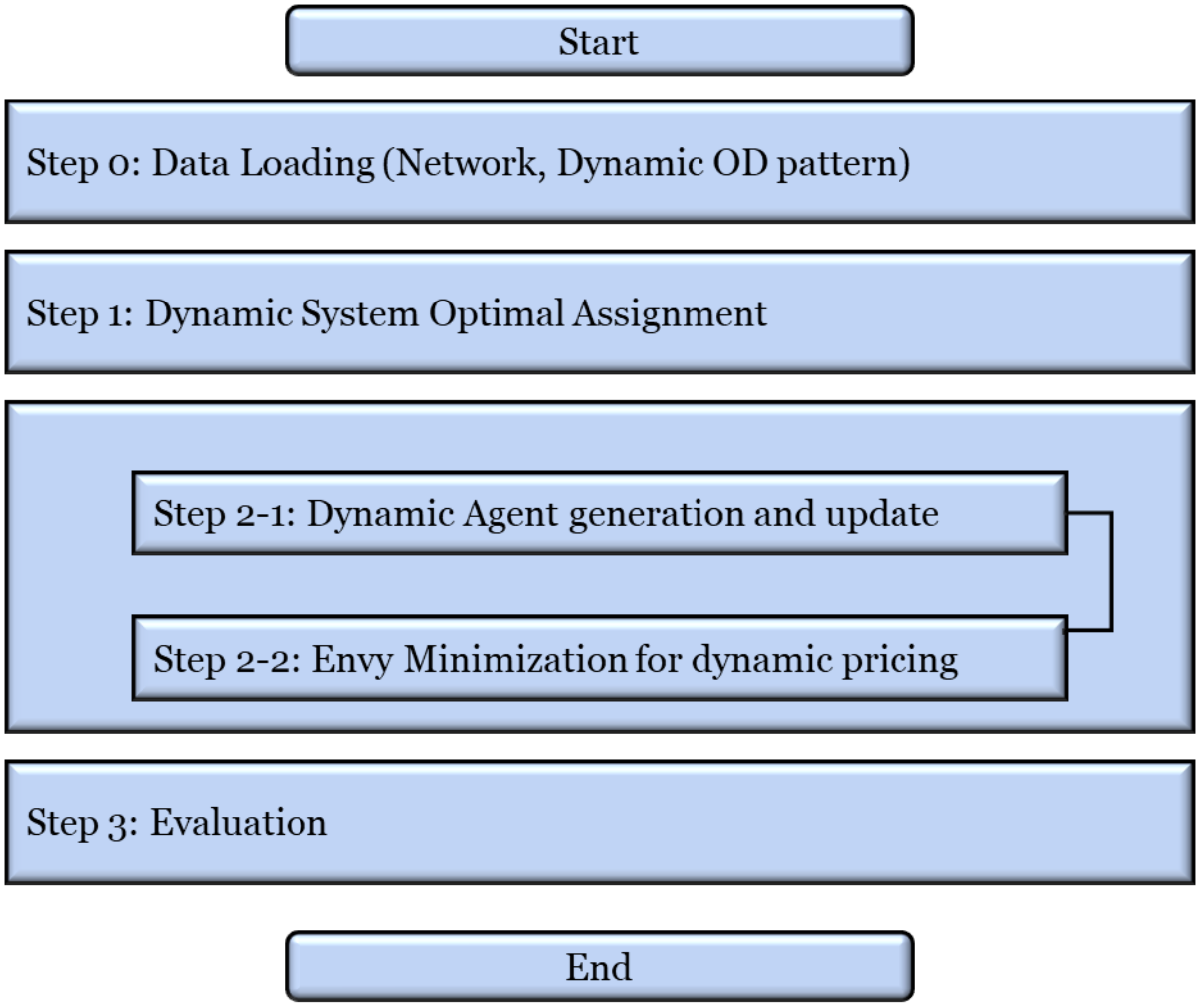

Figure 4.1 Solution Algorithm

4.8 Off-ramp Network Study

We implement the bi-level optimization approach on a hypothetical off-ramp network shown in Figure 4.2. It is composed of two OD pairs and 3 lanes. Lane 3 angles off to the right to become the exit ramp.

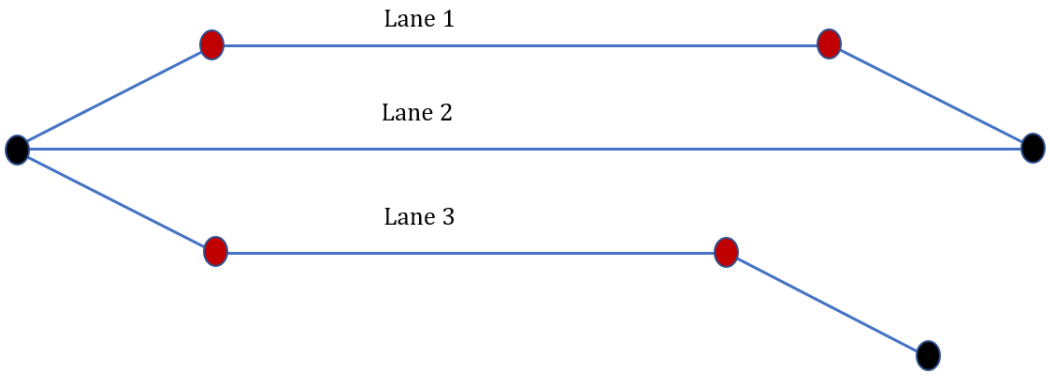

Figure 4.2 Illustrative Off-ramp Network

Traditional representation of networks involves nodes and links that signifiy actual nodes and links present on the network. However, such representations are inadequate to study lane changes. We propose a network transformation in Figure 4.3 in which we introduce additional virtual nodes that represent ”transfer points” from which lane changes can take place from vehicles in Lane 2 to Lane 3 in order to reach their destination. These points are introduced only for the network formulation, and are not physical points. They are needed to form conceptual links that represent the lane-to-lane vehicle movements over stratches of lanes. These nodes are connected by virtual links (shown in green) that are abstractions of the path the lane-changing vehicles would take.

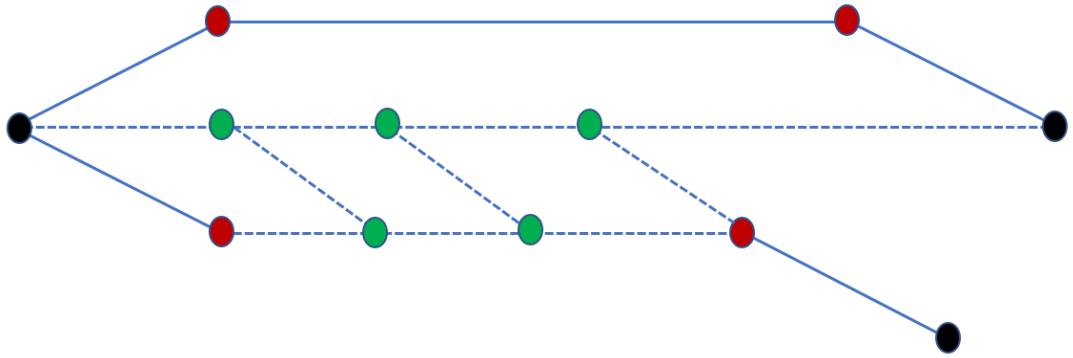

Figure 4.3 Transformed Network with Virtual Links and Nodes for Lane Changes

The node labels of the transformed network are shown in Figure 4.4. The two OD pairs in the network are (0-16) and (0-17)

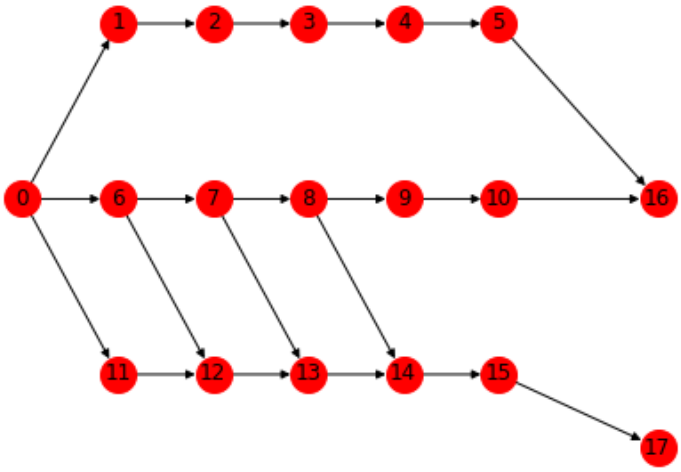

Figure 4.4 Node Labels

Table 3 provides further information about the network links and their link performance function parameters. The link performance function used in this study is a modified Greenshield model, the suitability of which is discussed in (Jayakrishnan et al., 1994). Note that the virtual links representing lane changes are also assigned a similar link performance function. We recognize that the cross-flows between lanes are fundamentally different than the longitudinal flows along the lanes, and that more elaborate studies are needed to find representative performance functions for the links representing the cross-flows. We expect future research that introduces a more direct time-based function that is able to capture the delays associated with lane changing, that may be calibrated with real-world data.

Table 3 Link characteristics

From	To	Length (ft)	k_j (veh/mile)	Free speed (m/s)
0	1	2500	160	30
1	2	400	160	30
2	3	400	160	30
3	4	400	160	30
4	5	400	160	30
5	16	2500	160	30
0	6	2500	160	30
6	7	400	160	30
7	8	400	160	30
8	9	400	160	30
9	10	400	160	30
10	16	2500	160	30
0	11	2500	160	30
11	12	400	160	30
12	13	400	160	30
13	14	400	160	30
14	15	400	160	30
15	17	2500	160	30
6	12	400	1000	30
7	13	400	1000	30
8	14	400	1000	30

4.9 Numerical Results

The two OD pairs (0-17 and 0-16)) are assigned a demand of 2500 vehicles/agents and 1875vehicles/agents respectively. The demand profile for agent generation is non-uniform, to represent congestion in the network which occurs during the middle of the time period. The value of time of agents are drawn from a lognormal distribution with the mean and variance of 0 and 0.5 respectively.

The results include a comparison of the DSO (proposed) solution with the DUE solution for the same network. Note that an argument can be made that a more appropriate comparison would be for the DUE solution for the original, untransformed network (AON), or with a slightly modified network that has fewer lane changing virtual nodes. The solution performance for those cases would be much worse, but we chose the same virtual network in the interest of consistency.

Figure 4.5 shows the convergence of the solution algorithm. Relative Dual Gap (Yang, Jayakrishnan 2011) was chosen to be the convergence metric. Rapid convergence was achieved, but from various experiments we observe that the rate of convergence was sensitive to the initial set size chosen in the Gradient Projection step.

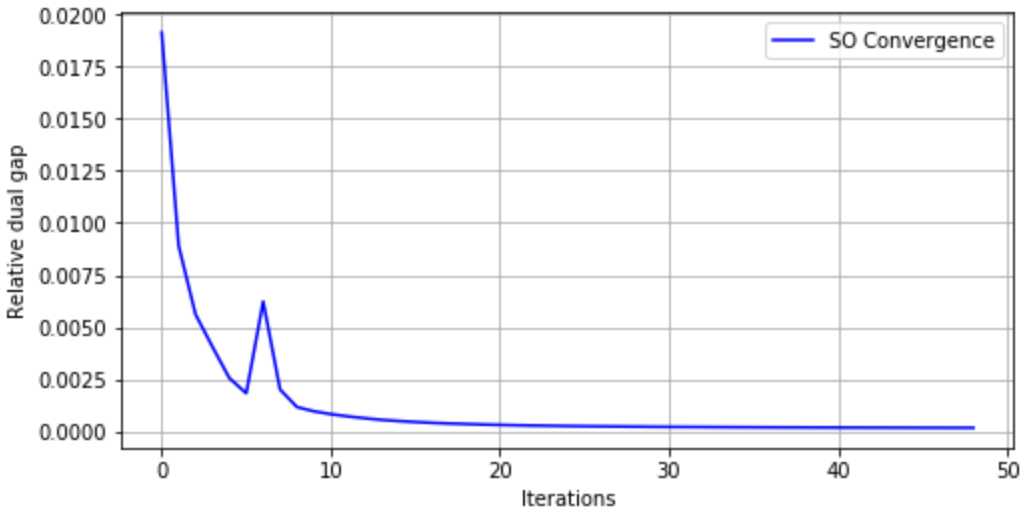

Figure 4.5 Convergence of the Solution Algorithm

Figure 4.6 depicts the convergence of the system travel time for both the DSO and DUE cases. As expected, the total travel time for the DSO traffic state is lower, by approximately 2%.

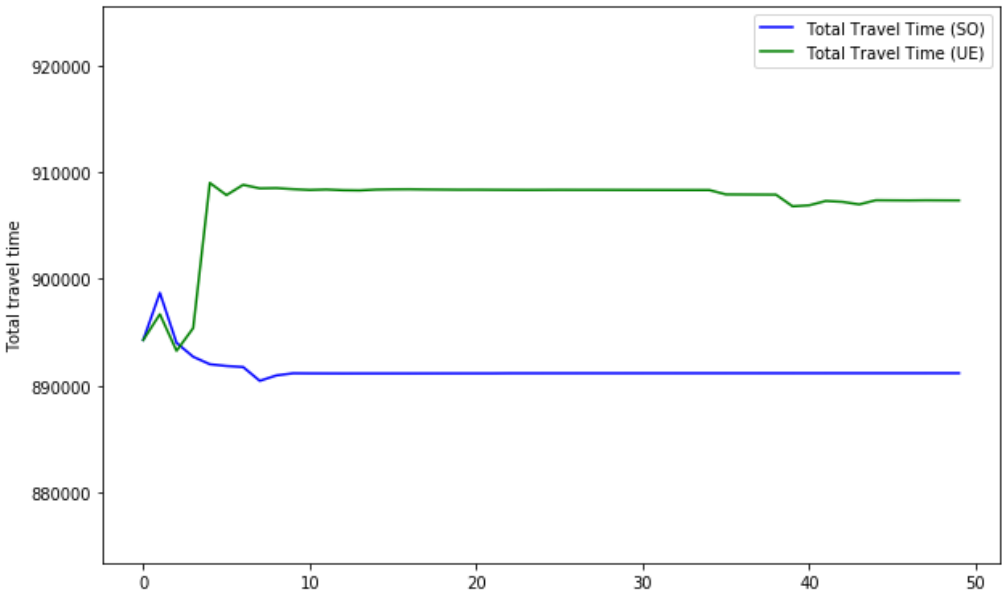

Figure 4.6 Travel times for SO and UE traffic conditions

Figure 4.7 depicts the average space mean speed observed in the network for both DSO and DUE conditions. It is computed by dividing the total VMT by the total VHT in the system at each time step. For both cases, the space mean speed shows a similar pattern when the network is in a free flow condition, but their patterns diverge at the onset of congestion. The space mean speed of the DSO condition is higher than that of the DUE condition. Furthermore, variance of the space mean speed for DSO is lower, which means the observed traffic speed is more stable.

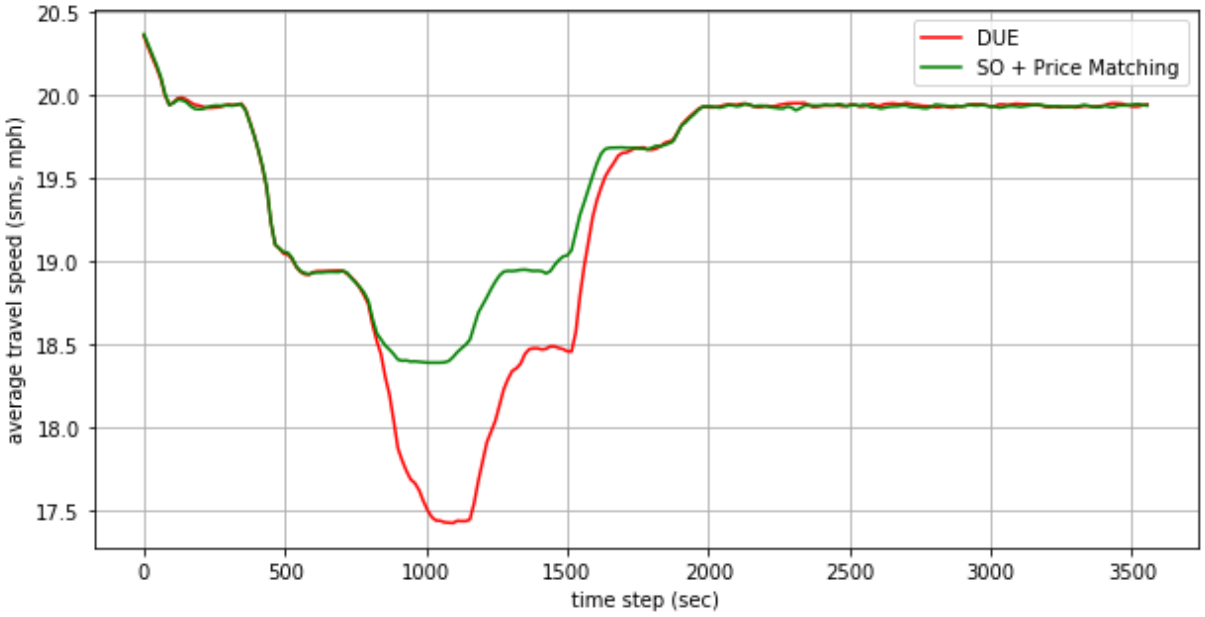

Figure 4.7 Average network Space Mean Speed (DUE vs DSO)

Figure 4.8 represents the amounts of tolls charged to the higher VOT agents and the compensation received by lower VOT drivers who slowed down in exchange for payments. Note that the amount

of tolls are matched with incentives at each time step (zero budget condition), and that the payments and tolls expectedly increase during congestion periods.

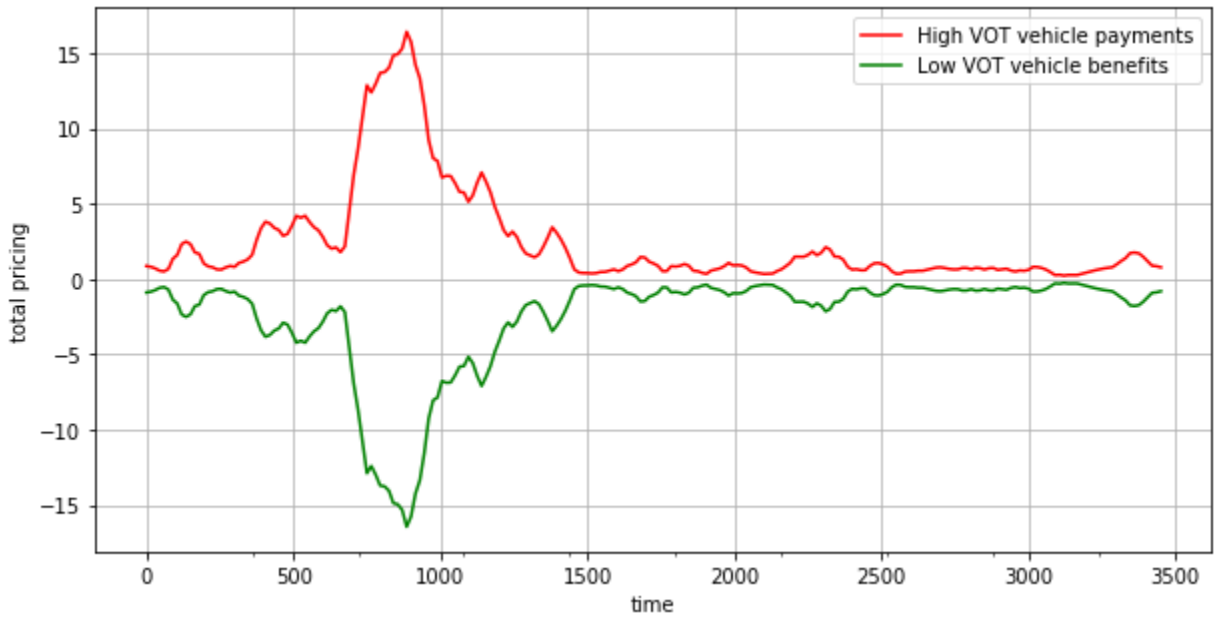

Figure 4.8 Incentives vs Tolls during analysis period

Finally, figure 4.9 shows the travel times of paths taken by OD1 (0-17) agents. The travel times are lower for DSO condition, however, we observe that agents traveled on similar paths for both cases. This is due to the fact that the network in study was small, which resulted in a lower number of possible paths for an OD pair. On larger networks, it is known that the SO conditions disperse demand spatially on the network more evenly than UE conditions (Boyce and Xiong, 2009).

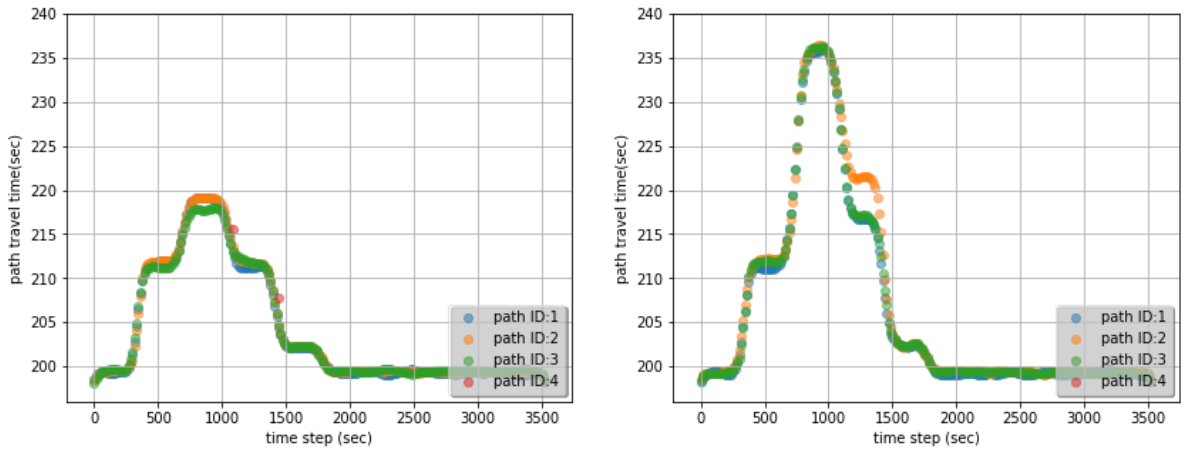

Figure 4.9 Path travel times (Origin 0 to Destination 17)

Chapter 5. Sensor Technologies for Enabling Peer-to-Peer Trading and Control

5.1 Introduction

Accurate real-time estimation of traffic states is a prerequisite to the successful deployment of any ITS application aimed at mitigating traffic congestion. Our proposed framework of routing vehicles on a lane-to-lane basis, which involves vehicles trading their position in time and space can only be realized in the field if the mediating agency (TMC, or a mobility service) has accurate information about traffic conditions. The measurement of traffic density has relied on traditional data collection methods such as loop-detectors or photographic techniques which have spatial or temporal limitations. Pavement-invasive detectors such as traditional loop detectors suffer from high installation and maintenance costs. Furthermore, data obtained from them are not always reliable. New technologies such as vehicle sensing, vehicle tracking, and wireless communication are expected to be capable of overcoming these drawbacks.

The 'Internet of Things' (IoT) and advances in sensor technologies offer efficient ways to monitor and estimate the state of traffic. Some high-end vehicles already come equipped with sensors to assist drivers with advanced functions such as Adaptive Cruise Control (ACC), Parking Assist System (PAS), Automated Emergency Braking System (AEBS), and Lane Keeping Assist System (LKAS). Such technologies are expected to be even more ubiquitous with the advent of Autonomous Vehicles. Therefore, it is evident that vehicle sensing technologies and data derived from them are poised to play a key role in the future of ITS (Intelligent Transport System)

applications. In this regard, the focus of our research is on the real-time estimation of traffic density from data obtained solely from radar sensors of CAPVs (Connected and Autonomous Probe Vehicles) in a traffic network. A radar equipped CAPVs can capture "local density" by detecting surrounding vehicles in its sensing area. A link-level traffic density can then be estimated at the TMC where local densities are collected from multiple CAPVs traveling on the link. In other words, spatially continuous link traffic conditions, i.e., traffic density, which cannot be observed from point detectors, can now be captured using a moving sensor system.

5.2 Literature Review

Some fusion methods integrating loop detectors and probes have been proposed when the probe vehicles in the network are sparse. (Qiu et al., 2010) introduced new real-time freeway traffic density estimation techniques that use a combination of both loop detector and IntelliDrive-based probe vehicle data. The IntelliDrive-based probe data of overtaken vehicle counts or passing vehicle counts are synchronized with up/down stream and on/off ramps loop detector data in real-time, and the system estimates traffic density using these datasets. (Wright and Horowitz, 2016) used probe data to supplement traditional, fixed-location loop detector data for density estimation. A method for supplementing data from fixed detection infrastructure with probe data while retaining the model-based filtering approach has been elusive, therefore, they recast the problem in a probabilistic framework to simplify the mathematics, and further develop an approach based on Rao-Blackwellization of particle filter (RBPF) as a solution.

(Herring et al., 2010) estimated and predicted traffic conditions in arterial networks using probe data. The proposed model for traffic condition estimation was evaluated using data from a fleet of

500 taxis in San Francisco, CA. (Seo and Kusakabe, 2015) proposed a method to estimate the traffic state (i.e., flow, density, and speed) based on probe vehicle data. As part of their study design, two probes, a leading probe vehicle and the following probe vehicle, drive on the same road stretch. The following probe observes the number of vehicles between itself and the leading probe. They calculate the cumulative count at the probe vehicle's current position and use it to estimate traffic density. (Seo et al., 2015) proposed an algorithm to estimate traffic flow, density, and speed by utilizing data from a probe equipped with spacing measurement equipment. They designed a probe with the capability of observing surrounding vehicles and capturing their spacing information. (Al-Sobky and Mousa, 2016) introduced a similar approach, but they used smartphones to capture the number of vehicles.

We note that the unit of density inferred by probe data (vehicles per square meter) is not a common unit for traffic density (vehicles per meter) used in transportation applications. (Nam et al., 2017), in a recent study, note that traffic density is closely correlated with the average number of detected vehicles on a road stretch, and proposed a method to convert sensing area-level traffic density to link-level traffic density by using an ordinary least squares conversion method.

In simple terms, traffic density is related to the vehicle count on a road unit, i.e., the number of vehicles per kilometer. Since the method of conversion in (Nam et al., 2017) is linear, there is an information loss in the process, which affects its accuracy.

We found Edie's definition (Edie, 1965) of traffic density to be the most appropriate for our study, since the space-time domain under consideration can be of any shape, thereby providing a generalized form of density estimation. This research proposes a methodological framework in which Edie's definition is applied to a CAPVs scenario.

5.3 Overview of traffic density estimation

The following table contains the definitions of the symbols used in this chapter.

Table 4 Variable definitions and notations

Symbol	Definition
n	*Number of vehicles in a link*
n^s	*Number of detected vehicles by a sensor equipped vehicle s*
$N([x_a, x_b]; t)$	*Number of vehicles in a link at time t*
$X\ ([x_a, x_b])$	*Space domain*
X	*Length of a link*
dt	*infinitesimal fraction of time*
τ_i	*Time spent of vehicle i in a link in a given period*
$k([x_a, x_b] \times [t_a, t_b])$	*Density of a link during a given time interval* $[t_a, t_b]$
J	*Set of time steps in the time interval* $[t_a, t_b]$
d_S	*Effective sensing distance of a sensor equipped vehicle*
d_{fS}	*Sensing distance of a front sensor*
d_{Rl}	*Sensing distance of a rear sensor*
d_{Sl}	*Effective sensing distance of a side lane*
VHT	*Vehicle Hours traveled*
VHT^s	*Vehicle Hours traveled of detected vehicles by sensor equipped vehicles*
$k([x_a, x_b] \times dt)$	*Density of a link during a very small time step*
$k([x_a, x_b] \times [t_a, t_b])$	*Density of a link during a given time interval* $[t_a, t_b]$
$k(d_S \times dt) = k_s$	*Local density measured by a sensor equipped vehicles*
$k(d_s[x_a, x_b] \times [t_a, t_b])$	*Density of a link measured by sensor vehicles at a given time interval* $[t_a, t_b]$
y_h	*Radar detection distance of the side lane*
y_s	*Distance of shaded area where radar cannot reach because of sensor angle*
θ_s	*Sensing range of a sensor*
l_v	*Average vehicle length*
s	*Spacing (distance between vehicle n and vehicle n+1*

Traffic density is calculated by counting the number of vehicles over a unit length of road stretch at a specific time, which can be inferred from an aerial snapshot. Without loss of generality, traffic density can also be derived from the cumulative number of vehicles and vehicle trajectories. In great detail, Edie (1965) described the relationships between density and vehicle hours travelled (VHT) in the Euclidian area of a region having a 2D dimension (of distance and time) as shown in Eq (5.1) to (5.4).

$$k_t = \frac{\partial n_t}{\partial x} = \lim_{\Delta x \to 0} \frac{n(x,t) - n(x+\Delta x,t)}{\Delta x} = \frac{N([x,x+\Delta x];t)}{X} \quad (5.1)$$

$$\bar{k} = \frac{1}{T}\int_0^T k_t dt \; = \frac{1}{T}\int_0^T \frac{N([x,x+\Delta x];t)}{X} dt = \frac{1}{X \cdot T}\int_0^T N([x, x+\Delta x]; t) dt \quad (5.2)$$

$$\sum_{i \in N} \tau_i = \int_0^T N([x, x+\Delta x]; t) dt = \int_0^T \int_0^X k(t,x) dx dt \; = X \cdot T \cdot \bar{k} \quad (5.3)$$

$$\bar{k} = \left(\frac{1}{X \cdot T}\right) \sum_{i \in N} \tau_i \quad (5.4)$$

When we discretize the time into exceedingly small fractions j ($j \in$ J), we can generalize the average density of a domain from the time-space diagram.

$$\bar{k}([x_a, x_b], \times [t_a, t_b]) \; = \frac{\sum_{j=1}^{J} N([x_a,x_b];t_j)}{J(x_b - x_a)} \quad ; \quad J = \frac{t_b - t_a}{timestep} \quad (5.5)$$

By restricting j to an infinitesimal step, we can assume that vehicles in the time space domain do not disappear in this time step. Furthermore, by discretizing time steps, we can conveniently obtain the number of vehicles and their associated VHT information from microscopic vehicle simulations or field applications. VHT can be derived as shown in Eq (5.6)

$$VHT_J \approx \sum_{j=1}^{J} N\big([x_a, x_b]; t_j\big)\, \Delta t_j = \; J \; k([x_a, x_b] \times [t_a, t_b])(x_b - x_a)\Delta t_j \quad (5.6)$$

$$= J \; k([x_a, x_b] \times [t_a, t_b])(x_b - x_a)\frac{t_b - t_a}{J} = k([x_a, x_b] \times [t_a, t_b])(x_b - x_a)(t_b - t_a)$$

From Eq (6), it follows that traffic density can be calculated by dividing the total vehicle hours travelled by the Euclidean area of length and time dimensions (Eq 5.7). This approximation equation is equivalent to the density definition by (Edie, 1965) and (Makigami et al., 1971):

$$k([x_a, x_b] \times [t_a, t_b]) = \frac{VHT_J}{(x_b - x_a)(t_b - t_a)} = \frac{VHT_J}{XT} \quad (5.7)$$

(Jin, 2010) also notes that the equation (5.7) approximates Edie's definition of traffic density in a time-space domain and this equation can be applied to multiple lane cases. Furthermore, the domain can be a rectangle, circle, or any other arbitrary shape (Daganzo, 1997). Edie's definition has been widely employed in traffic density estimation methods by using probes equipped with sensors. Ozarki et al. (2015) propose a usage of probe to estimate traffic density. A probe system using image processing technology can capture the time-space region between a probe and its leading vehicle, which is vehicle spacing. From the knowledge of the travel time spent by a probe, they estimate the traffic condition by employing Edie's definition. (Seo et al., 2015) also employ a similar approach. They design probe vehicles equipped with GPS and mono-eye cameras to record spacing information and develop a method traffic condition monitoring algorithm.

5.4 Traffic density estimation method using radar sensing data

This section describes the details of the radar technology as well as the equipment used for estimating density in road stretches.

5.4.1 Specification of a radar sensor-equipped CAPVs

Among its many uses, a radar sensor-equipped vehicle is designed to efficiently observe surrounding traffic conditions. In our earlier work in Nam et al. (2017), we proposed a traffic density estimation method by utilizing a radar sensor equipped probe developed by Korea Institute of Civil Engineering and Building Technology (KICT). The probe vehicle has multiple sensors, including a GPS unit, high-resolution radars working with 77-gigahertz microchips, and computing processors. Applications in the main processor manipulate incoming data from sensors

and then compute local traffic density. The radar system of the probe vehicle is capable of observing multiple surrounding vehicles on a real-time basis and then tracing their trajectories which are then used to calculate VHT. Currently, the probe, called TRADOS (TRAffic Density Observation System), has an onboard real-time traffic monitoring tool, which can sense traffic conditions in its vicinity (e.g., local density).

Figure 5.1 shows a conceptual diagram of how the sensor-equipped CAPVs detects adjacent vehicles. Radars are located at the front and rear bumpers that detect vehicles in four regions surrounding the CAPVs: front-end, rear-end center, left and right side. In the front, there are two radars: a forward long-range radar, and a mid-range radar, both of which are widely used for ACC applications. In our study, the long-range radar performs the role of detecting vehicles on the same lane, and the mid-range radar is adapted to detect vehicles on the left/right side lanes. The CAPV has three radars in the rear. Two side backward sensors designed for Blind Spot Detection (BSD) can detect vehicles driving in the left/right lanes. Finally, the backward long-range sensor is used to detect vehicles following the CAPVs in the same lane.

Applications in the computing processors synchronize different sensor data on a time basis and store each detected vehicles' relative position data, which is then be converted into second-by-second vehicle trajectory data. By differentiating the trajectories with respect to time, we can infer the travel speed of detected vehicles. Similarly, the CAPV can also infer acceleration/deceleration of the detected vehicles, if required.

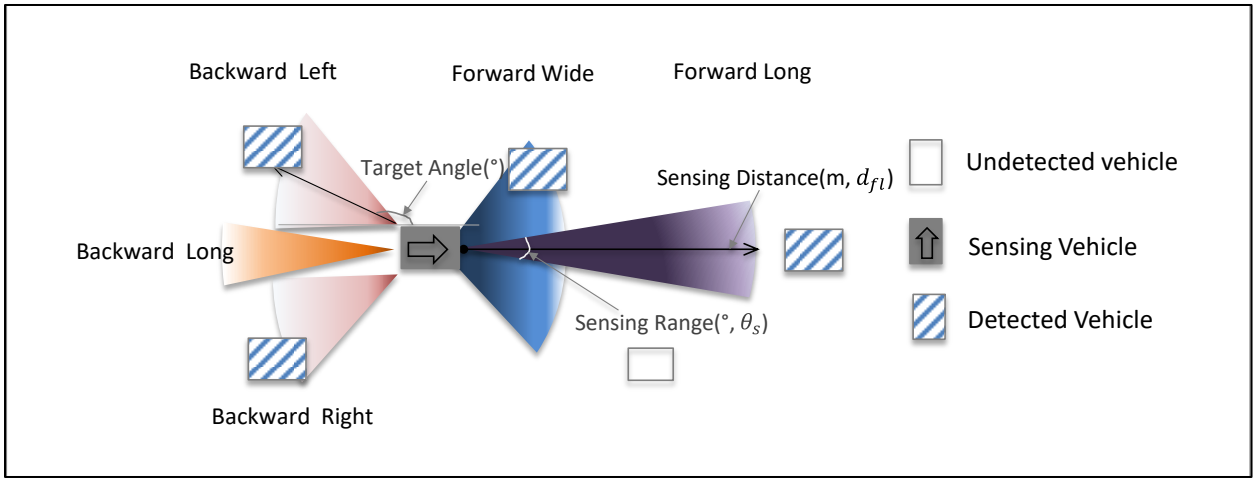

Figure 5.1 Sensing vehicle and its sensing range specifications

For this study, the following radar configuration is assumed as shown in Table 5.

Table 5 Radar configuration of CAPV

Sensor Code	Name	Target Angle (°)	Sensing Range (°)	Sensing Distance(m)
1	Forward Long	0	10	30
2	Forward Wide	0	60	10
3	Backward Left	160	40	10
4	Backward Right	200	40	10
5	Backward Long	180	20	20

As mentioned earlier, in our previous research in (Nam et al., 2017), we used an ordinary least squares conversion method to convert the density per square meter to density per linear meter, as depicted in equation 5.8.

$$k(d_S \times t) \approx \alpha \cdot \frac{N(d_S;t)}{A_s} \quad \text{where } \alpha \text{ is a converting parameter} \tag{5.8}$$

After a CAPV has crossed the road section, the section density can be estimated by averaging local densities at every time step *j*.

$$\hat{k}([x_a, x_b] \times [t_a, t_b]) \doteq \frac{\sum_{j=1}^{J} \alpha \cdot N(d_S;t_j)}{A_S J} = \frac{\sum_{j=1}^{J} \alpha \cdot N(d_S;t_j)/A_S}{J} = \frac{\sum_{j=1}^{J} k_j}{J} \tag{5.9}$$

In the case of multiple CAPVs traversing the road sections, equation (5.9) can be generalized by averaging section densities of S CAPVs as in equation (5.10).

$$\hat{k}([x_a, x_b] \times [t_a, t_b]) \doteq \frac{\sum_{s \in S} \sum_{j=1}^{J} \alpha \cdot N(d_S;t_j)}{A_S JS} = \frac{\sum_{s \in S} \sum_{j=1}^{J} \alpha \cdot N(d_S;t_j)/A_S}{JS} = \frac{\sum_{s \in S} \sum_{j=1}^{J} k_j}{JS} \tag{5.10}$$

Hereinafter, we shall refer to this method as "Area-based method" (Nam et al, 2017) and compare their estimates to our proposed method.

5.5 Proposed Estimation method for single lane traffic density with sensors

In our approach, we consider the geometric spans of sensors and their effective sensing distance (d_s). Instead of simply counting the number of vehicles on the link as used in the Area-based method, we use an important property of Edie's definition that the time-space domain in Eq (5.8) can take any form, such as rectangular or polygonal. Figure 5.2(a) depicts a time-space diagram that shows trajectories of all vehicles traveling on a road section with a single lane and the time-space effective sensing domain of a radar-equipped CAPV. Since a CAPV moves along traffic, the shape of the time-space diagram of the sensing area is not a rectangle but an arbitrary polygon as shown in Figure 5.2(b). As shown in Eq (1) to (8), by dividing the total vehicle hours travelled

of detected vehicles by the CAPV's time-space domain, we can estimate the traffic density of the road section. Thus, the value of traffic density is an estimated value from the sampled time-space domain of a CAPV.

Data obtained by the CAPV can be used not only to identify and trace surrounding vehicles' trajectories, but also to calculate the total vehicle travel time in the sensing area. The total sensing time-space domain is the shaded polygon shown in Figure 5.2(b). The density of the domain is estimated by calculating total detected-vehicle travel hours over the area of the shaded polygon (Eq 5.11), which can also be obtained by the same derivation process for Eq (5.7). The advantage of this method is that it does not calculate a local density every time step. Only a section density can be estimated by combining detected and current vehicles' travel time until a sensor vehicle passes a domain. In Figure 5.3 (a), a CAPV has two sensors: Front sensor and Rear sensor. The sensor domain is the sum of sensing distance of those two sensors ($d_{Fl} + d_{Rl}$). Four vehicles, including the CAPV itself, have been detected when a CAPV drives along the section.

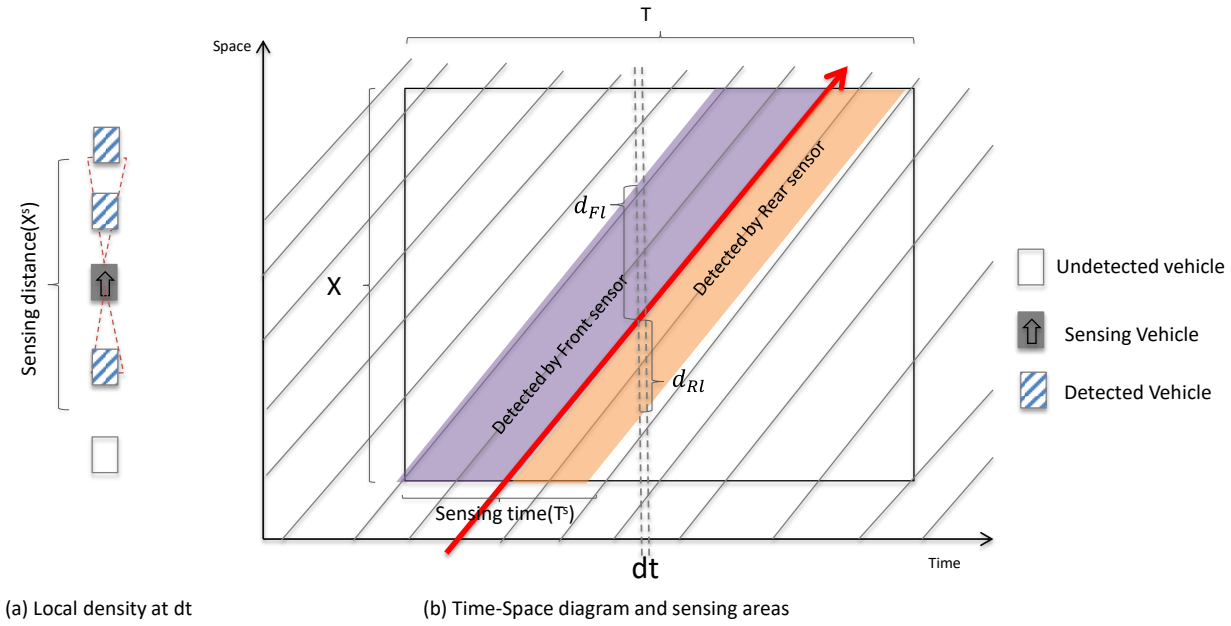

Figure 5.2 Time-space diagram example of vehicle directions

$$\hat{k}([x_a, x_b] \times [t_a, t_b]) \fallingdotseq k(d_s[x_a, x_b] \times [t_a, t_b]) = \frac{\sum_{j=1}^{J} VHT_j^s}{\sum_i d_{si} \cdot J} = \frac{VHT^s}{\sum_i d_{si} \cdot J} \tag{5.11}$$

5.6 Extension to the estimation for multiple lanes with multiple sensors

Since a CAPV has multiple radars at various positions, the CAPV can also detect vehicles in adjacent lanes. In addition to the forward long-range radar (FL) and backward long-range radar (BL), it also has a forward mid-range wide (FW), and rear left (RL) and read right (RR) radars. Figure 5.3 depicts the sensing area and its specification of front mid-range and rear side(left) radars. The FL and BL sensors can detect vehicles driving in the same lane, whereas FW sensor and both rear side sensors (RL and RR) can detect vehicles in the side lanes. The vehicle detecting performance of radars depends on their sensing ranges and angles. In this section, we describe how

radars detect vehicles on multiple lanes and how we use this capability in the proposed traffic density estimation method.

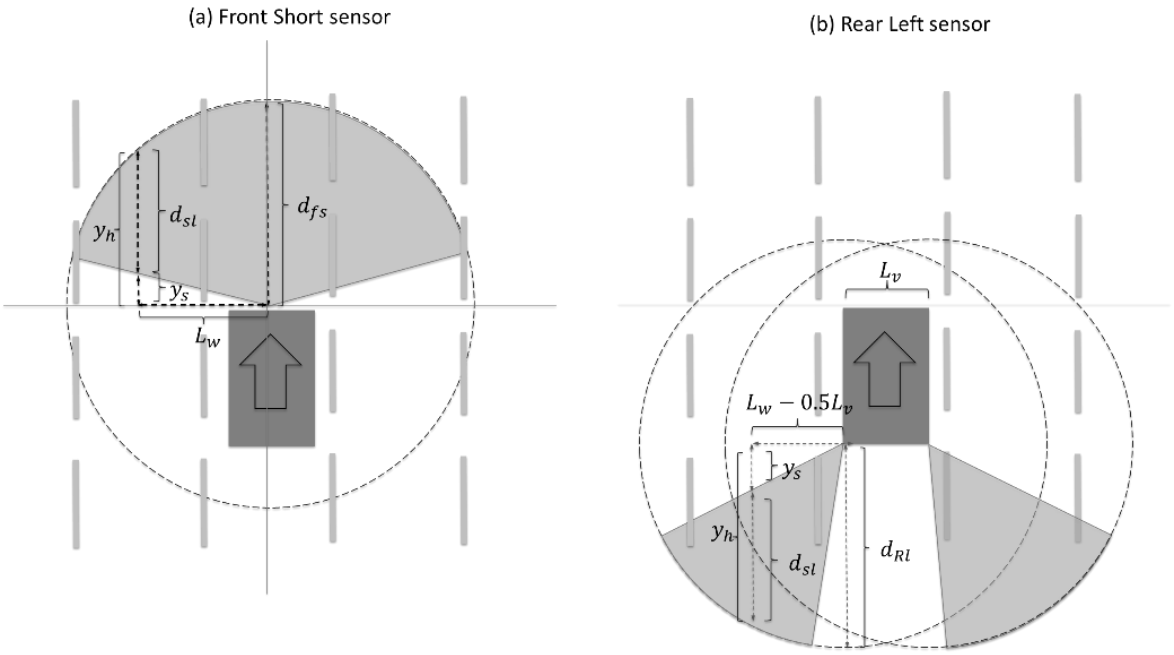

Figure 5.3 Vehicle sensing ranges for multiple lanes

Eq (5.12) - Eq (5.14) illustrate how the sensing range of a side lane for FW is calculated. The detection range of FW is wide enough that vehicles driving beside a CAPV can also detect adjacent vehicles. However, it is evident that the sensing range on side lanes are shorter than a sensor's direction because of the sensor's effective pulse length and its radiation angle. Firstly, radar detection distance of a side lane (y_h) is shorter than the corresponding detection distance on the driving lane. Furthermore, a CAPV has shaded areas (y_s) that a radar cannot cover due to the radar radiation angle as shown in Figure 3. Here, L_w is lane width and θ_s is sensing range. Thus,

assuming that a CAPV drives along the centerline of a lane and the sensing range of FW sensor (θ_s) is wide enough to detect vehicles in nearby lanes, an effective detection distance of the side lane (d_{sl}) is a radar detection distance of the side lane (y_h) minus an average distance of shaded area (y_s) as calculated in Eq (5.13). Effective sensing distance of a side lane for rear sensors can be calculated similarly.

$$y_h = \sqrt{d_{fw}^2 - L_w^2} \tag{5.12}$$

$$y_s = L_w \tan\left(\frac{\pi}{2} - \frac{\theta_s}{2}\right) \tag{5.13}$$

$$d_{sl} = \begin{cases} y_h - y_s & \text{if } sl \text{ is a co-directional lane} \\ 0 & \text{if } sl \text{ is an opposite lane} \end{cases} \tag{5.14}$$

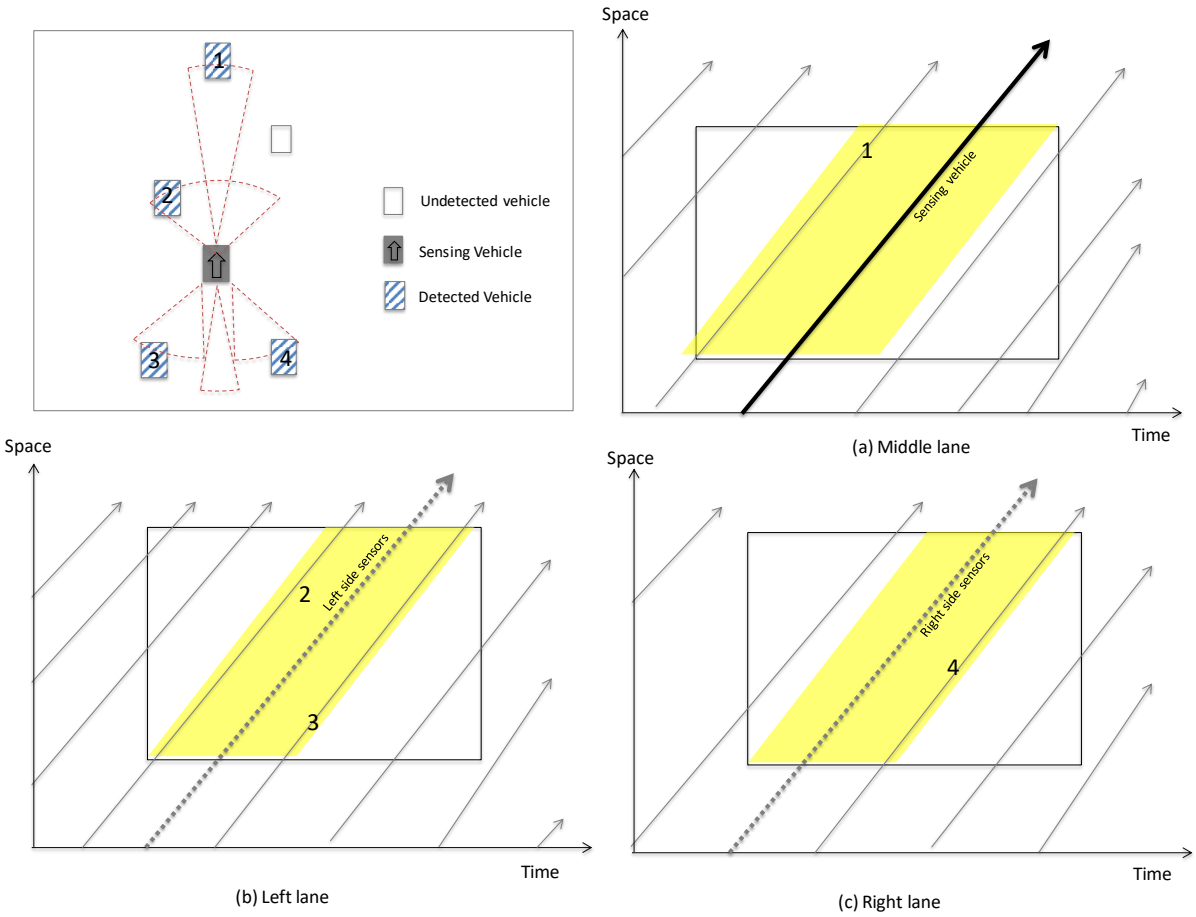

Figure 5.4 Time-space diagram example of Vehicle detections for multiple lanes

By regarding the effective detection distance of side lane (d_{sl}) as an effective sensor distance (d_s), we can estimate a time-space domain from Eq (5.11) with a set of multiple sensors. We have discussed how multiple sensors of a CAPV can detect adjacent vehicles even if they are not in line with the CAPV. Figure 5.4 shows the example of vehicle detection in such a case. There are five vehicles near a CAPV traveling on the middle lane. Out of the five vehicles, four vehicles are detected, whose trajectories are depicted in Figure 5.4. The shaded area in each graph indicates the time-space domain of the sensing area of each lane. Some trajectories of vehicles will be sampled

in the road section as a CAPV drives on a road stretch with sensors. From the captured trajectories in the shaded area, we can calculate traffic density by summing up all detected vehicles travel times inside the shaded area as shown by Eq (5.11).

5.7 Evaluation of Proposed Algorithm

The accuracy of any probe-based traffic estimation algorithm is highly dependent on diverse factors such as the market penetration rate (MPR) of probe vehicles, surrounding environment, and level of service. Obtaining ground truth data for comparison in the real world is time-consuming and prohibitively expensive since capturing every vehicle's trajectory is not feasible. The trajectory data of Next Generation SIMulation (NGSIM) can be an option for basic validation or proof of concept for our algorithm, however in reality, we need a richer source of data to account for all the various scenarios to test in our study. Therefore, we chose traffic simulation as a tool to implement the proposed algorithm and also to get 'ground-truth' data of traffic density which is then used as a basis for comparison with the traffic densities obtained by our algorithm.

In the simulation model, we can set MPR of CAPVs, the road environment, and the performance characteristics of radars. The simulation model has two types of vehicles in terms of sensing capabilities: CAPVs equipped with radar sensing technology, and regular vehicles composed of a representative mix of vehicles such as autos, buses, and trucks without sensing functionality that can be found on a typical urban road network. Each CAPV also sends collected data to a central computing server, which then estimates the road section's traffic density using the proposed algorithm. We employ a commercial microsimulation model called PARAMICS which can depict real traffic conditions at the agent level.

5.7.1 Test Network and Radar Vehicle Configuration

To evaluate our algorithm, we chose a simple network shown in Figure 5.5, comprising a single stretch of freeway with three lanes, containing one origin zone and one destination zone. To simulate traffic congestion, the number of lanes in Link 13 decreases from 3 to 2 so that the bottleneck effect occurs at the connection between Link 11 to Link 13. A real-life equivalent of the lane drop could be roadwork being performed on the outermost lane of Link 13.

The simulation duration for evaluation is one hour. In practice, it has been observed that the simulation software behaves erratically at the boundary conditions, meaning the beginning and end periods of the simulation. To avoid errors occurring due to the edge effects, which usually happen during warm up and clearance time in simulation, the simulation time was set 1.5 hours and the evaluation is conducted only for one hour, starting at 0.1 hours and ending at 1.1 hours. Finally, the total O-D demand was set to 5000 vehicles for the simulation period.

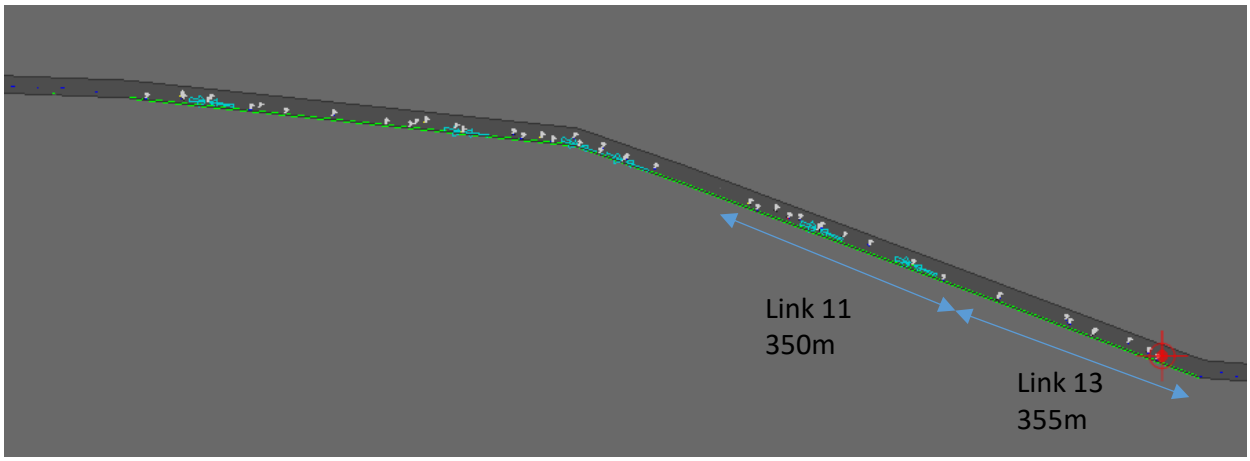

Figure 5.5 Study network and analysis target links

The simulation was run for various proportions of sensor vehicles to evaluate the performance of the proposed algorithm with respect to the MPR of CAPVs. As it is well known, the simulation results are generally affected by the random seed number associated with each simulation run. To get more robust numerical results, we performed multiple simulation runs (10 times) with randomly generated seed numbers. Averaging results from multiple simulation runs produce a tighter bound on the performance of our algorithm and establish more confidence in the validity of our results. The traffic density was updated every 1 minute. The link-level traffic density estimate of any time period that did not contain CAPV data was extrapolated from the previous time step's traffic density estimate.

5.7.2 Simulation Results

The plots in Figure 5.6 display the estimated densities in Link 13 in comparison with the real density over the entire simulation period, for different MPR of CAPV. The blue line indicates the real (i.e., ground truth, Eq 5.7) density that is calculated using the total VHT over the entire time-

space domain of Link 13. The green line indicates traffic densities calculated using the proposed method (Eq 5.11 and Eq 5.14). Finally, the red line represents the density obtained by the Area-based density estimation method (Eq 5.10) that only uses the average local density in the time-space domain.

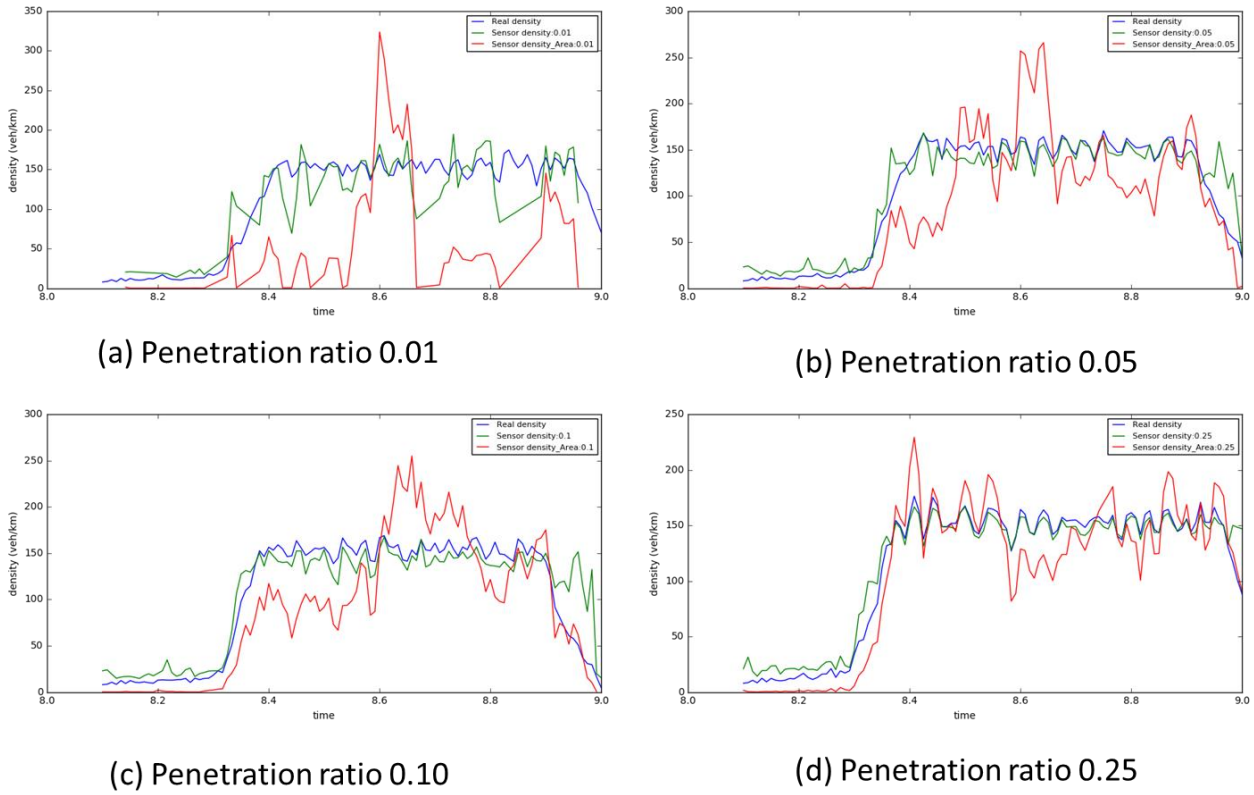

Figure 5.6 Estimated densities in comparison with real density

Overall, the proposed method outperforms the Area-based method at all penetration rates. Even at the lowest penetration case of 1%, the proposed algorithm is more accurate than the Area-based method. Table 6 depicts the performance of the proposed algorithm with respect to root mean square error (RMSE) and relative error (RE) given by the absolute error divided by the observed value. Specifically, its performance is significantly higher when the penetration rate is low. This

high performance is because the proposed method considers the relationship between VHT of detected vehicles and the area of sensing domains whereas the Area-based method only relies on the number of detected vehicles. For instance, the number of detected vehicles is unstable in congested or transitional conditions where stop and go traffic exists. Furthermore, the proposed method considers adjacent geometries such as current driving lane and the availability of side lanes, which area-based estimation methods neglect in their analysis. Although our algorithm performs better in absolute terms as the penetration ratio increases, the relative improvement is not significantly larger after the 5% penetration rate scenario.

Table 6 Summary of evaluations

MPR	RMSE			Relative Error		
	Proposed	Area-based	Improvement (%)	Proposed	Area-based	Improvement (%)
1%	22.81	78.59	71.0	0.21	0.52	60.1
5%	13.93	55.44	74.9	0.20	0.44	54.8
10%	12.09	35.05	65.5	0.21	0.37	43.4
25%	9.84	23.01	57.2	0.20	0.32	38.6

The performance of the proposed algorithm, however, tends to deteriorate during the times when queues are building up and/or clearing as shown in Figure 5.7. A probable reason is that the traffic condition is heterogeneous at the beginning of congestion. In other words, the downstream of the link is severely congested whereas the upstream is still in free-flow condition. In this case, CAPVs are more likely to be located on the congested road section, therefore congestion is more weighted during this period. Similarly, transitional conditions such as queues clearing, the sensed area from different sensor vehicles tend to overlap in the congested region, thereby overestimating the real density.

We also divided the simulation period into various flow regimes to investigate if the accuracy of our density estimation was significantly different in varied conditions. The flow regimes are defined as free flow, a transition from free flow to congested, congested, and queue-clearing conditions at the end of the simulation period. The RMSE results are shown in figure 5.7, which exhibit similar patterns as the overall results shown earlier. The proposed method shows marked improvements in steady state traffic conditions.

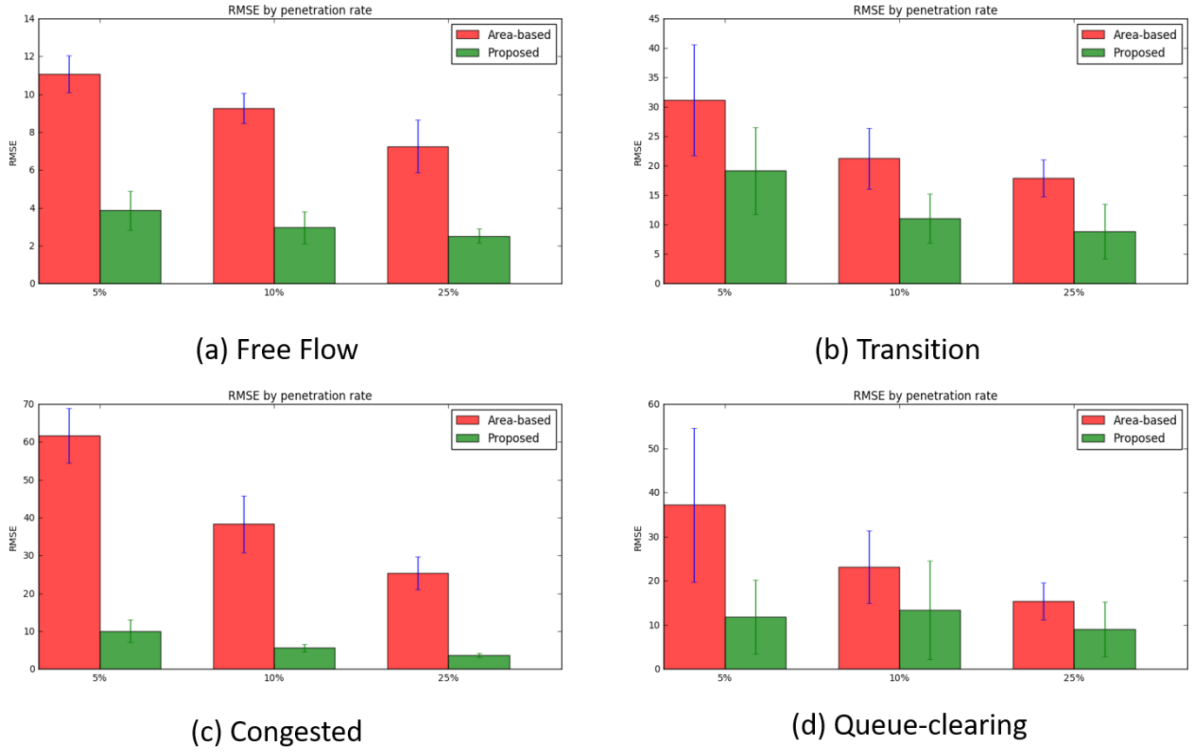

Figure 5.7 RMSE comparisons by flow regime

5.8 Discussion

In the previous sections, we outlined a new algorithm for estimating traffic density using CAPVs. Instead of accounting for only the number of vehicles in the sensing area, we also consider Edie's definition to calculate traffic density from vehicle trajectories such as vehicle hours travelled in the Euclidian time-space domain. This is a novel approach because previous methods rely upon simple linear conversion factors to translate vehicles per square kilometer into vehicles per kilometer. The proposed method technically considers other factors such as geometries, sensing distance, vehicle speed, and dynamics of traffic flow. Additionally, we have extended our method to multiple lane scenarios. The proposed algorithm was tested on simple networks by using microscopic simulation (PARAMICS) and its APIs. Measures of effectiveness such as RMSE and Relative Errors, were computed for various radar-vehicle market penetration rates of 1%, 5%, 10%, and 25%. The proposed algorithm shows promising results, outperforming the naive Area-based method in almost all scenarios and all traffic flow regimes.

5.9 Deep Learning Approach to Traffic Estimation

Although the previous method can capture traffic states during stationary traffic conditions such as non-congested and fully congested conditions, it is vulnerable during flow transition periods. Specifically, the performance deteriorates during the onset of congestion and queue-clearing conditions, in comparison with its performance in other states. From multiple experiments, we found that the over-estimating relationship has distinctive patterns. This pattern is nonlinear and highly situation-dependent, therefore could be studied using Machine learning algorithms, which learn non-linear patterns from all possible features.

5.9.1 Background

The capabilities of Deep Learning algorithms are increasingly being recognized in the fields of traffic estimation and prediction (Li et al., 2017; Ma et al., 2015; Polson and Sokolov, 2017; Tian and Pan, 2015; Yi et al., 2017). One common conclusion that has emerged in the field of traffic flow prediction is that deep learning methods are successfully able to identify nonlinearity of traffic flow according to time and time-lag characteristics, and that deep learning algorithms can accurately predict traffic fundamentals. Recurrent Neural Networks (RNN) (Rumelhart et al., 1986) have been utilized by (Li et al., 2017; Liu et al., 2006; Oh et al., 2005; van Lint et al., 2005) to predict traffic flows from prior traffic condition. RNN models, however, have a well-known limitation known as the "Vanishing Gradient Problem". Due to this property, the effect of the prior steps' traffic conditions tends to drastically weaken over time, thus deterring the implementation of time-lag properties of traffic dynamics. (Ji and Hong, 2019; Li et al., 2017; Ma et al., 2015; Tian and Pan, 2015) point out this property and recommend Long-Short Term Memory Neural Networks (Hochreiter and Schmidhuber, 1997), a scheme within the broad category of deep learning methods, as an effective tool to counteract this problem. They report that this LSTM approach could result in better estimation of traffic conditions and can better capture the time-lag properties of traffic dynamics.

Most recent LSTM applications in transportation research, however, focus on a traffic condition prediction where ground truth values at a certain location in prior timesteps are given and the model predicts the traffic condition of the next time step. In other words, the scope of contemporary research has been the prediction of traffic density at pre-defined fixed-point detectors. However, our scope of traffic density estimation is potentially network-level since our source of data are

CAPs that travel throughout the network. With an assumption that we do not have a sectional level of ground truth traffic densities at every timestep, the proposed model estimates the ground truth traffic density by utilizing data from vehicles sensor and geo-spatial information. Thus, our traffic estimation process does not include previous step's ground truth traffic densities as input variables. We propose a multivariate input variable-based LSTM neural network model that is explained in detail in the following section.

5.9.2 Deep Learning-based Estimation Framework

The following figure shows the conceptual framework of the proposed methodology. Hereinafter, we will call the proposed model as STREAM-LSTM (Simulation-based TRaffic density Estimation AlgorithM-Long-Short Term Memory). A traffic management center collects various pieces of information from CAPs passing a road section every 0.5 seconds and stores the data in a moving time horizon window vector of n time steps. In our study, we set the moving horizon to be 5-time steps. Traffic density is highly affected by prior traffic conditions. The time-horizon window has a pattern that are captured by CAPs during the moving horizon. We call this pattern a "Sensor Signature". The LSTM network (Tian and Pan, 2015) recognizes the current signature (input layer) and previous time step's layer pattern (LSTM layer). The advantage of employing LSTM networks in this context is that they do not suffer from the well-known "vanishing gradient" problem (Ma et al., 2015; Polson and Sokolov, 2017; Tian and Pan, 2015). Simply stated, this means that they can consider not only quite recent prior conditions but also relatively longer prior conditions, as the phrase "Long Short-Term memory" implies. Our proposed framework takes the advantage of the memory layers that automatically determine the time lag between input and output. In traffic estimation domain, traffic conditions collected from CAPs might be locally biased

since CAPs only capture adjacent traffic conditions. In other words, there exists a time lag between a CAP and actual traffic density when traffic is in transional period. Furthermore, some CAPs approaching congestion can be used as an indicator of increasing density. LSTM recognizes those time-lag conditions using temporally-varying Sensor Signatures.

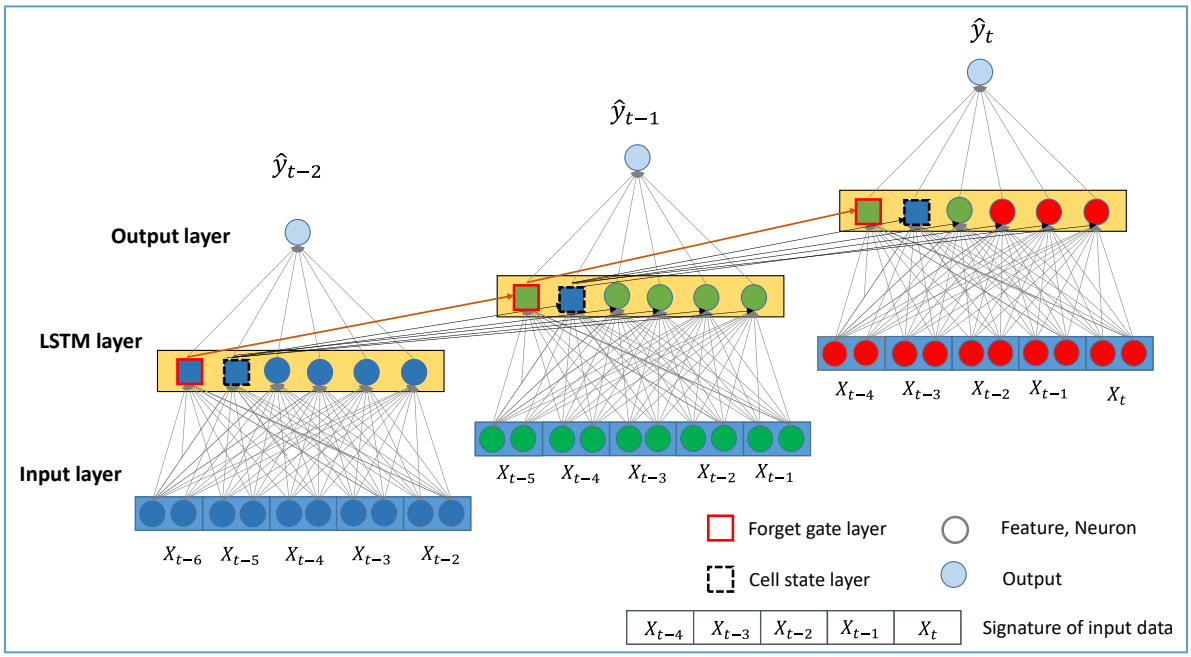

Figure 5.8 Design of LSTM for signature data

This model can take multiple features as input variables from CAPs as shown in Figure 5.8. The model input vector at t is denoted as $x_t = (x_{1,t}, x_{2,t}, x_{3,t}, \cdots, x_{\tau,t})$. A neuron (i_t) in the input layer at time t (Equation 5.15) consists of an input $(x_{i,t})$, a hidden vector of previous time step (h_{t-1}), weights for the two vectors (W_i, U_i), and bias b_i. To reflect time-relevant characteristics in the data, this model uses a "forget gate layer" (Equation 5.16) and a "cell state layer" (Equation 5.17) to store temporal information which is the output of neuron states in the previous time step. Forget layer f is called a transfer function that is determined to be either forgotten or alive from the

previous states by cell state layer. For example, the forget layer in our method determines the time period of considering time lags between sensor input and traffic density. If the sensor data of past time periods does not affect the density of the current time step, the cell state layer decides to not use the forget layer. The function can take any form such as linear, sigmoid, tanh, or ReLU. From each neuron state, density is estimated by Equation (5.18).

$$i_t = \sigma_g(W_i x_{\ i,t} + U_i h_{t-1} + b_i) \quad \text{Eq (5.15)}$$

$$f_t = \ \sigma_g\left(W_f x_t + U_f h_{t-1} + b_f\right) \quad \text{Eq (5.16)}$$

$$c_t = f_t \circ c_{t-1} + i_i \circ \sigma_c(W_C x_t + U_c h_{t-1} + b_c) \quad \text{Eq (5.17)}$$

$$\hat{y}(t) = f(\sum_i^I w_i n_i(t) + b_o) \quad \text{Eq (5.18)}$$

where

x_t: Input vector at t

h_{t-1}: a hidden vector of previous time step

i_t : Input layer at t

c_t: Cell state layer at t

f_t : Forget gate layer at t

$\hat{y}_t$: Estimated output at t

σ_h, σ_y: Activation function

W_h, U_h: Weights of a layer h (it plays a role in connecting perceptrons among layers)

b_h, b_c, b_o: Bias vector

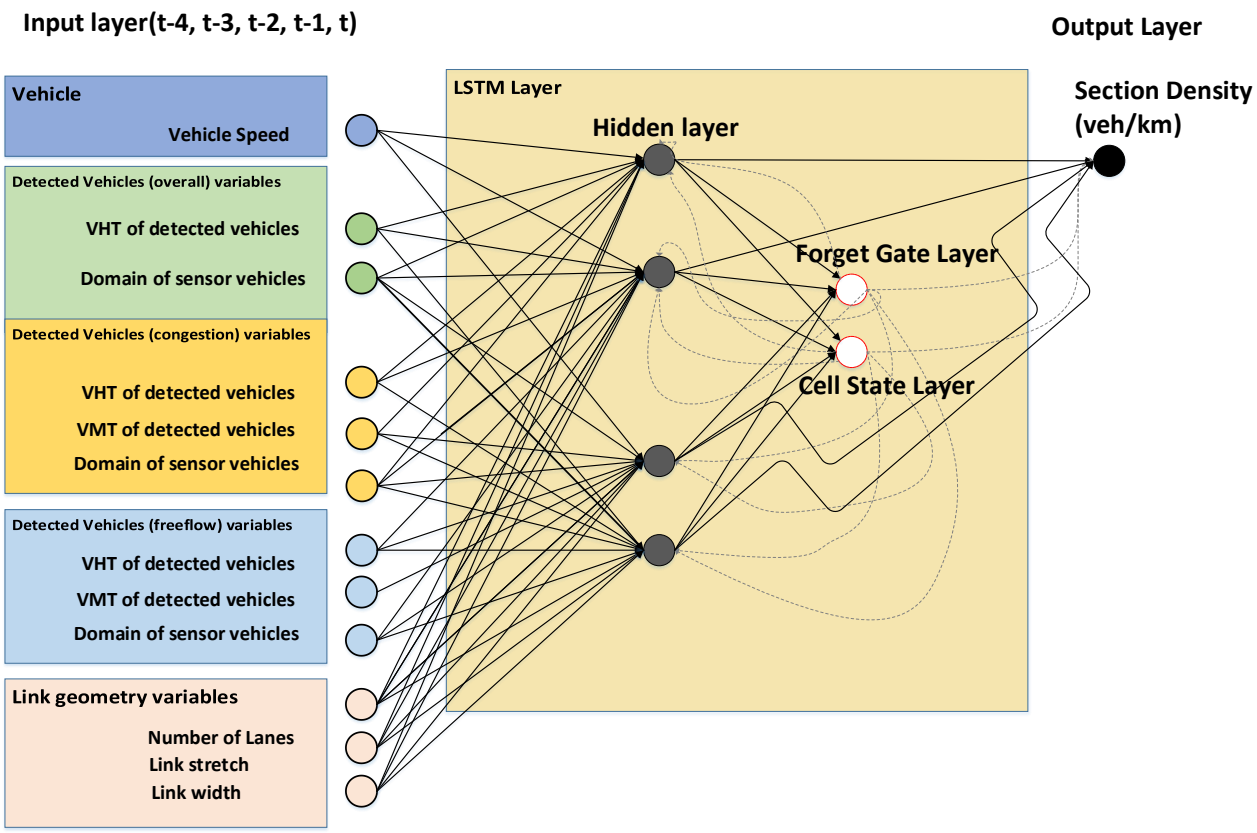

Figure 5.9 Input-output variables and LSTM network design

After multiple experiments, we select various input variables that are known to have an effect on traffic density, as shown in Figure 5.9. First, we consider the travel speed of a sensor vehicle. We refer to the well-known Edie's definition that traffic density is a function of vehicle travel time over a time-space domain. The traffic pattern in non-congested conditions is significantly different from that in congested conditions, as can be seen in Figure 5.10. With this insight, we categorize the traffic condition into two regimes and calculate the variables (VHT, VMT, Sensor time-space domain) in each traffic regime. We set the congestion criterion of the expressway in this study to 80 km/hour.

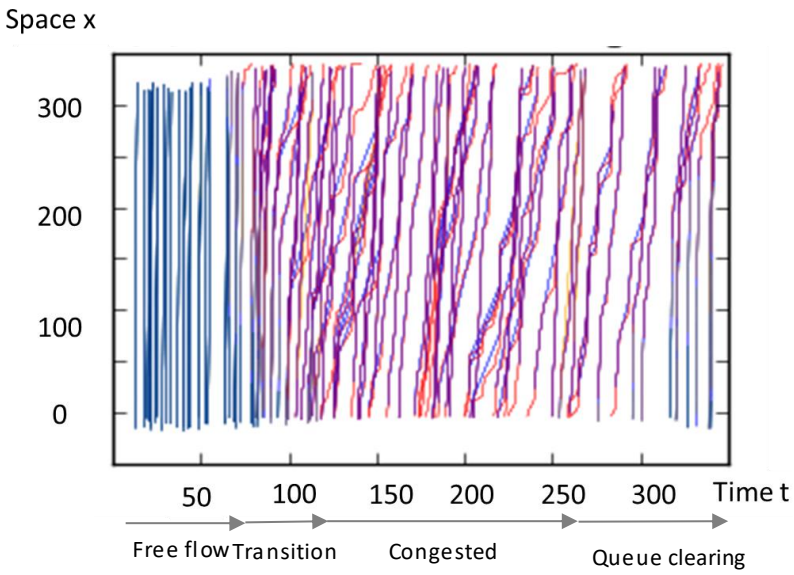

Figure 5.10 Vehicle trajectory variation according to the congestion level

5.9.3 Simulation Environment

This research evaluates the proposed method by using a microscopic simulation program (PARAMICS). The testbed for our evaluation is a simple traffic network used in the previous section, hereafter called the hypothetical network. This network contains one single stretch of freeway, with 3 lanes, and one origin-destination pair. The entire simulation period is set to be 1.5 hours, out of which the first 0.25 hours and the last 0.25 hours are discarded due to the peculiarities of the simulation software where we have previously observed erratic vehicle behavior around the boundary conditions (beginning and end of the simulation). The period of evaluation is set to be the middle 1 hour.

The demand on this O-D pair is set to be 5000 vehicles for the simulation period. For our study, congestion is artificially induced in the network by dropping the number of lanes abruptly from 3

lanes on link 13 to 2 lanes on its immediate downstream link 11. The network was simulated for different market penetration of sensor vehicles, and for various sensor-vehicle characteristics, such as sensing distance, target angle, etc.

5.9.4 Results

The complete dataset is segregated into two parts: training data and test data. These datasets contain information collected by the CAPs and have both static (link geometry) and dynamic (vehicle sensed, link flow, etc.) information. The training dataset is used by the model to build relationships between link density and data from CAPs. The trained model is then deployed on the test data to evaluate its accuracy. This procedure is repeated for different market penetration ratios.

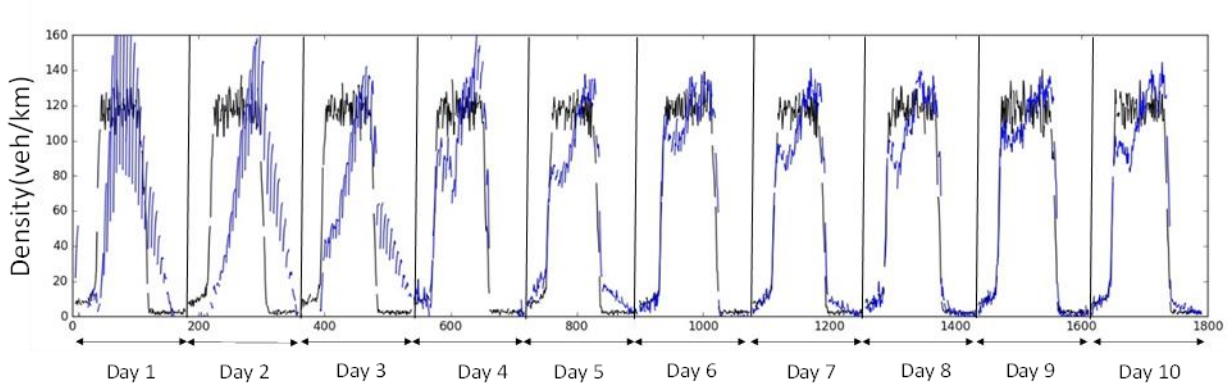

Figure 5.11 (a) Training Process for day 1 to 10 (link 13)

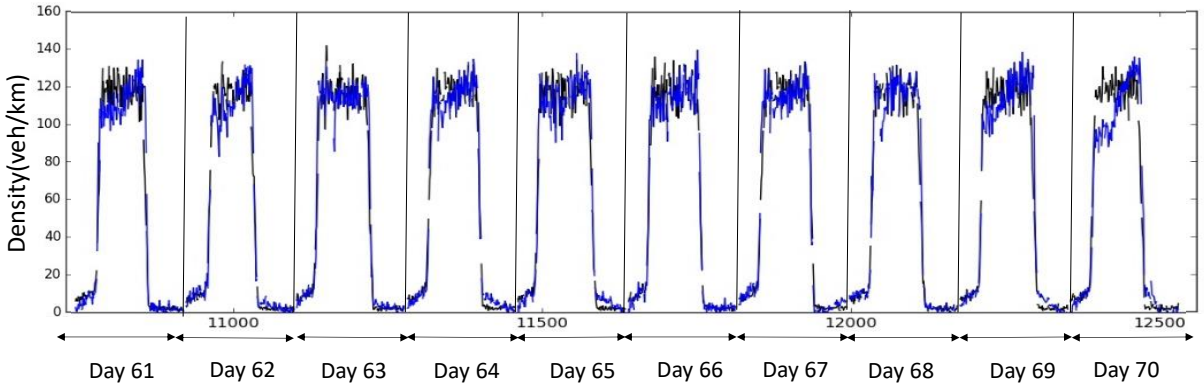

Figure 5.12 (b) Training process for day 61 to 70 (link 13)

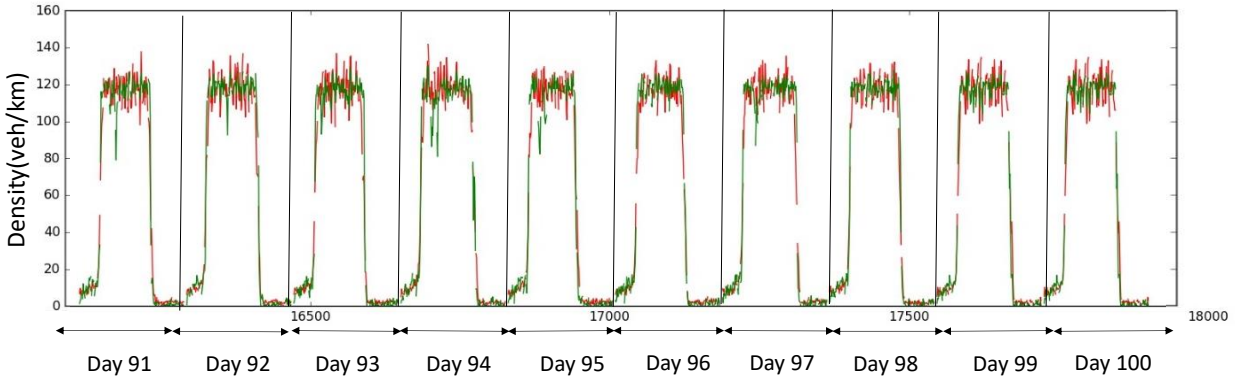

Figure 5.13 (c) Test results for day 91 to 100 (link 13)

Figures 5.13 (a), (b), and (c) shows how the model is trained on data obtained from a specific link (link# 13) on a simple hypothetical network, when the sensor vehicles have a market share of 25%. The x-axis and y-axis represent learning time and estimated densities, respectively. Note that the data here are simulated, which means data from different training runs could conceivably be thought of as traffic data from different days. Real density is shown in the black line, while the estimated density is shown in blue in Figures 5.13 (a) and (b), and green in Figure 5.13 (c). Specifically, Figure 5.13 (a) shows the training over the first 10 days. We can see that in the first few runs, the algorithm is not very accurate in estimating density, but that is to be expected, as it

needs more data to correct itself. The degree of accuracy is significantly improved from repeated learning (Figure 5.13 (b)), as is evident from noting the difference between Run # 1 and, say, Run# 6 onwards.

Figure 5.14 indicates the estimated densities averaged over the test runs of our proposed method in comparison with STREAM, which uses Edies's generalized definition detailed in Equation (1). The performance of the STREAM-LSTM is compared with that of a density estimation method of STREAM. The proposed methodology shows an improvement over Edie's method (STREAM). The simulation period of one hour is characterized by various flow regimes and it would be instructive to observe the performance of our algorithm in different traffic conditions.

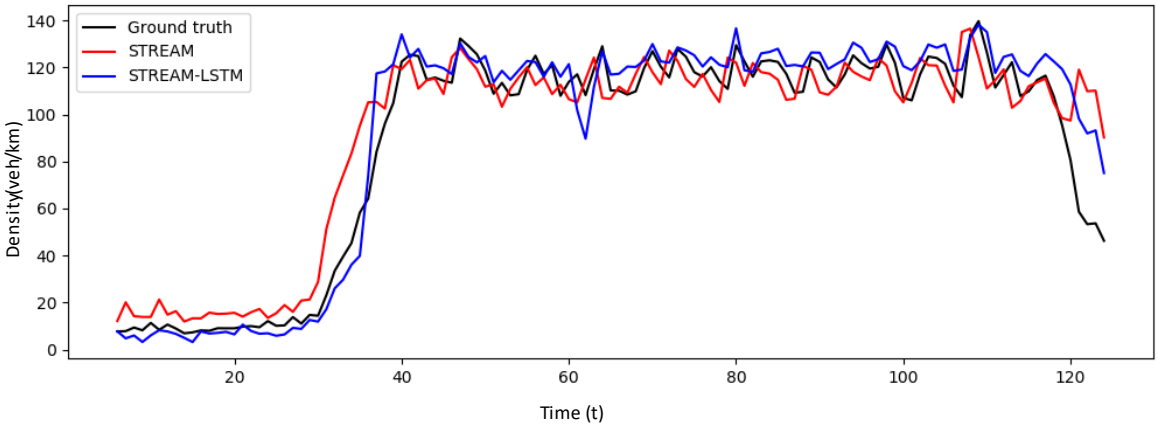

Figure 5.14 Overall comparisons between the proposed STREAM-LSTM and STREAM

The simulation period can be roughly divided into four flow regimes: free-flow conditions, transition from free flow to congested conditions, congested condition, and queue clearing condition at the very end (Figure 5.14). As expected, STREAM (red line) tends to estimate traffic density poorly at the onset of congestion and during queue clearing conditions. Our model

accurately estimates traffic density in Free-flow, Transition, and Congested conditions (Figure 5.15). Although overestimation still remains a problem in the Queue clearing condition, the STREAM-LSTM method converges to the actual density faster than STREAM.

Our evaluation results confirm that the proposed method performs better than previous methods. This is because our proposed method fully utilizes the signature of multiple information gathered from multiple CAPs. Additionally, LSTM Neural Networks can efficiently memorize the relationship between the signature and time-lag characteristics of traffic densities.

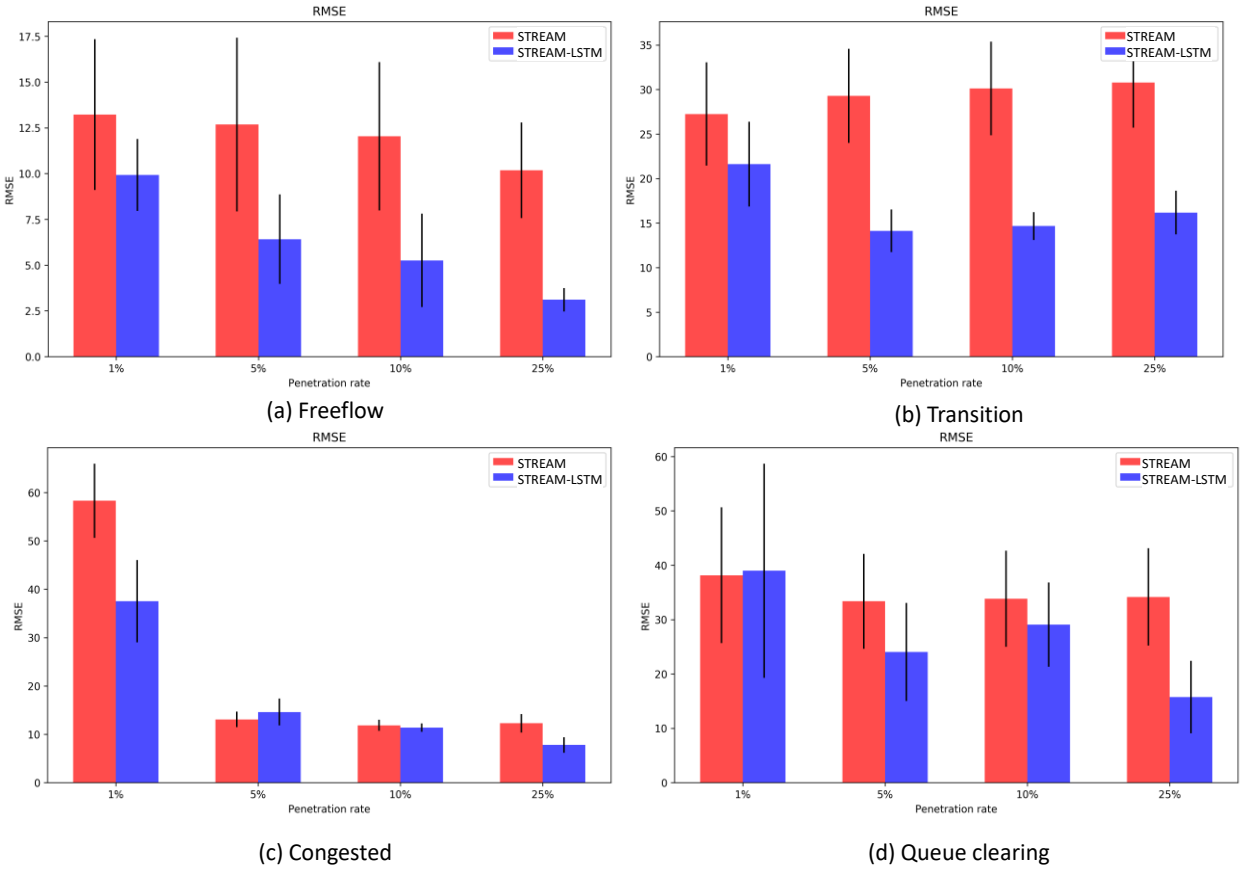

Figure 5.15 RMSE comparison in different flow regimes

By means of comparison, we also calculated the estimated densities on link 13 over the same test dataset using Edie's definition. The numerical values for Root Mean Squared Error and Relative Error using both methods at different penetration rates are shown in Table 7. The performance gets better as the penetration rate increases, with an almost 45% improvement in RMSE and 66% improvement in Relate Error in the 25% market penetration scenario.

Table 7 Evaluation results for the proposed method (link 13)

Penetration rate	RMSE			Relative Error		
	STREAM-LSTM	STREAM	Improve (%)	STREAM-LSTM	STREAM	Improve (%)
1%	32.69	49.15	33.50	0.36	0.50	27.80
5%	14.08	16.29	13.54	0.18	0.30	40.14
10%	12.12	15.69	22.74	0.15	0.30	49.68
25%	8.88	15.97	44.36	0.11	0.34	66.11

5.9.5 Discussion

In this chapter, we proposed two approaches for estimating traffic states, including a Deep Learning LSTM approach, which is a non-parametric method to estimate traffic density. This research was partially motivated by CAPs technology and current research literature on probe-based traffic density estimation methods. Our simulation analysis shows that a mathematical algorithm (STREAM) tends to overestimate density in certain traffic conditions. This study proposes a method to estimate the traffic density for a single link using a STREAM-LSTM model. The performance of the STREAM-LSTM method is compared with that of a density estimation method of STREAM.

Our model accurately estimates traffic density in Free-flow, Transition, and Congested conditions. Although overestimation still remains a problem in the queue clearing condition, the STREAM-LSTM method converges to the actual density faster than STREAM. This is because our proposed method fully utilizes the signature of multiple information gathered from CAPs. The other reason is that LSTM Neural Network can efficiently memorize the relationship between the signature and time-lag characteristics of traffic densities. Our research focuses on the accuracy of traffic density estimation in the domain of CAPs and evaluate the proposed method by multiple simulation runs. Statistically reliable information is also an important aspect in traffic management and advanced traffic information systems. There are reasonable methods to capture reliability such as Monte-Carlo simulations, which is a direction for our future research. Factors affecting traffic conditions such as geometry and heterogeneity of vehicles have not considered in this study, but are under consideration in our current and future research.

It is evident that the traffic characteristics of traffic flow on one link have an impact on those nearby links. Therefore, it stands to reason that if we formulate these relationships between links and present those as additional input data to our LTSM model, its accuracy can be expected to improve.

Chapter 6. Conclusions and Future Research

Vehicles equipped with wireless communication technologies and advanced driver assistance systems present an opportunity for futuristic mobility platforms to relieve traffic congestion by making better use of existing capacity and promote equity. In this dissertation, we presented a decentralized lane-based negotiation framework under which lower VOT vehicles can trade their positions in time and space to higher VOT vehicles in exchange for monetary benefits. We first presented a proof of concept using simulation and found such negotiations to have a positive impact on traffic under certain levels of market penetration. We used an agent-based Dynamic Traffic Assignment model to optimize this system and compute the optimal set of benefits to be distributed to trading vehicles. The system was optimized using a bi-level framework in which time-dependent origin-destination flows were computed by a dynamic traffic assignment model, using a gradient projection algorithm. The output from this module was then used to minimize the "envy" in the system accruing from vehicles who were prescribed inferior routes. Numerical results from running our optimization scheme on an illustrative off-ramp network show that the proposed model converges to both envy-free and system optimum traffic states, even at a net zero budget, meaning this system can be used by transportation agencies without exacting tolls or giving subsidies.

Our proposed framework of routing vehicles on a lane-to-lane basis can only be realized in the field if the mediating agency (TMC, or a mobility service) has accurate information about real-time traffic conditions. We propose multiple algorithms, including a LSTM (Long Short Term

Memory) neural network architecture-based framework to estimate real-time traffic states solely using information collected from sensor-equipped probe vehicles, without the need for any other data such as those obtained from traditional embedded loop detectors. Measures of effectiveness such as RMSE and Relative Errors, were computed for various radar-vehicle market penetration rates of 1%, 5%, 10%, and 25% and numerical results show a clear advantage of our proposed algorithms over existing schemes.

In addition, because traffic density has a close relationship with other fundamental traffic flow variables such as flow and speed, a high degree of accuracy in the estimation of density brings us one step closer to more accurately estimating these other performance indicators as well. Our results show that the proposed model outperforms existing methods. However, there is still variation in its performance under different traffic conditions. There are some traffic conditions, such as queue clearing, where the proposed model's performance is better than mathematical models, but not by a significant amount. Our model can also be extended, without significant computational overhead, to a multiple link scenario. The proposed method can be used in the real-time lane-wise queue-length estimation and prediction in urban road networks. These should serve as crucial inputs for the safety and efficiency of CAV-based mobility platforms in the near future.

In the following sections, we propose some extensions of our current research and directions for future research.

6.1 Integrated Mobility Framework

An immediate extension of our work is to integrate the different parts outlined in the dissertation into a single, comprehensive framework. At present, the lane-change negotiations happen in a

microsimulation model, but the optimization and traffic-state estimation frameworks are standalone, and not connected to each other. One insight we gained from this research – perhaps too late – is that the choice of microsimulation model is crucial. While commercial simulation software platforms provide attractive GUIs and ease of use, they do so at the expense of flexibility. For our detailed mobility framework to be built in a single, integrated environment, we need to have absolute control of every single aspect of vehicle behavior. This, unfortunately, is wellnear impossible in most commercial platforms, despite the developers' claims. Our immediate future research involves porting all the existing modules of our framework to an open-source software environment, in which it would be easier to carry out traffic simulation, dynamic optimization, and machine learning techniques in real time, using a single programming language.

6.2 Traffic Management Agency Tools to Recommend P2P Negotiations

We proposed an expanded network in our optimization scheme to allow for lane changes between the middle lane and the rightmost lane. For such ad hoc schemes to be possible in the real world, we need to have more detailed studies to determine under what traffic conditions such lane changes can occur safely. A promising approach is to generate large datasets from simulation and use those data in a reinforcement learning framework to gain insights into the complex interactions between CAV and non-CAV vehicles in mixed autonomy traffic, and how they are affected by traffic conditions, roadway geometry, and other factors. We envision various applications of this work – for example, the development of traffic management tools that inform transportation agencies of optimal times and locations where such negotiations may take place.

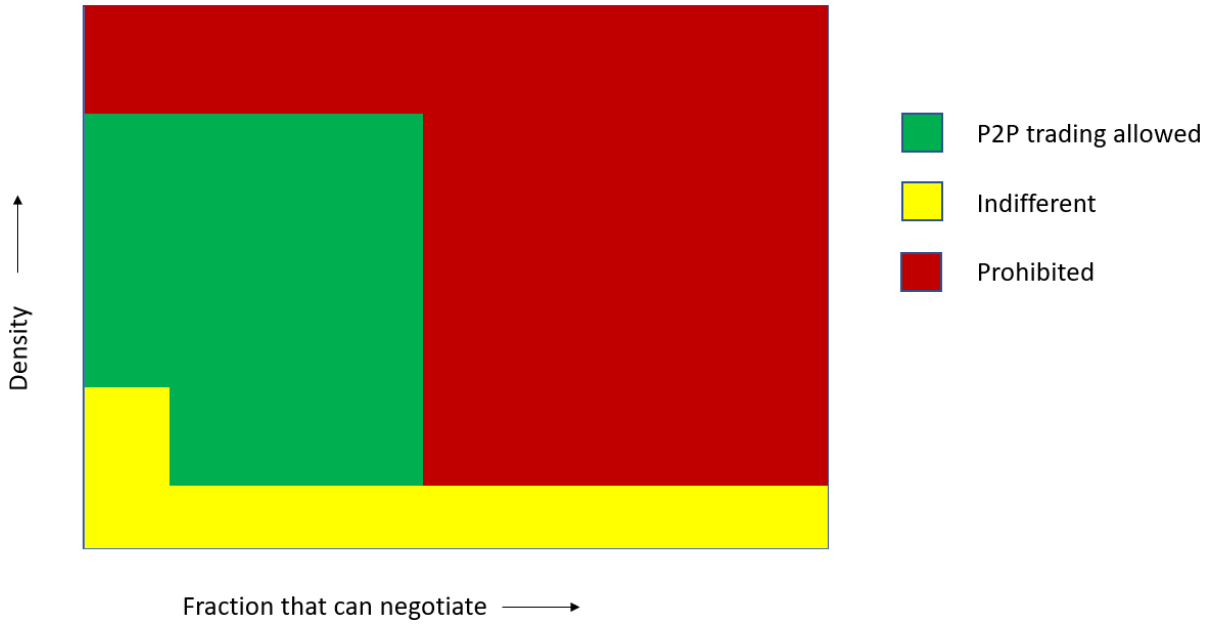

Figure 6.1 Conceptual decision tool for allowing Peer-to-Peer lane changes

6.3 Area-Based Negotiations Involving Multiple Vehicles

In our study, we only focused on the negotiation between a high VOT driver who wants to "cut in line" and a lower VOT driver who trades their spot by slowing down, in exchange for benefits. However, in reality, when a vehicle slows down, it also slows down the vehicles behind it. Our present framework only allows for benefits to be distributed to the first vehicle, with no compensation to the vehicles behind it. As such, a fairer pricing mechanism needs to take this into account.

6.4 Broadening the Scope of Agents for Futuristic Mobility Services

The widely understood definition of agents in agent-based models is one where agents are singular entities, with certain heterogeneous characteristics, control inputs, and goals. In the context of

future mobility services, this definition needs to be challenged and expanded. We live in an era of a rapidly changing mobility landscape, where the concept of vehicle ownership is itself in flux. Ownership can be individual, fractional, or fleet-based. In such scenarios, negotiations between agents takes entirely new forms, and needs to be studied. Furthermore, to realistically situate future mobility services within Smart Cities, we need to expand the definition of agents to include infrastructure (signal controls, sensors, etc.) and model all the complex interactions between various classes of agents in a network. On a larger scale, we understand transportation systems to be multi-modal in nature, and with multiple stakeholders. Future agent-based models, therefore, should reflect these characteristics.

6.5 Extending the Framework to Incorporate Environmental Considerations

Currently, the heterogeneous nature of agents in the system is defined based on value of time. A future direction of research would be to incorporate emissions in the pricing framework. For instance, an electric vehicle slowing down and changing lanes has a smaller carbon footprint than a gas-powered vehicle performing the same action. This has direct implications on the pricing and optimization structures. Future research can go in the direction of objective function formulations in which the total number of lane changes per unit distance is restricted for some vehicles, or price-matching mechanisms where different classes of vehicles are offered different benefits in negotiations.

6.6 Extensions of Envy Proxies for Equity Considerations

The current definition of envy as proposed by Nam et al., (2017) is one in which agents can only compare their valuations with other agents who have the same origin and destination. This is a reasonable definition that serves as a suitable proxy for inequities in the network resulting from

some agents in the network being prescribed sub-optimal path alternatives. However, it may be worthwhile to explore if other proxies of equity can be devised. We propose a candidate scheme where, in addition to the existing envy minimization, agents also perform a “local” comparison with other agents traveling on the same link as them, at the same time as them.

References

Al-Sobky, A.S.A., Mousa, R.M., 2016. Traffic density determination and its applications using smartphone. Alexandria Eng. J. 55, 513–523. https://doi.org/10.1016/j.aej.2015.12.010

Ali, Y, Haque, M.M., Zheng, Z., Washington, S., Yildirimoglu, M., 2019. A hazard-based duration model to quantify the impact of connected driving environment on safety during mandatory lane-changing. Transp. Res. Part C Emerg. Technol. 106, 113–131. https://doi.org/10.1016/j.trc.2019.07.015

Ali, Yasir, Zheng, Z., Haque, M.M., Wang, M., 2019. A game theory-based approach for modelling mandatory lane-changing behaviour in a connected environment. Transp. Res. Part C Emerg. Technol. 106, 220–242. https://doi.org/10.1016/j.trc.2019.07.011

Asadi, B., Vahidi, A., 2011. Predictive cruise control: Utilizing upcoming traffic signal information for improving fuel economy and reducing trip time. IEEE Trans. Control Syst. Technol. 19, 707–714. https://doi.org/10.1109/TCST.2010.2047860

Barceló, J., Casas, J., Ferrer, J.L., García, D., 1999. Modelling Advanced Transport Telematic Applications with Microscopic Simulators: The Case of AIMSUN2, in: Traffic and Mobility. pp. 205–221. https://doi.org/10.1007/978-3-642-60236-8_14

Beckmann, M., McGuire, C.B., Winsten, C.B., 1956. Studies in the Economics of Transportation. Yale University Press: New Haven.

Ben-elia, E., Ettema, D., 2009. Carrots versus sticks : Rewarding commuters for avoiding the rush-hour — a study of willingness to participate Faculty of Geosciences Key Words :

Abstract This paper deals with the potential participation in a reward scheme to avoid 16, 68–76.

Boyce, D., Xiong, Q., 2009. User-Optimal and System-Optimal Route Choices for a Large Road Network. Rev. Netw. Econ. https://doi.org/10.2202/1446-9022.1058

Brams, S.J., Taylor, A.D., 1996. Fair Division: From Cake-Cutting to Dispute Resolution. Cambridge Univ. Press.

Burris, M.W., 2003. The toll-price component of travel demand elasticity. Int. J. Transp. Econ.

Cameron, G.D.B., Duncan, G.I.D., 1996. PARAMICS - Parallel microscopic simulation of road traffic. J. Supercomput. 10, 25–53. https://doi.org/10.1007/BF00128098

Chiu, Y., 2014. Active Traffic and Demand Management System.

Choudhury, C.F., Email, T.F., Ben-akiva, M.E., Rao, A., 2006. Modeling Cooperative Lane Changing and Forced Merging Behavior. Transp. Sci. 1–16.

Choudhury, C.F., Ramanujam, V., Ben-Akiva, M.E., 2009. Modeling Acceleration Decisions for Freeway Merges. Transp. Res. Rec. J. Transp. Res. Board 2124, 45–57. https://doi.org/10.3141/2124-05

Daganzo, C.F., 1997. Fundamentals of Transportation and Traffic Operations, Fundamentals of Transportation and Traffic Operations. https://doi.org/10.1108/9780585475301

Dial, R.B., 1999. Network-Optimized Road Pricing: Part II: Algorithms and Examples. Oper. Res. 47, 327–336. https://doi.org/10.1287/opre.47.2.327

Edie, L., 1965. Discussion of traffic stream measurements and definitions. Proc. Second Int. Symp. Theory Traffic Flow, London 1963.

Edie, L.C., Herman, R., Lam, T.N., 1980. Observed Multilane Speed Distribution and the Kinetic Theory of Vehicular Traffic. Transp. Sci. 14, 55–76. https://doi.org/10.1287/trsc.14.1.55

Fritszhe, H., 1994. A model for traffic simulation. Traffic Eng. Control 35, 317–321.

Gafarian, A. V, Munjal, P.K., Pahl, J., 1971. An experimental validation of two Boltzmann-type statistical models for multi-lane traffic flow. Transp. Res. 5, 211–224. https://doi.org/10.1016/0041-1647(71)90022-0

Gerdts, M., Karrenberg, S., Müller-Beler, B., Stock, G., 2009. Generating locally optimal trajectories for an automatically driven car. Optim. Eng. 10, 439–463. https://doi.org/10.1007/s11081-008-9047-1

Gipps, P.G., 1981. A behavioural car-following model for computer simulation. Transp. Res. Part B 15, 105–111. https://doi.org/10.1016/0191-2615(81)90037-0

Hartline, J., Yan, Q., 2011. Envy, truth, and profit, in: Proceedings of the ACM Conference on Electronic Commerce. ACM Press, New York, New York, USA, pp. 243–252. https://doi.org/10.1145/1993574.1993612

He, F., Yin, Y., Shirmohammadi, N., Nie, Y.M., 2013. Tradable credit schemes on networks with mixed equilibrium behaviors. Transp. Res. Part B Methodol. 57, 47–65. https://doi.org/10.1016/j.trb.2013.08.016

Helbing, D., 1996. Gas-kinetic derivation of Navier-Stokes-like traffic equations. Phys. Rev. E - Stat. Physics, Plasmas, Fluids, Relat. Interdiscip. Top. 53, 2366–2381. https://doi.org/10.1103/physreve.53.2366

Herring, R., Hofleitner, A., Abbeel, P., Bayen, A., 2010. Estimating arterial traffic conditions using sparse probe data, in: IEEE Conference on Intelligent Transportation Systems, Proceedings, ITSC. pp. 929–936. https://doi.org/10.1109/ITSC.2010.5624994

Hochreiter, S., Schmidhuber, J., 1997. Long Short-Term Memory. Neural Comput. 9, 1735–1780. https://doi.org/10.1162/neco.1997.9.8.1735

Hoogendoorn, S.P., Bovy, P.H.L., 1998. Modeling Multiple User-Class Traffic. Transp. Res. Rec. J. Transp. Res. Board 1644, 57–69. https://doi.org/10.3141/1644-07

Ji, B., Hong, E.J., 2019. Deep-learning-based real-time road traffic prediction using long-term evolution access data. Sensors (Switzerland) 19. https://doi.org/10.3390/s19235327

Jin, W.-L., 2010. Macroscopic Characteristics of Lane-Changing Traffic. Transp. Res. Rec. J. Transp. Res. Board 2188, 55–63. https://doi.org/10.3141/2188-07

Khattak, Z.H., Smith, B.L., Park, H., Fontaine, M.D., 2020. Cooperative lane control application for fully connected and automated vehicles at multilane freeways. Transp. Res. Part C Emerg. Technol. 111, 294–317. https://doi.org/10.1016/j.trc.2019.11.007

Li, Y., Yu, R., Shahabi, C., Liu, Y., 2017. Diffusion convolutional recurrent neural network: Data-driven traffic forecasting. arXiv.

Liang, K.Y., Deng, Q., Martensson, J., Ma, X., Johansson, K.H., 2015. The influence of traffic

on heavy-duty vehicle platoon formation, in: IEEE Intelligent Vehicles Symposium, Proceedings. Institute of Electrical and Electronics Engineers Inc., pp. 150–155. https://doi.org/10.1109/IVS.2015.7225678

Lima, P.F., Martensson, J., Wahlberg, B., 2018. Stability conditions for linear time-varying model predictive control in autonomous driving, in: 2017 IEEE 56th Annual Conference on Decision and Control, CDC 2017. Institute of Electrical and Electronics Engineers Inc., pp. 2775–2782. https://doi.org/10.1109/CDC.2017.8264062

Liu, H., Van Zuylen, H., Van Lint, H., Salomons, M., 2006. Predicting Urban Arterial Travel Time with State-Space Neural Networks and Kalman Filters. Transp. Res. Rec. J. Transp. Res. Board 1968, 99–108. https://doi.org/10.1177/0361198106196800112

Liu, L.N., McDonald, J.F., 1998. Efficient Congestion Tolls in the Presence of Unpriced Congestion: A Peak and Off-Peak Simulation Model. J. Urban Econ. 44, 352–366. https://doi.org/10.1006/juec.1997.2073

Liu, R., Liu, H., Kwak, D., Xiang, Y., Borcea, C., Nath, B., Iftode, L., 2015. Themis: A participatory navigation system for balanced traffic routing, in: IEEE Vehicular Networking Conference, VNC. IEEE Computer Society, pp. 159–166. https://doi.org/10.1109/VNC.2014.7013335

Lloret-Batlle, R., Jayakrishnan, R., 2016. Envy-minimizing pareto efficient intersection control with brokered utility exchanges under user heterogeneity. Transp. Res. Part B Methodol. 94, 22–42. https://doi.org/10.1016/j.trb.2016.08.014

Lloret Batlle, R., 2017. Peer-to-Peer and Collaborative Consumption of Supply in Transportation Systems. ProQuest Diss. Theses.

Ma, X., Tao, Z., Wang, Yinhai, Yu, H., Wang, Yunpeng, 2015. Long short-term memory neural network for traffic speed prediction using remote microwave sensor data. Transp. Res. Part C Emerg. Technol. 54, 187–197. https://doi.org/10.1016/j.trc.2015.03.014

Makigami, Y., Newell, G.F., Rothery, R., 1971. Three-Dimensional Representation of Traffic Flow. Transp. Sci. 5, 302–313. https://doi.org/10.1287/trsc.5.3.302

Nam, D., Lavanya, R., Yang, I., Jeon, W.H., Jayakrishnan, R., 2017. Traffic Density Estimation Using Radar Sensor Data from Probe Vehicles, ITS World Congress 2017 Montreal, October 29 – November 2.

Nelson, P., 1995. A kinetic model of vehicular traffic and its associated bimodal equilibrium solutions. Transp. Theory Stat. Phys. 24, 383–409. https://doi.org/10.1080/00411459508205136

Ngo, V., Hofman, T., Steinbuch, M., Serrarens, A., 2012. Optimal Control of the gearshift command for hybrid electric vehicles. IEEE Trans. Veh. Technol. 61, 3531–3543. https://doi.org/10.1109/TVT.2012.2207922

Nie, Y. (Marco), 2015. A New Tradable Credit Scheme for the Morning Commute Problem. Networks Spat. Econ. 15, 719–741. https://doi.org/10.1007/s11067-013-9192-8

Nie, Y.M., 2012. Transaction costs and tradable mobility credits. Transp. Res. Part B Methodol. 46, 189–203. https://doi.org/10.1016/j.trb.2011.10.002

Nie, Y.M., Yin, Y., 2013. Managing rush hour travel choices with tradable credit scheme. Transp. Res. Part B Methodol. 50, 1–19. https://doi.org/10.1016/j.trb.2013.01.004

Nilsson, J., Brannstrom, M., Coelingh, E., Fredriksson, J., 2017. Lane Change Maneuvers for Automated Vehicles. IEEE Trans. Intell. Transp. Syst. 18, 1087–1096. https://doi.org/10.1109/TITS.2016.2597966

Ntousakis, I.A., Nikolos, I.K., Papageorgiou, M., 2016. Optimal vehicle trajectory planning in the context of cooperative merging on highways. Transp. Res. Part C Emerg. Technol. 71. https://doi.org/10.1016/j.trc.2016.08.007

Oh, C., Ritchie, S.G., Oh, J.-S., 2005. Exploring the Relationship between Data Aggregation and Predictability to Provide Better Predictive Traffic Information. Transp. Res. Rec. J. Transp. Res. Board 1935, 28–36. https://doi.org/10.1177/0361198105193500104

Paden, B., Čáp, M., Yong, S.Z., Yershov, D., Frazzoli, E., 2016. A survey of motion planning and control techniques for self-driving urban vehicles. IEEE Trans. Intell. Veh. 1, 33–55. https://doi.org/10.1109/TIV.2016.2578706

Pan, J., Khan, M.A., Popa, I.S., Zeitouni, K., Borcea, C., 2012. Proactive vehicle re-routing strategies for congestion avoidance, in: Proceedings - IEEE International Conference on Distributed Computing in Sensor Systems, DCOSS 2012. pp. 265–272. https://doi.org/10.1109/DCOSS.2012.29

Park, H., Smith, B.L., 2012. Investigating Benefits of IntelliDrive in Freeway Operations: Lane Changing Advisory Case Study. J. Transp. Eng. 138, 1113–1122.

https://doi.org/10.1061/(ASCE)TE.1943-5436.0000407

Paveri-Fontana, S.L., 1975. On Boltzmann-like treatments for traffic flow: A critical review of the basic model and an alternative proposal for dilute traffic analysis. Transp. Res. 9, 225–235. https://doi.org/10.1016/0041-1647(75)90063-5

Plessen, M.G., Lima, P.F., Martensson, J., Bemporad, A., Wahlberg, B., 2018. Trajectory planning under vehicle dimension constraints using sequential linear programming, in: IEEE Conference on Intelligent Transportation Systems, Proceedings, ITSC. Institute of Electrical and Electronics Engineers Inc., pp. 1–6. https://doi.org/10.1109/ITSC.2017.8317665

Polson, N.G., Sokolov, V.O., 2017. Deep learning for short-term traffic flow prediction. Transp. Res. Part C Emerg. Technol. 79, 1–17. https://doi.org/10.1016/j.trc.2017.02.024

Pourazarm, S., Cassandras, C.G., Malikopoulos, A., 2015. Optimal routing of electric vehicles in networks with charging nodes: A dynamic programming approach, in: 2014 IEEE International Electric Vehicle Conference, IEVC 2014. Institute of Electrical and Electronics Engineers Inc. https://doi.org/10.1109/IEVC.2014.7056110

Prigogine, I., Herman, R., 1971. KINETIC THEORY OF VEHICULAR TRAFFIC.

Qiu, T.Z., Lu, X.-Y., Chow, A.H.F., Shladover, S.E., 2010. Estimation of Freeway Traffic Density with Loop Detector and Probe Vehicle Data. Transp. Res. Rec. J. Transp. Res. Board 2178, 21–29. https://doi.org/10.3141/2178-03

Roncoli, C., Bekiaris-Liberis, N., Papageorgiou, M., 2017. Lane-Changing Feedback Control for

Efficient Lane Assignment at Motorway Bottlenecks. Transp. Res. Rec. J. Transp. Res. Board 2625, 20–31. https://doi.org/10.3141/2625-03

Roncoli, C., Papageorgiou, M., Papamichail, I., 2015. Traffic flow optimisation in presence of vehicle automation and communication systems - Part II: Optimal control for multi-lane motorways. Transp. Res. Part C Emerg. Technol. 57, 260–275. https://doi.org/10.1016/j.trc.2015.05.011

Roncoli, C., Papamichail, I., Papageorgiou, M., 2016. Hierarchical model predictive control for multi-lane motorways in presence of Vehicle Automation and Communication Systems. Transp. Res. Part C Emerg. Technol. https://doi.org/10.1016/j.trc.2015.11.008

Roughgarden, T., 2002. How unfair is optimal routing?, in: Proceedings of the Annual ACM-SIAM Symposium on Discrete Algorithms. pp. 203–204.

Rumelhart, D.E., Hinton, G.E., Williams, R.J., 1986. Learning representations by back-propagating errors. Nature 323, 533–536. https://doi.org/10.1038/323533a0

Saerens, B., Diehl, M., Van Den Bulck, E., 2010. Optimal control using pontryagin's maximum principle and dynamic programming. Lect. Notes Control Inf. Sci. 402, 119–138. https://doi.org/10.1007/978-1-84996-071-7_8

Seo, T., Kusakabe, T., 2015. Probe vehicle-based traffic flow estimation method without fundamental diagram, in: Transportation Research Procedia. Elsevier, pp. 149–163. https://doi.org/10.1016/j.trpro.2015.07.009

Seo, T., Kusakabe, T., Asakura, Y., 2015. Estimation of flow and density using probe vehicles

with spacing measurement equipment. Transp. Res. Part C Emerg. Technol. 53, 134–150. https://doi.org/10.1016/j.trc.2015.01.033

Small, K.A., 1992. Urban Transportation Economics. Harwood Academic Publishers, Switzerland.

Tian, Y., Pan, L., 2015. Predicting Short-Term Traffic Flow by Long Short-Term Memory Recurrent Neural Network, in: 2015 IEEE International Conference on Smart City/SocialCom/SustainCom (SmartCity). pp. 153–158. https://doi.org/10.1109/SmartCity.2015.63

Treiber, M., Hennecke, A., Helbing, D., 1999. Derivation, properties, and simulation of a gas-kinetic-based, nonlocal traffic model. Phys. Rev. E - Stat. Physics, Plasmas, Fluids, Relat. Interdiscip. Top. 59, 239–253. https://doi.org/10.1103/PhysRevE.59.239

Van Den Bosch, A., Van Arem, B., Mahmod, M., Misener, J., 2011. Reducing time delays on congested road networks using social navigation, in: 2011 IEEE Forum on Integrated and Sustainable Transportation Systems, FISTS 2011. pp. 26–31. https://doi.org/10.1109/FISTS.2011.5973596

van Lint, J.W.C., Hoogendoorn, S.P., van Zuylen, H.J., 2005. Accurate freeway travel time prediction with state-space neural networks under missing data. Transp. Res. Part C Emerg. Technol. 13, 347–369. https://doi.org/10.1016/j.trc.2005.03.001

Varian, H.R., 1974. Equity, envy, and efficiency. J. Econ. Theory 9, 63–91. https://doi.org/https://doi.org/10.1016/0022-0531(74)90075-1

Wang, T., Cassandras, C.G., Pourazarm, S., 2014. Energy-aware vehicle routing in networks with Charging nodes, in: IFAC Proceedings Volumes (IFAC-PapersOnline). IFAC Secretariat, pp. 9611–9616. https://doi.org/10.3182/20140824-6-za-1003.00814

Wright, M., Horowitz, R., 2016. Fusing loop and GPS probe measurements to estimate freeway density. IEEE Trans. Intell. Transp. Syst. 17, 3577–3590. https://doi.org/10.1109/TITS.2016.2565438

Xiao, L., Gao, F., 2010. A comprehensive review of the development of adaptive cruise control systems. Veh. Syst. Dyn. 48, 1167–1192. https://doi.org/10.1080/00423110903365910

Yang, H., Wang, X., 2011. Managing network mobility with tradable credits. Transp. Res. Part B Methodol. 45, 580–594. https://doi.org/10.1016/j.trb.2010.10.002

Yang, H., Zhang, X., 2003. Optimal Toll Design in Second-Best Link-Based Congestion Pricing. Transp. Res. Rec. 1857, 85–92. https://doi.org/10.3141/1857-10

Yi, H., Heejin, J., Bae, S., 2017. Deep Neural Networks for traffic flow prediction, in: 2017 IEEE International Conference on Big Data and Smart Computing, BigComp 2017. Institute of Electrical and Electronics Engineers Inc., pp. 328–331. https://doi.org/10.1109/BIGCOMP.2017.7881687

Zhang, Y., Ioannou, P.A., 2017. Combined Variable Speed Limit and Lane Change Control for Highway Traffic. IEEE Trans. Intell. Transp. Syst. 18, 1812–1823. https://doi.org/10.1109/TITS.2016.2616493

Zhou, L., Burris, M.W., Baker, R.T., Geiselbrecht, T., 2009. Impact of Incentives on Toll Road

Use by Trucks. Transp. Res. Rec. J. Transp. Res. Board 2115, 84–93.

https://doi.org/10.3141/2115-11